University of Alberta

Regulation of *Wolbachia* density within *Drosophila simulans*

by

Jennifer Ann Haukedal

A thesis submitted to the Faculty of Graduate Studies and Research

in partial fulfillment of the requirements for the degree of

Doctor of Philosophy

in

Physiology, Cell and Developmental Biology

Department of Biological Sciences

©Jennifer Ann Haukedal

Fall 2013

Edmonton, Alberta

Permission is hereby granted to the University of Alberta Libraries to reproduce single copies of this thesis and to lend or sell such copies for private, scholarly or scientific research purposes only. Where the thesis is converted to, or otherwise made available in digital form, the University of Alberta will advise potential users of the thesis of these terms.

The author reserves all other publication and other rights in association with the copyright in the thesis and, except as herein before provided, neither the thesis nor any substantial portion thereof may be printed or otherwise reproduced in any material form whatsoever without the author's prior written permission.

Abstract

The endosymbiont *Wolbachia pipientis* is a Gram negative alpha proteobacterium and is found in a wide range of insects, spiders and mites, nematodes, and crustaceans. *Wolbachia* is responsible for several reproductive manipulations within its host, most notably, cytoplasmic incompatibility (CI). CI is a form of conditional male sterility by which infected males can only successfully mate with females infected with the same *Wolbachia* strain. *Wolbachia* density within developing sperm has been implicated in determination of the penetrence of CI within populations. To this end, this study examines two distinct factors that may regulate *Wolbachia* density in *Drosophila simulans*: replication of the WO phage and oxidative stress imbalance between host and symbiont.

The replication of the WO phage, a temperate bacteriophage found within the *w*Ri genome has previously been correlated with *Wolbachia* density and CI. In *D. simulans*, only one of the three phage genomes is undergoing replication, WORiC, and replication of WORiC does not appear to correlate with *Wolbachia* density.

D. simulans infected with *w*Ri (DSR) contains a higher amount of reactive oxygen species (ROS) when compared with uninfected flies (DSRT). The exogenous feeding of the antioxidant compounds glutathione and ascorbic acid increases *Wolbachia* density three fold in males, females, and their testes and ovaries. This increase in density is not attributed to amino acid scavenging or an

increase in fly fitness. In developing sperm, the ROS-producing enzyme NADPH oxidase is found exclusively in the nuclear region and does not appear to differ between DSR and DSRT. Dual oxidase, another member of the NADPH oxidase family, however, was found in close association with *Wolbachia*-containing vesicles. *In vitro,* the NADPH oxidase inhibitors VAS2870, apocynin, and DPI had varying abilities to inhibit the amount of total ROS found in DSR and DSRT; homogenates from DSR were more susceptible to apocynin and DPI than DSRT. Exogenous feeding of apocynin and VAS2870, however, did not change *Wolbachia* density in young males.

Unlike other *Wolbachia*-host systems, the activity of the WO phage in *w*Ri does not appear to be a factor that is regulating *Wolbachia* density. This may be due to a very low level of replicating phage and a relatively high *Wolbachia* titer. A redox-dependent mechanism of regulation of *Wolbachia* density is more likely and dual oxidase is a strong candidate as the key component of this regulation.

Acknowledgements

First and foremost, I'd like to thank Dr. Harriet Harris for giving me the opportunity to join her lab, for her wealth of knowledge that she shared with me and, most importantly, for having the utmost confidence in me when I was sure that I wasn't going to make it through. I'm also very grateful to have a co-supervisor, Dr. Andrew Keddie, who has never lacked for advice and made me realize the important aspects of being a scientist. I've been very fortunate to have a very supportive committee; Dr. Andrew Simmonds and Dr. Shelagh Campbell have always been generous and helpful with any problems I've come to them with and I thank them for that.

I don't think I would have made it through those days when nothing works out if not for my past and present lab members. Dr. Lesley Brennan and Philip Batista have been great friends and co-workers and have helped me get through experiments, writing, and, on bad days, a couple pints of beer. I've also had the good fortune to mentor undergraduate summer students every year. David Catterall, Kenile Awoh, Chantalle Grant, Amanda Cook, and Kailey Michnel have been extremely helpful and enthusiastic in the lab.

I'd like to thank Troy Locke, in the MBSU, for the hours of chats we've had about techniques and equipment and life in general. Arlene Oatway in the microscopy facility has been a wonderful resource as well.

Finally, I would have not gotten this far without the support of my husband and best friend for the past 9 years, Evan Haukedal.

Table of Contents

Tables

Figures

List of symbols, nomenclature, and abbreviations

α – alpha

AA – ascorbic acid, reduced state

Aa23 – *Aedes albopictus* embryonic cell line, infected with *Wolbachia*

Aa23T – *Aedes albopictus* embryonic cell line, uninfected

AEL – after egg laying

ANOVA – analysis of variance

Apocynin – 4-hydroxy-3-methoxyacetophenone

CySCs – somatic cyst stem cells

Cys – cysteine

CI – cytoplasmic incompatibility

DCFDA – 2′,7′-dichlorofluorescin diacetate

DHA – dihydroascorbic acid, oxidized state

DPI – diphenyleneiodium

DSR – *Drosophila simulans* Riverside strain, infected with *Wolbachia w*Ri

DSRT – *Drosophila simulans* Riverside, uninfected

Duox (*duox*) – dual oxidase

FAC – ferric ammonium chloride

Glu – glutamic acid

Gly – glycine

GSCs – germline stem cells

GSH – glutathione, reduced form

GSSG – glutathione, oxidized form

$HO^{\cdot}$ – hydroxyl radical

H_2O_2 – hydrogen peroxide

λ – Lambda bacteriophage

MK – male killing

MTase (*MTase*) – *Wolbachia* parB-containing adenine methyltransferase

MYA – million years ago

NADPH – nicotinamide adenine dinucleotide phosphate

Nox (*Nox*) – NADPH oxidase

O_2^{-} - superoxide

ORF – open reading frame

PBS – phosphate buffered saline

PCNA – proliferating cell nuclear antigen

PCR – polymerase chain reaction

PKCβIII – protein kinase C beta 3

qPCR – quantitative polymerase chain reaction

ROS – reactive oxygen species

SNBP – small nuclear basic protein

SOD – superoxide dismutase

T4SS – type four secretion system

VAS2870 – 3-benzyl-7-(benzoxazolyl)thio-1,2,3-triazolo[4,5-d]pyrimidine

*w*AlbB – *Wolbachia* infecting *Aedes albopictus*

*w*Bm – *Wolbachia* infecting *Brugia malaya*

*w*Bol1 – *Wolbachia* infecting *Hypolimnas bolina*

*w*Mel – *Wolbachia* infecting *Drosophila melanogaster*

*w*MelPop – *Wolbachia* infecting *Drosophila melanogaster*, pathogenic strain

*w*Pip – *Wolbachia* infecting *Culex pipiens*

*w*Ri – *Wolbachia* infecting *Drosophila simulans* Riverside

Wsp (*wsp*) – *Wolbachia* surface protein

*w*VitA – *Wolbachia* infecting *Nasonia vitripennis*

1. Introduction
1.1 Symbiosis

The term symbiosis is ancient Greek for "living together" and describes close relationships between members of different species. Bacterial symbiosis in animals, in particular, is a nearly ubiquitous phenomenon and some of these symbionts are endosymbiotic, which means they reside within host cytoplasm.

Macro- and micro-organismal symbiotic relationships can broadly be divided into mutualistic and parasitic classes. While the spectrum of symbiosis can include intermediary relationships such as commensalism (one organism benefits with no detriment or benefit to the other), the current work here will make no assumptions that a completely benign and intimate commensal relationship between eukaryotic and prokaryotic organisms can, in fact, exist.

Mutualism occurs when both species benefit from the association and can occur with or without a division of labour. Leafcutter ants, for example, culture farms of fungi with the leaf fragments they procure. The leaves provide a source of nutrition for the fungus and the ants consume specialized hyphal swellings off the fungi that only occur when the fungi have been properly cultivated [reviewed in (Caldera et al., 2009)]. This system also includes several bacterial species of Enterobacteriaceae which function to convert plant biomass into vitamins and amino acids for the ants (Aylward et al., 2012) .

Parasitism describes close relationships where one partner benefits to the detriment of the other. Classic examples of parasitism include intestinal tract

helminthic infections (tapeworms, flatworms, roundworms, etc.) that require the host environment to complete their developmental life cycle, and bacteriophages that hijack bacterial host machinery in order to replicate. Parasitism, however, is normally not quite so clearly described in many animal-bacterial associations; the effects that a parasite can confer are often subtle. Slight reductions in fecundity, changes in immune function, or lifespan may not have a noticeable effect on the host. To complicate things further, the parasite might actually provide a benefit alongside several parasitic effects; some bacterial symbionts boost immunity while at the same time reducing fecundity (*e.g*. male-killing *Spiroplasma* increases resistance to parasitic nematodes) (Jaenike et al., 2010).

1.1.1 Primary and Secondary Symbioses in Insects

Bacterial endosymbionts in insects and other arthropods are a common phenomenon and are generally classified into two groups, primary and secondary. Primary endosymbiotic associations are obligate for survival of both the host and the bacteria; these symbionts are generally housed in a specialized organ called a bacteriome and specialized cells called bacteriocytes. Primary symbiotic relationships are also ancient; estimated evolutionary timelines indicate a 270 million year association (Dale and Moran, 2006). These symbionts are completely adapted to an intracellular lifestyle and their genome size is a reflection of this; many are less than 1Mb (Wernegreen, 2002). One of the most widely studied primary symbiotic relationships is the pea aphid, *Acyrthosiphon pisum* Harris, and its residing bacteria, *Buchnera aphidicola*. This aphid species is

a phloem sap feeder and depends on *Buchnera* to provide essential amino acids that cannot be obtained through diet (Gunduz and Douglas, 2009).

Secondary symbionts are not always required for host survival and are usually defined as facultative. Although generally located throughout various organs and tissues in a host they often are packed in specific cell types. The benefits they confer to their host are varied. In female *Trichogramma bourarachae* Pintureau, a parasitic wasp, and the mosquito *Aedes albopictus* Skuse harboring *Wolbachia pipientis*, a marked increase in fecundity is observed compared to uninfected females (Dobson et al., 2004; Vavre et al., 1999). Similarly, female *Metaseiulus occidentalis* Nesbitt, a predatory mite, display increased fecundity when infected with the secondary symbiont *Cardinium hertigii* (Weeks and Stouthamer, 2004). A secondary symbiont of *A. pisum, Hamiltonella defensa*, confers resistance to parasitoid wasps (Oliver et al., 2003) but, interestingly, this protection is lost if the bacteria loses its bacteriophage (Weldon et al., 2013).

Horizontal transfer of secondary symbionts occasionally occurs between different hosts and, therefore, the evolution of the bacterium does not necessarily co-align with that of the host. Secondary symbionts also exhibit genome reduction, but this is a moderate reduction in comparison to primary symbionts. Examples of secondary symbionts include *Spiroplasma spp*, *Cardinium spp*, and *Wolbachia pipientis*; these three all induce some type of reproductive manipulations to their host (Harris et al., 2010). Insects can be singly infected with either a primary or

secondary symbiont, or they may have multiple infections (e.g. a primary and a secondary, or several secondaries).

1.2 *Drosophila simulans*

Drosophila simulans was first described by AH Sturtevant in the early 1920's during hybridization experiments with different *Drosophila* species (Sturtevant 1920). *Drosophila simulans* is closely related to *D. melanogaster* in morphology and genetic composition. Hybrids originating from *D. melanogaster* females and *D. simulans* males can be obtained, however, progeny are sterile if the parents are not infected with *Wolbachia*. Hybrid males from the same mating scheme infected with *Wolbachia* die at larval stages (Ferree and Sullivan, 2006). Despite the similarity between the two species, genetic manipulation of *D. simulans* is not currently available due to the lack of P-element sequences available in *D. melanogaster* (Kimura and Kidwell, 1994).

1.2.1 *Drosophila* Spermatogenesis

In *Drosophila*, spermatogenesis proceeds spatially throughout the tubular-shaped testis, beginning at the apical tip and proceeding towards the basal end. The apical tip is composed of three different cell types: non-dividing stromal hub cells, germline stem cells (GSCs), and somatic cyst stem cells (CySCs). Of these cells, only the GSCs are destined to become mature sperm. Mitotic division of GSCs and CySCs is asymmetrical in nature; the mother cell retains its position adjacent to the hub cells via E-cadherin based adherens junctions (Inaba et al., 2010) and the daughter cell moves on to differentiate [reviewed in (de Cuevas and

Matunis, 2011)]. Maintenance of the stem cell niche is regulated largely by the JAK-STAT signaling cascade (Singh et al., 2010). Mother cells destined to remain in the niche will continuously receive signals from the hub cells, while daughter cells destined to differentiate will be isolated from these signals.

The daughter cells, gonialblasts, undergo 4 successive rounds of mitosis and the result is a 16-cell syncytium, which begins the meiotic cycle. Throughout the mitotic divisions, the CySCs encase the gonialblasts (Gönczy and DiNardo, 1996). An extended G2 phase occurs during meiosis where the cells grow in volume approximately 25-fold and become primary spermatocytes. Regulating the G2/M checkpoint are 4 necessary genes: *spermatocytes arrest, cannonball, always early* and *meiosis I arrest*; mutations in any one of these genes results in cell cycle arrest (Lin et al., 1996). Following meiosis I and II, the spermatocytes begin a remarkable morphological change which results in 64 elongated spermatids. During an intermediate elongation stage, termed the "canoe stage", core histones are replaced with the small nuclear basic proteins (SNBPs or protamines) Mst35Ba, Mst35Bb, and Mst77F (Raja and Renkawitz-pohl, 2005; Rathke et al., 2007).

Until recently, the compact nature of post-meiotic chromosomes was thought to inhibit transcriptional activity; however post-meiotic chromosomes do produce transcripts and at least one transcript from the gene *scotti* is required for sperm individualization (Barreau et al., 2008; Vibranovski et al., 2010).

Individualization is the process of separating the syncytial 64 spermatocysts into 64 single sperm cells. During individualization, the volume of cytoplasm decreases dramatically, essentially leaving only the chromosomes and the proteins that compact them. An "individualization complex" (IC) is a cytoskeleton/membrane complex containing cytoplasm and organelles that transverses down the sperm cyst distally from the nucleus. Once the IC travels to the end of the sperm tails, it is referred to as a "waste bag" and is degraded within the testes lumen (Fabrizio et al., 1998; Tokuyasu et al., 1972). Mature sperm are then stored in the seminal vesicle.

1.2.2 *Drosophila* Early Fertilization Events

Mature oocytes are arrested in metaphase I of meiosis until passage through the oviduct when meiosis I and II are completed. The resulting 4 haploid nuclei become the maternal pronucleus and 3 polar bodies. Sperm (including the tail) with highly condensed chromosomes due to the replacement of histones with protamines during spermatogenesis enter oocytes. Immediately upon entry, the sperm plasma membrane is broken down by the gene products from s*neaky* and *misfire* (Ohsako et al., 2003; Wilson et al., 2006). Following plasma membrane breakdown, paternal protamines are removed and replaced with maternal histones H3.3, H4, H2A, and H2B. This removal of protamines and deposition of histone H3.3 onto the paternal chromatin is dependent on the chromatin assembly factor, HIRA (Bonnefoy et al., 2007; Loppin et al., 2005; Raja and Renkawitz-pohl, 2005).

Upon histone addition to the paternal pronucleus, the chromosomes are less compact and able to undergo replication in preparation for the first zygotic mitosis. During replication, the maternal and paternal pronuclei migrate towards one another and eventually fuse. The separation of the maternal pronucleus from the 3 polar bodies and the subsequent migration towards the paternal pronucleus is dependent on the gene product of *KLP3A*, a kinesin-like protein, in *Drosophila* (Williams et al., 1997).

After DNA synthesis, nuclear envelope breakdown, and chromosome condensation, the fused pronuclei enter prophase and begin the first zygotic mitosis. A unique feature of many insects, including *Drosophila*, is the ability of the maternal chromosomes to proceed through anaphase independently of the paternal chromosomes (Callaini et al., 1997); this may be an underlying mechanism that allows for parthenogenesis in insects.

1.3 *Wolbachia pipientis*

Wolbachia are obligate intracellular secondary bacterial symbionts that infect a wide variety of arthropods and filarial nematodes. *Wolbachia* was first described by Hertig and Wolbach in 1924 and were described as “Rickettsia-like mircroorganims” (Hertig and Wolbach, 1924).Today, it is estimated that between 40 - 66% of all insect species alone harbor this bacterium (Hilgenboecker et al., 2008; Zug and Hammerstein, 2012).

Wolbachia are pleiomorphic; cells can be round or oval, and between 0.4µm to 1.0µm. In host cytoplasm, each *Wolbachia* cell is contained within a Golgi-derived host vacuole and appears to divide by binary fission, and vacuoles can contain several *Wolbachia* cells after fission (Cho et al., 2011; Nigro and Louis, 1989; Oh et al., 2000; Popov et al., 1998). Because of its obligate nature, attempts to culture *Wolbachia* outside of host cells have been unsuccessful to date. *Wolbachia* can be purified from host cells and maintained in culture medium for up to 7 days, but bacterial replication does not occur without re-inoculation back into host cells (Gamston and Rasgon, 2007; Rasgon et al., 2006).

1.3.1 *Wolbachia* Nomenclature and Phylogeny

Currently, all *Wolbachia* bacteria belong to one species, *Wolbachia pipientis* (Lo et al., 2007) which is a member of the α-proteobacteria class. *Wolbachia* are usually named according to the host that they infect. For example *w*Ri, is the *Wolbachia* infecting *Drosophila simulans* Riverside, *w*Pip infects *Culex pipiens*, while *w*Mel infects *Drosophila melanogaster*.

Within this single species, there are 10 supergroups A through K [although supergroup G is no longer recognized (Baldo and Werren, 2007)]. Generally speaking, *Wolbachia* that infect nematodes are members of supergroups C, D, and J (Fenn et al., 2006; Ferri et al., 2011), and most recently, I (Haegeman et al., 2009). Supergroup F has recently been shown to infect both nematodes and arthropods (Casiraghi et al., 2005; Covacin and Barker, 2007; Lefoulon et al., 2012; Panaram and Marshall, 2007). Supergroups A and B belong to *Wolbachia*

infecting arthropods such as *D. melanogaster* (fruit fly), *Nasonia vitripennis* and *Asobara tabida* (both parasitoid wasps), and *Aedes albopictus* (Asian tiger mosquito) (Werren et al., 1995). It has been estimated that supergroups A and B diverged approximately 32 MYA and divergence from the earliest ancestor of *Wolbachia* occurred about 50 – 55 MYA (Clark et al., 1999).

16S rRNA sequencing indicates that the closest relatives of *Wolbachia* are *Ehrlichia spp.* and *Anaplasma spp* (Drancourt and Raoult, 1994; O'Neill et al., 1992). Both genera contain tick-borne human pathogens: *Ehrlichia chaffeensis* is the cause of ehrlichiosis in humans and *Anaplasma phagocytophilum* causes human granulocytic anaplasmosis [reviewed in (Paddock and Childs, 2003) and (Dumler et al., 2005), respectively] . To date, however, there is no evidence that *Wolbachia* can infect vertebrates.

1.3.2 *Wolbachia* Genomes

The first *Wolbachia* genome sequenced in 2004 was *w*Mel (*Wolbachia* infecting *Drosophila melanogaster*) (Wu et al., 2004). The *w*Mel genome sequence revealed several surprising and interesting features which have also been found in subsequent sequences of other *Wolbachia* strains (Wu et al., 2004). Among these to date:

1. At 1.2Mbp, the *w*Mel genome is much reduced compared to free living bacteria. This is a result of a long-term intracellular lifestyle within the eukaryotic host. Genes that have been lost include: cell envelope

biogenesis genes, lipopolysaccharide production genes, and genes responsible for cell wall components (Wu et al., 2004).

2. *Wolbachia* genomes carry a surprisingly high amount of repetitive and mobile elements. 14.2% of the *w*Mel genome is composed of repeat sequences which include insertion sequence elements, retrotransposons, and uncharacterized mobile elements. *w*Mel also carries two prophage regions, termed WOMelA and WOMelB.
3. *w*Mel contains 23 proteins that are composed of 1-11 anykrin repeat domains, which is the highest density of ankyrin domain proteins in all bacteria. wPip, the *Wolbachia* found in *Culex pipiens* has 60 ankyrin containing proteins (Klasson et al., 2008). Ankyrin repeat-containing proteins are thought to facilitate protein-protein interactions. Although 12 of these genes have since been cloned and expressed in whole flies (Yamada et al., 2011), no functional roles have been determined to date.
4. *Wolbachia* genomes contain two operons that comprise a functional type IV secretion system (T4SS). T4SSs are best studied in the bacteria *Agrobacterium tumefaciens* and this system is used to deliver DNA into susceptible plants and causes crown galls [reviewed in (Pitzschke and Hirt, 2010)]. When the T4SS of 37 strains of *Wolbachia* infecting insects, crustaceans, nematodes, and arachnids were sequenced, a high degree of conservation was found between all of the components (Pichon et al., 2009). It is not currently known what molecules *Wolbachia* are able to deliver via this system.

Since 2004, additional *Wolbachia* strain genomes have been sequenced including wBm (infecting *Brugia malayi* TRS) (Foster et al., 2005), wPip (infecting *Culex pipiens* Pel) (Klasson et al., 2008), *w*Ri (infecting *Drosophila simulans* Riverside) (Klasson et al., 2009), *w*AlbB (infecting *Aedes albopictus* Houston) (Mavingui et al., 2012), and *w*Bol1 (infecting *Hypolimnas bolina*) (Duplouy et al., 2013).

1.3.3 *Wolbachia* Phenotypes

Wolbachia can exert a wide range of phenotypic effects on its hosts; it exists as a mutualist, a reproductive manipulator, or a parasite. As a mutualist, *Wolbachia* has been shown to act as a nutritional source in bedbugs (Hosokawa et al., 2010), and is required for reproduction in many nematodes and oogenesis in some insects (Dedeine et al., 2001; Hoerauf et al., 2003). As a reproductive manipulator, *Wolbachia* alters host reproduction dramatically using several different strategies. All manipulations hinge on the fact that *Wolbachia* are solely maternally inherited and reproductive phenotypes always benefit females in a given population to ensure that the bacteria succeed in future generations. *Wolbachia* can cause feminization of genetic males, can cause male-killing, induce parthenogenesis, and can cause a form of conditional male sterility called cytoplasmic incompatibility (CI). In a parasitic, laboratory induced *Wolbachia* infection, *w*MelPop (popcorn strain) infects *Drosophila melanogaster* and undergoes massive over-replication once adulthood is reached and cell division ceases, and decreases the lifespan of the fly by approximately 50% (Min and

Benzer, 1997). It is not currently known what factors are responsible for the timing and trophism of the increased replication of *w*MelPop. The perplexing ability of *Wolbachia* to "phenotype switch" when trans-infected into new hosts makes the molecular mechanisms of these interactions difficult to elucidate. *w*Inn, for example, naturally infects *Drosophila innubila* and is a male-killing strain however when trans-infected into *D. simulans* and *D. melanogaster*, no reproductive manipulations occur (Veneti et al., 2012).

1.3.3.1 Male Killing

Wolbachia-induced male killing (MK) was first identified in *Adalia bipunctata* (the two-spot ladybird beetle) and *Acraea encedon* (a butterfly) (Hurst et al., 2013). Eggs laid by infected females produce only half of the viable offspring that uninfected females produce, and this is attributed to mortality of nearly all of the embryos destined to be males. An unusual form of male killing occurs in the moth *Ostrinia scapulalis* Matsudo, whereby infected ZZ males die during embryogenesis or early larval development but females (ZW) die if cured of *Wolbachia* and this phenotype influences the *doublesex* sex-determining gene (Sugimoto and Ishikawa, 2012). When the male-killing *Wolbachia* strain *w*Inn (infecting *D. innubila*) was transferred to *D. simulans* and *D. melanogaster*, a complete loss of reproductive phenotypes was observed (Veneti et al., 2012). Recently it was reported that the male-killing *Wolbachia* of *D. bifasciata* acts by impairing chromatin remodeling and spindle formation in male embryos.

Defective mitosis occurs in all stages of embryogenesis and eventually accumulates and induces mortality (Riparbelli et al., 2012).

1.3.3.2 Parthenogenesis

Parthenogenesis is a naturally occurring phenomenon that is prevalent in hymenopteran species and can occur in mites, thrips, and aphids. The most common form of parthenogenesis is arrhenytoky; haploid males arise from unfertilized eggs and diploid females result from sexual fertilization.

Complete parthenogenesis, or thelytoky, occurs when unfertilized eggs develop as homozygous diploid females [reviewed in (Rabeling and Kronauer, 2013)]. This results in reduced numbers of male offspring and often completely eliminates males in populations. Queen honey bees, for example, can produce clonal daughter queens via thelytoky and can also produce diploid female worker bees through sexual reproduction. The switch in reproductive behavior in queen bees is thought to be under the control of *th* (*thelytoky*) gene, which encodes a transcription factor (Lattorff et al., 2007).

In 1990, Stouthamer and others discovered that, under antibiotic treatment, four species of the parasitoid wasp *Trichogramma* converted from male-less thelytoky populations into sexually reproducing arrhenytokous populations (Stouthamer et al., 1990). In this sexually reproducing population, unfertilized eggs developed into haploid males. While it was clear that symbiotic bacteria were responsible for this reproductive manipulation (Stouthamer and Werren,

1993), it wasn't until the PCR reaction was commonly available that *Wolbachia* was identified as the agent (Zchori-Fein et al., 1994).

While the molecular mechanisms of *Wolbachia* induced parthenogenesis are unknown, studies have shown that *Wolbachia* can influence ploidy through two distinct mechanisms. In infected *Trichogramma spp.*, the first mitotic division is incomplete; chromosomes fail to segregate in anaphase which leads to a diploid cell. In infected *Muscidifurax uniraptor*, the first mitotic division is normal but diploidy occurs when the two daughter cells fuse (Gottlieb et al., 2011; Pannebakker et al., 2004; Stouthamer and Kazmert, 1994).

1.3.3.3 Feminization

Wolbachia induced feminization is the conversion of genetic males into functional females and this occurs mainly in crustaceans (Bouchon et al., 1998; Rousset et al., 1992). In *Armadillidium vulgare*, the pill woodlouse, *Wolbachia* influences the production of the androgenic gland hormone from the androgenic gland. This masculinizing hormone, when injected, is able to phenotypically convert females into males (Martin et al., 1999). How *Wolbachia* interacts with the androgenic gland to modulate levels of this hormone is currently unknown.

1.3.4 Cytoplasmic Incompatibility

1.3.4.1 Cytoplasmic incompatibility benefits infected females

In 1973, Yen and Barr demonstrated that the etiological agent of cytoplasmic incompatibility was *Wolbachia* in *Culex pipiens* (Yen and Barr 1973). It wasn't until 1989 that *Wolbachia*-induced CI was described in *D. simulans* (Binnington and Hoffmann 1989); the *w*Ri and *D. simulans* model continues to be used towards determining the molecular mechanisms of CI.

Cytoplasmic incompatibility is a form of conditional male sterility induced by many different strains of *Wolbachia* that increases the proportion of infected individuals in populations and confers a benefit to infected females. Infected females can successfully mate with any male, regardless of his infection status, and the embryos will be viable and carry *Wolbachia.* When infected males fertilize eggs from uninfected females, the resulting zygote does not complete the first mitosis. CI penetrence (the proportion of embryos that die as a result of an incompatible cross) can range from 25% - 100%, depending on the bacterial and host strain (Bourtzis et al., 1996).

Wolbachia does not have any positive or negative effects on fecundity in *D. sechellia* and *D. ananassae* (Bourtzis et al., 1996). *Nasonia vitripennis* also does not benefit in fecundity from *Wolbachia* infections once host genetic background is controlled (Bordenstein and Werren, 2000).

CI is thus responsible for a phenomenon termed “cytoplasmic drive” (Turelli and Hoffmann, 1991)in which infected females have a distinct advantage over uninfected females and this results in a rapid spread of *Wolbachia* throughout populations in a short amount of time (Turelli and Hoffmann, 1995).

1.3.4.2 Molecular mechanisms of CI

CI presents itself within the first mitotic division following fertilization. Upon fertilization, protamine removal in the paternal pronucleus appears normal (Landmann et al., 2009). The paternal pronucleus suffers from delays in nuclear envelope breakdown (Tram and Sullivan, 2002), deposition of histones H3.3 and H4 (Landmann et al., 2009), and chromosome condensation (Lassya and Karr, 1996). HIRA, a chaperone of H3.3, is also down-regulated in males that exhibit strong CI (Zheng et al., 2011). While the maternal pronuclear chromosomes condense normally in preparation for metaphase, the paternal chromosomes lag behind and remain decondensed. This leads to death of the embryo (Lassya and Karr, 1996).

The asynchronous chromosome condensation is related to the deposition of maternal histones onto the paternal chromosome. In incompatible crosses, the deposition of histones H3.3 and H4 onto the paternal chromosomes are delayed when compared to deposition onto the maternal chromosomes (Landmann et al., 2009). PCNA, a marker for DNA replication, is retained upon the paternal chromosomes while the maternal chromosomes complete replication and proceed

through mitosis. In mutant PCNA *D. melanogaster*, maternal histones H4 and H2A are unable to deposit onto the paternal chromosomes (Loppin et al., 2005).

D. melanogaster and *D. simulans* infected with *Wolbachia* express lower levels of the H3.3 binding protein HIRA; HIRA mutant *D. melanogaster* display CI phenotypes upon fertilization (Zheng et al., 2011). HIRA is essential for histone H3.3 binding to the male pronuclear chromosomes, although not required for the removal of protamines immediately following fertilization (Bonnefoy et al., 2007).

Despite the delay in male pronuclear chromosome condensation, maternal chromosomes in CI crosses proceed through anaphase normally in *D. simulans* (Callaini et al., 1997). As the maternal chromosomes migrate to the spindle poles, aberrant condensation of the paternal chromosomes gives rise to a "chromosome bridge" (Lassya and Karr, 1996), which ultimately results in death of the embryo.

1.3.4.3 CI Effector Molecules

Recently, Bossan et al (2011) have shown that as few as two factors are likely to be involved in the CI phenotype in a mathematical model termed "the goalkeeper model." They argue that two factors, *x* and *y*, contribute to whether CI will occur between infected and uninfected animals and fit their model to known experimental data. The amount of the two factors will determine, in males, if the sperm is modified (mod), and in females, if the cytoplasmic composition will rescue that modification (resc). If at least one mod factor is in excess of the resc

factors, CI will occur and, alternatively, if the resc factors are in excess of the mod factors, CI will not occur (Bossan et al., 2011). Several candidate modification effector molecules have been studied in recent years, although there is not yet substantial evidence that they are directly related to CI opposed to a molecule that simply mimics the CI phenotype.

It is assumed that an effector molecule that *Wolbachia* produces to hijack its host's reproduction would be delivered into the host cytoplasm or nucleus via the T4SS. In the past several years, the pathogenesis of the tick-borne pathogen *Anaplasma phagocytophilium* has been closely studied and the effector molecules that are delivered could be used as a model to understand *Wolbachia*'s reproductive manipulations. This bacterium infects human neutrophils and downregulates the innate immune system and inhibits apoptosis and autophagy [reviewed in (Rikihisa, 2010)]. In 2004, Park et al. discovered the *A. phagocytophilium* protein AnkA in the nucleus of an infected human neutrophil cell line and that AnkA was binding specific sites on the host chromosomes (Park et al., 2004). AnkA is a 160kDa ankyrin repeat domain-containing protein and is secreted into the host nucleus via the T4SS (Caturegli et al., 2000; Lin et al., 2007). Several years later, it was found that AnkA specifically decreases expression of the NAPDH oxidase protein gp91 to avoid the deleterious effects of targeted reactive oxygen generation by the host (Garcia-Garcia et al., 2009). *Wolbachia* are closely related to *Anaplasma spp*., presumably have a functional T4SS, and contain many ankyrin repeat domain-containing proteins. Despite the

parallels between the two α-proteobacteria, no such effector molecule in *Wolbachia* has been functionally described.

Polyacrylamide gel electrophoresis and mass spectrometry of the proteins found in infected and uninfected mosquito gonads revealed the presence of a *w*Pip-encoded DNA binding protein in infected tissues. This binding protein, HU beta, is particularly exciting because it is a small basic protein and could conceivably function as a protamine during histone replacement in spermatogenesis (Beckmann et al., 2013). Further investigation into HU beta localization and its role in CI will prove interesting.

Finally, two dimensional polyacrylamide gel electrophoresis of the proteins within 15 minute post-fertilization embryos revealed that infected eggs harbor a unique bacterial DNA adenine methyltransferase (met2) (H. Braig, personal communication). In *D. simulans*, this methyltransferase is carried within the prophage WORiB region, however, other *Wolbachia* strains carry an additional copy within their WO-A prophages (Saridaki et al., 2011). *Met2* is described as an "orphan methyltransferase" because it is presumably not part of any restriction modification (R-M) system (reviewed in (Tock and Dryden, 2005)). Southern blot analyses of the presence of *met2* within the genomes of 11 *Wolbachia* strains revealed that *met2* is present in CI causing strains and is either absent or disrupted in strains that are mod(-) (Saridaki et al., 2011).

Transgenic expression of wMel *met2* in *D. melanogaster* was recently reported using the UAS/GAL4 system (Yamada et al., 2011). This study revealed

no modification of phenotype in flies expressing *met2* ubiquitously and, similarly, when expressed specifically in the ovaries, no rescue phenotype was apparent in CI crosses. Although these data suggest that constitutive expression of the *met2* gene does not alone drive the CI phenotype, it is still unclear what type of regulation *met2* or any of the phage-related genes are subject to and how this affects the mechanism of CI.

1.4 Regulation of *Wolbachia* density in insect hosts

1.4.1 *Wolbachia* density and CI

The bacterial dosage model, when applied to CI, predicts that high densities of *Wolbachia* lead to a high concentration of the unknown effector molecule and result in a high penetrence of the CI phenotype in a population.

In *Ephestia kuehniella*, the Mediterranean flour moth, two different naturally-occurring strains of *Wolbachia* have been described (Sasaki and Ishikawa, 1999). *w*KueYo, found in *E. kuehniella* Yokohama, is a strong CI inducer, while *w*KueTS, found in *E. kuehniella* Tsuchiura, is a relatively weaker inducer of CI. A strong positive correlation was found to exist between the *Wolbachia* density in the testes of these moths and the strength of CI (Ikeda et al., 2003). Interestingly, when *E. kuehniella* was artificially trans-infected with the *Wolbachia* from *Cadra cautella* (the almond moth), the opposite effect was observed; *E. kuehniella* containing *w*CauB has a high *Wolbachia* density and a

lower CI level than either of the naturally occurring *E. kuehniella/w*Kue systems (Ikeda et al., 2003).

In two planthopper species, *Laodelphax striatellus* and *Sogatella furcifera*, *Wolbachia* density is strongly correlated with high and low CI, respectively. In *L. striatellus*, *Wolbachia* density remains high as long as 15 days into adulthood and CI levels also remain at nearly 100% throughout aging. In *S. furcifera*, *Wolbachia* density steadily declines between adults 1– 15 days old, and CI levels drop in relative proportion to the bacterial load (Noda et al., 2001).

In *D. melanogaster,* wMelPop, the virulent, over-replicating strain of *Wolbachia*, does not cause CI but causes early mortality due to massive replication in the brain, nervous tissues, and muscles (Min and Benzer, 1997). When *w*MelPop was transferred into *D. simulans*, the new population displayed complete CI but kept the 50% reduction in lifespan. One of the main differences in the CI trophism of *w*MelPop in the two different hosts was the localization of the bacteria to the developing sperm bundles in *D. simulans* testes while in *D. melanogaster w*MelPop is only found in the somatic cells in the testes (McGraw et al., 2001). Here, *w*MelPop density is approximately 25 fold higher than the density of naturally occurring *w*Ri in the testes of *D. simulans* (McGraw et al., 2001).

Recently it was shown that *Wolbachia* titer is correlated with the host gene *gurken* (*grk*) (Serbus et al., 2011). *Grk* mRNA forms complexes with the proteins squid and Hrb27C and normally has a role in regulating microtubule organization

in the ovaries. In *D. melanogaster* and *D. simulans*, *grk* mutants have reduced *Wolbachia* densities in oocytes, and overexpression of *grk* mRNA increases *Wolbachia* titer. This system appears to work as a feedback loop; high *Wolbachia* densities lead to translation, and inactivation, of *grk* mRNA. This process is largely independent of microtubules (Serbus et al., 2011).

*D. melanogaster w*MelCS and *D. simulans w*Cof are both mod(-) strains and display different tissue tropism; the former does not infect developing sperm while the latter does. This indicates that not all mod(-) strains of *Wolbachia* are incapable of colonizing developing sperm (McGraw et al., 2001).

It is not clear what factors are responsible for determining the density of *Wolbachia*. It has been suggested that *Wolbachia* replication follows host replication; studies in *Aedes albopictus* diapause eggs, whose cell division is halted until they are hydrated, indicate that *Wolbachia* are also not dividing. Once cell division resumes in the host eggs, *Wolbachia* resumes division as well (Ruang-areerate et al., 2004). In general, the effects of *Wolbachia* density can be inconsistent, but the resulting phenotypes depend on the host and *Wolbachia* strain.

1.4.2 *Wolbachia* density and trophism during spermatogenesis

While the underlying molecular mechanism of CI remains unknown, it is largely assumed that there is a distinct modification to sperm chromatin during spermatogenesis.

Clark and others (2003) have proposed three specific classes of spermatocyst infection with *Wolbachia.* Type I infections are described by detection of *Wolbachia* in the spermatocytes and/or the spermatids. Type II infections are characterized by the presence of *Wolbachia* only within somatic portions of the spermatocyst. Finally, type III infections do not contain any detectable *Wolbachia* within the developing cysts. They argue that, in order for the CI phenotype to manifest, type I infections must be present.

In high density strains, *Wolbachia* are present in all stages of spermatogenesis except fully mature, individualized sperm and tend to segregate in a manner similar to that of mitochondria (Dudkina and Kiseleva, 2005). During elongation of spermatids, *Wolbachia* observed under scanning electron microscopy appear to increase approximately 8-fold; this is followed by complete bacterial removal along with the cytoplasmic components in the individualization complex (Dudkina and Kiseleva, 2005).

1.4.3 The WO phage[i]

The *Wolbachia* of *D. simulans*, *w*Ri, has acquired four prophage elements that are integrated into the bacterial genome as 18 - 77kb sequences, termed WORiA, WORiB (two identical copies) and WORiC (Klasson et al., 2009). In contrast *w*Mel, found in *Drosophila melanogaster*, has one WO-A, one WO-B and a small pyocin-like element. All of these prophage elements are integrated into the *Wolbachia c*hromosome at unique sites. Masui *et al* (2000) were the first to demonstrate the existence of the prophage WO in *Wolbachia* of the cricket

Teleogryllus taiwanemma and later in *D. simulans* (*w*Cof, *w*Ri), the moths *Ephestia kuehniella* (*w*CauB, *w*CauA, *w*Kue, *w*Sca) and *Corcyra cepharonica* (*w*Cep) (Masui *et al*., 2001) using electron microscopy and PCR. The WO prophages from *Wolbachia* infecting *D. simulans, D. melanogaster, C. pipiens, T. taiwanemma, Nasonia vitripennis* and *E. kuehniella* have been sequenced (Fujii et al., 2004; Klasson et al., 2009, 2008; Masui et al., 2001; Salzberg et al., 2009; Tanaka et al., 2009). WO phage genome sequences from *w*Ri, *w*Mel, and *w*Pip are inferred from their respective bacterial chromosome genome sequencing projects. WOcauB2 and WOcauB3 are two strains of WO phages infecting *Wolbachia* of *E. kuehniella* that have been sequenced from the lytic phase (Tanaka et al., 2009). With respect to WO phages, little is known about their gene expression, lytic activity, or influence on the phenotypic properties of their hosts. Bacteriophages are believed to be the mobile genetic elements responsible for the high level of genetic diversity in *Wolbachia* (Bordenstein and Wernegreen, 2004; Ishmael et al., 2009; Wu et al., 2004) through lateral transfer between co-infecting strains.

Bacteriophages can influence the level of virulence of bacterial pathogens (Canchaya et al., 2003) and can change the phenotypic properties of closely related strains of bacteria. In *Wolbachia*-infected *Drosophila*, *Culex, Nasonia* and other insects, WO prophages appear to be temperate, that is, they have an integrated prophage form and can also generate virions which result in bacterial lysis. When temperate bacteriophages infect sensitive bacteria their viral genomes direct DNA replication of the phage, cell lysis and the release of progeny, or, if the lytic state is suppressed, they integrate into the bacterial

chromosome in the form of a prophage, in what is known as the lysogenic state. In *Escherichia coli*, lambdoid prophages are stably integrated into the host chromosome and do not undergo lytic induction until the bacterial SOS response is activated (Little and Michalowski, 2010).

Typically, mature WO phage particles are detected using primers specific to the open reading frame encoding a putative minor capsid protein C (ORF7) (Masui et al., 2001). In *w*Ri of *D. simulans*, however, ORF7 is present in all four prophage insertions [WRi_005560], [WRi_007170], [WRi_010220], and [WRi_012630] and so the presence of ORF7 is not a specific indicator of which phage is active.

1.4.4 WO Phage nomenclature

The nomenclature surrounding the WO phages from different *Wolbachia* strains varies. Originally, the phage found in *w*Kue was tentatively named WO (Masui et al., 2001), irrespective of how many types of integrated prophages were present. When *w*Mel was sequenced (Wu et al., 2004), the two prophage inserts were named WO-A and WO-B respective to the origin of replication. Two phage types in *w*Ri, WO-A and WO-B, were named based on sequence homology to the wMel phages, with the addition of one more phage type, WO-C (Klasson et al., 2009). WOPip is present as five integrated copies in the *Wolbachia* of *C. pipiens* and these are designated WOPip1 through 5. They have been reported to be more closely related to WO-B of *w*Mel than WO-A of *w*Mel (Klasson et al., 2008).

1.4.5 The phage density model

In the parasitoid wasp, *N. vitripennis*, Bordenstein *et al* (2006) used a quantitative PCR assay to demonstrate that *Wolbachia* titer, which correlates with CI intensity, is inversely related to copy number of temperate WOVitA. This relationship, known as the Phage Density Model, predicts that low CI strains of *Wolbachia* will have a high number of phage particles, and, conversely, high CI strains of *Wolbachia* will have low titers of phage particles (Bordenstein et al., 2006; Kent and Bordenstein, 2011). In *D. simulans*, however, it is not known which of the diverse prophage elements give rise to lytic viruses, how their lytic properties are regulated, or the effect of lysis on host phenotype. Although most tailed bacteriophages have evolved a temperate lifestyle, it is not yet known if the prophage elements in *w*Ri are functional, defective, satellite phages, or agents of gene transfer (Casjens, 2003).

During periods of stress, lysogenic bacteriophages will often replicate and lyse their hosts through induction of the bacterial SOS response. In *Escherichia coli* infected with Lambda (λ) phage components of the SOS response will inactivate the phage CI repressor and this leads to induction of viral replication and lysis of the host cell. It is not currently known if *Wolbachia* contains a functional SOS response and whether the WO phage lytic cycle is controlled by this. The bacterial SOS response can be induced by conditions that are typically

stressful to the host. DNA damage, lack of nutrients, or sub-optimal temperatures can all induce this pathway.

1.4.4 The *Drosophila* redox system

1.4.4.1 Reactive oxygen and antioxidant enzymes

Reactive oxygen species (ROS) are damaging oxygen radicals that are produced naturally as a by-product of cellular respiration and innate immunity. They include H_2O_2, $O_2^{\cdot}$, and OH-, and are continually neutralized by antioxidants during normal cellular processes. The finely tuned relationship between ROS and antioxidants composes the cellular redox balance; this can be easily perturbed by bacterial infection or other exogenous ROS stresses the cell may encounter. Upon disruption of redox balance, cells may become susceptible to the damaging effects of ROS; this can include DNA damage and lipid peroxidation. Enzymatic antioxidants include families of glutathione peroxidase, superoxide dismutase, catalase, peroxiredoxin, and thioredoxin [reviewed in (Mathers et al., 2004)].

Previous work in our laboratory has shown that in the mosquito cell line Aa23, *Wolbachia* infection increases the amount of ROS generated and the protein expression of the host CuZn superoxide dismutase, peroxiredoxin, and glutathione peroxidase and the *Wolbachia* bacterioferritin and iron superoxide dismustase (Brennan et al., 2008).

1.4.4.2 Glutathione

Glutathione is a small tripeptide (Gly-Glu-Cys) that acts to reduce H_2O_2 to H_2O and is continually recycled within a cell between the reduced and oxidized form (GSH to GSSG) via enzymes glutathione peroxidase and glutathione reductase, respectively. In *Drosophila*, however, glutathione reductase isn't present and it is thought that thioredoxin is responsible for GSSG to GSH reduction (Cheng et al., 2007; Maiorino et al., 2007). Glutathione synthesis is accomplished, in part, by the enzyme glutamate-cysteine ligase (Biterova and Barycki, 2009), which, when overexpressed in *D. melanogaster* extends lifespan (Orr et al., 2005). After short term exposure of *Drosophila* to paraquat, a ROS inducer, glutathione supplementation can increase survivorship significantly (Bonilla et al., 2006).

1.4.4.3 The NADPH oxidase family

Upon bacterial infection, insects and mammals are capable of generating excess and directed ROS in a process known as an oxidative burst. During this event, a complex of proteins is recruited to the site of infection and highly concentrated bursts of ROS target the bacterial cells to eliminate them. The key protein families involved in the oxidative burst are NADPH (nicotinamide adenine dinucleotide phosphate) oxidase (Nox) and dual oxidase (Duox), for which *Drosophila* has single functional homologs (dNox, dDuox, respectively) (Ha et al., 2005)'. Humans have 7 NADPH oxidase family members, Nox1, Nox2, Nox3, Nox4, Nox5, Duox1 and Duox2 (Kawahara et al., 2007). It is currently not

known whether natural *Wolbachia* infections induce the NADPH oxidase complex or whether *Wolbachia* density can be influenced by excess ROS produced by the host.

Many Gram negative bacteria have evolved methods to cope with the oxidative burst. Generally this is accomplished by up-regulation of the available antioxidant components in the bacterial cell. Access to glutamate, one of the three amino acids that comprise glutathione, can enhance the resistance to oxidative bursts in *Neisseria meningitidis* that infect human polymorphonuclear neutrophil leucocytes. Because glutamate is a component of glutathione, this resistance is attributed to an increased pool of bioavailable components to produce glutathione (Talà et al., 2011). *Salmonella typhimurium* has a large antioxidant repertoire; periplasmic superoxide dismutase and cytoplasmic catalases and peroxidases are able to neutralize the oxidative burst generated in infected mouse macrophages (Aussel et al., 2011). *Escherichia coli* also contains two periplasmic CuZn SODs which can protect cells against external superoxide (Korshunov and Imlay, 2002). The *w*Ri genome contains Fe^{2+}SOD, and although it is expressed in infected Aa23 cells (Brennan et al., 2008), it is unknown if this plays a role in combating the excess ROS found within infected host cells.

1.4.4.4 Dual oxidase

The gene for *Drosophila* dual oxidase (*dDuox*) [CG3131 and GD22800 for *D. melanogaster* and *D. simulans*, respectively] is located on chromosome 2L and is expressed most abundantly in the ovaries of young females (Graveley et al.,

2011) . dDuox is composed of 1536 amino acids and contains 3 EF hand domains (which bind calcium ions), 9 trans-membrane domains, and a NAD/FAD binding domain. Duox generates hydrogen peroxide by the transfer of electrons from NAD(P)H to molecular oxygen (Ameziane-El-Hassani et al., 2005).

In *D. melanogaster,* Duox is most well known for its role in gut immunity (Ha et al., 2005). Duox-RNAi flies are short lived when fed live yeast (opposed to heat-killed yeast that is normally included in fly food) and the process appears to be regulated by the Gαq-PLCβ-$Ca2^{+}$ signaling pathway (Ha et al., 2009a). Duox-produced H_2O_2 is also a important signaling molecule in *Drosophila* embryos; H_2O_2 contributes to the inflammation response and wound healing (Moreira et al., 2010). The activation of Duox, in response to wound healing, is initiated by an instantaneous calcium flash (Razzell et al., 2013).

In humans, Duox is regulated, in part, by the dual oxidase maturation factors DuoxA1 and Duox A2. These co-factors enable Duox1 and Duox 2, respectively, to translocate to the plasma membrane after post-translational modifications in the Golgi (Hoste et al., 2012; Morand et al., 2009). It is not known if these factors and mechanisms are present in *Drosophila.*

1.4.4.5 NADPH oxidase

Drosophila NADPH oxidase (*dNox*; CG34399) is an ortholog of human *Nox5* (Ritsick et al., 2007) and spans a 6.6kb region on chromosome 2R. Similar to Duox, Nox proteins have several trans-membrane domains however, human Nox5 differs from the other Nox family members by containing 3 intracellular N-

terminal calcium EF hand motifs. In humans, Nox5 proteins are found in spermatocytes, spleen and lymph nodes and generate superoxide in the presence of Ca^{2+} through a calmodulin binding site (Bánfi et al., 2004, 2001b; Tirone and Cox, 2007),(Tirone and Cox, 2007). In *Anopheles gambiae* infected with *Plasmodium berghei,* Nox5 contributes to plasmodial immunity (Oliveira et al., 2012). To date, only one record of Nox5 in *Drosophila* exists; Nox5 contributes to smooth muscle contraction and, therefore, Nox5 mutant females cannot correctly oviposit (Ritsick et al., 2007). The contribution of Nox5 to spermatogenesis in *Drosophila* has not yet been examined.

1.4.4.6 NADPH oxidase family inhibitors

Unfortunately, the chemistry and targets of the commonly used NADPH oxidase inhibitors apocynin, DPI, and VAS2870 are not well understood (Gatto et al., 2013a; Wind et al., 2010; Wingler et al., 2012). The difficulty arises from the functional plasticity and redundancy of the different enzymes and the fact that, in humans, Nox 1 - 4 primarily produces superoxide while Nox5 and Duox 1 and 2 produce H_2O_2. Due to the generally more dangerous nature of superoxide, the enzyme superoxide dismutase quickly can convert superoxide into hydrogen peroxide.

VAS2870 (3-benzyl-7-(benzoxazolyl)thio-1,2,3-triazolo[4,5-d]pyrimidine) is a relatively novel NADPH oxidase inhibitor that inhibits Duox-produced H_2O_2 (Niethammer et al., 2009). Unlike other NADPH oxidase inhibitors, VAS2870 does not block the assembly of the NADPH oxidase subunits (Gatto et al., 2013b),

does not have any antioxidant properties (Wind et al., 2010), and does not inhibit xanthine oxidase or eNOS (endothelial nitric oxide synthase, in humans)(other radical-producing enzymes) (Wind et al., 2010). VAS2870 also potently blocks ROS generation by Nox2 in human neutrophils in a PKCβII-independent manner (Gatto et al., 2013b).

Apocynin (4-hydroxy-3-methoxyacetophenone) acts to inhibit translocation of the catalytic subunits that comprise Nox enzymes to the membrane of phagocytic and non-phagocytic cells in humans [reviewed in (Stefanska and Pawliczak, 2008)]. Apocynin has been criticized as a non-specific NADPH oxidase inhibitor recently because it has been shown to have weak antioxidant properties and may only inhibit NADPH oxidase in the present of myeloperoxidase, which is primarily found in human leukocytes (Castor et al., 2010; Heumüller et al., 2008; Petrônio et al., 2013).

Diphenylene iodonium (DPI) was one of the first NADPH oxidase inhibitors used to inhibit NADPH oxidase derived ROS; DPI, however, also blocks xanthine oxidase and is considered a general flavoprotein inhibitor (Wind et al., 2010). DPI specifically blocks the activity of Nox5 in human spermatozoa (Musset et al., 2012).

1.5 Thesis objectives

While it is clear that *Wolbachia* trophism and density in developing sperm play a role in CI modifications, the factors that modulate localization and

replication of *w*Ri are largely unknown. The aim of this work was to investigate two separate factors that could possibly regulate *w*Ri density, specifically in males:

A. The phage density model (Bordenstein et al., 2006) predicts that *Wolbachia* density is controlled, largely in part, by the lytic activity of the temperate phage WO and that a negative correlation exists between phage replication and CI levels. This relationship has only been shown in the parasitoid wasp *N. vitripennis*. The objective of this study was to examine the role of the WO phages of *w*Ri in the control of bacterial replication in DSR. I hypothesized that: 1) Out of the 4 prophages present in the *w*Ri genome, measurements of extra-chromosomal gene copy will determine which of the prophages was capable of extra-chromosomal replication, and; 2) the replication of the phage, when compared to measurements of *Wolbachia* density, will display a negative correlation.

B. *Wolbachia*-infected *D. simulans* Riverside experiences higher levels of ROS production, a more robust antioxidant response, and added DNA damage when compared to uninfected flies (Brennan et al., 2012). The source of ROS or how this affects *w*Ri density in this system is not currently known. I hypothesized that: 1) *w*Ri density is, at least in part, modulated by a redox mechanism that controls bacterial numbers based on the amount of ROS present in the system, and; 2) This ROS is generated by the host proteins dNox and/or dDuox.

2. *Materials and Methods*

2.1 Fly stocks and maintenance

Drosophila simulans Riverside (DSR), containing the *Wolbachia* strain *w*Ri, was maintained in the laboratory alongside a parallel *Wolbachia*-cured line DSRT (treated). The DSR line was originally obtained from the University of Bangor, in Bangor, UK. Flies were housed at room temperature in 8 ounce media bottles with Styrofoam plugs. One liter of fly media contained 34g sucrose, 42g cornmeal, 4.5g agar, and 12-15g yeast extract in tap water. Flies were placed on new media every 3 to 4 weeks. *Wolbachia* infection was routinely confirmed by PCR using primers specific to the *Wolbachia* surface protein gene *wsp* (Zhou et al., 1998). Flies were aged by removing all adults in the bottles and collecting newly eclosed adults 0 to 5 days later.

2.2 DNA extractions and determination of DNA concentration and purity

DNA from DSR and DSRT was generally extracted using one of two methods. For larger groups of flies (5 -15 individuals), genomic DNA was extracted using the DNeasy Blood and Tissue Kit (Qiagen # 69506) according to the manufacturer's instructions for animal tissues. The insect homogenate was incubated in Proteinase K at 56°C overnight, instead of 1 hour as the protocol recommended.

For smaller groups of flies (1 – 5 individuals), genomic DNA was extracted using an ethanol precipitation procedure. Flies were homogenized in 1.5ml centrifuge tubes containing 50µl of lysis buffer (50mM Tris, 5mM EDTA, 100mM NaCl, 1% SDS, pH 8.0) using sterile plastic pestles and a mechanical homogenizer. 150µl of lysis buffer was added to the homogenate and the samples were incubated overnight in 20 mg/ml Proteinase K at 56°C. After incubation, samples were centrifuged at 500g for 2 minutes to pellet the large debris. The supernatant was collected, and to this, $1/8^{th}$ volume of 8M ammonium acetate was added. Following this, 2 volumes of absolute ethanol were added to the samples and samples were held at either -20°C or 4°C for 1 hour or overnight, respectively. Following the incubation, samples were spun at 14 000g for 30 minutes to pellet the precipitated DNA. The supernatant was removed and the white pellet was washed with 500µl 70% ethanol, then spun at 14 000g for another 10 minutes. Following centrifugation, the supernatant was completely removed and discarded and the tubes were left open on the bench for the pellets to dry for 5 minutes. Pellets were resuspended in 100 – 200µl of TE buffer (10mM Tris, 1mM EDTA, pH 8.0).

DNA concentration and purity was measured using the Nanodrop ND 1000 (Thermo Scientific). Absorption was measured at 240, 260, and 280nm and the ratios between 260/240 and 260/280 were calculated. Both ratios were deemed acceptable if they were 2.0 ± 0.4.

2.3 Protein extractions from whole flies

Protein was extracted from DSR and DSRT using the Bio Rad Ready Prep Protein Extraction Kit (Soluble/Insoluble) (# 163-2085) following the manufacturer's protocol. Approximately 50 flies were homogenized in a dounce homogenizer using the "A" type pestle in 1 ml of lysis buffer (included in kit) on ice. Samples were transferred to 2ml microfuge tubes and the suspension was sonicated for 4-5 x 30 second bursts, chilling on ice in between bursts. The samples were centrifuged at 14 000g for 25 minutes at 4°C. The supernatant was collected and transferred to a new tube. Another 1 ml of lysis buffer was added to the remaining pellet and this was sonicated 2 x 30 seconds then re-centrifuged for 25 minutes at 4°C. The supernatant from the second extraction was pooled with the supernatant from the first and this comprised the soluble fraction of the extraction.

The insoluble fraction (the remaining pellet) was re-suspended in 0.5ml of rehydration/sample buffer (included in kit) containing 10µl of TBP (tributylphosphine) reducing agent. The sample was vortexed until the pellet was completely solubilized. The tubes were then centrifuged at 14 000g for 15 minutes at room temperature to pellet cellular debris and the resulting supernatant was collected and transferred to a clean centrifuge tube. This supernatant comprised the insoluble fraction of the extraction.

2.4 Sequence acquisition and alignments

Nucleotide and protein sequences were retrieved from the National Center for Biotechnology Information [http://www.ncbi.nlm.nih.gov]. Because the *D. simulans* genome is not yet fully annotated, *D. melanogaster* sequences were generally used for comparisons. Sequences were aligned using ClustalW2, a general purpose multiple sequence alignment program [http://www.ebi.ac.uk/Tools/msa/clustalw2/] using the recommended settings.

Specific protein domains were estimated using InterProScan Sequence Search [http://www.ebi.ac.uk/Tools/pfa/iprscan/].

2.5 General polymerase chain reaction protocol

Unless otherwise stated, PCR reactions were performed using a standardized procedure. In a 25µl reaction volume, each PCR reaction contained 1.25 units (0.25µl) of *Taq* DNA polymerase (Qiagen # 20120), 1X PCR Buffer (2.5µl; Qiagen, included with *Taq*), 50nM each (0.5µl total) of dCTP, dGTP, dTTP, and dATP (Invitrogen dNTP mix, PCR grade; #18427-013), 0.4µM (0.5µl each) of each forward and reverse primer, and double distilled water to volume the reaction up to 25µl. PCR reactions were run in the MJ Mini Personal Thermocycler (Bio Rad Laboratories) and the thermal profile was as follows: a 5 minute 95°C denaturation step to begin the reaction, 35 cycles consisting of 95°C – 30 seconds, 55°C – 30 seconds, and 72°C – 30 seconds, and a 5 minute 72°C extension to complete the program. A variation to this set program occurred when amplicon sizes were exceptionally large, in which case, the 30 second extension step was increased up to 2 minutes. Primers were designed to have melting

temperatures as close to 60°C as possible and this enabled a 55°C annealing temperature for the majority of reactions.

2.5.1 Agarose gel electrophoresis of PCR products

Agarose gels were cast using 1.5% *w/v* Ultra Pure™ Agarose (Invitrogen #15510-027) in 0.5x TBE (5x TBE containing 54g Tris, 27.5g boric acid, 20ml of 0.5M EDTA pH 8.0 in 1L of ddH_2O). The solution was heated until boiling in a standard microwave and 5µl of 10mg/ml ethidium bromide (Sigma Aldrich # E7637) was added. The solution was allowed to cool in the fume hood until it ceased steaming and was then cast into the agarose gel electrophoresis apparatus. Once cooled and solidified, the gel was submerged in 0.5x TBE and 15µl of PCR samples were electrophoresed at 100V for approximately one hour. Bands were visualized on a UV light box and photographed.

2.6 Primer design and quantitative PCR primer validation

Sequences for specific genes were retrieved from the National Center for Biotechnology Information [http://www.ncbi.nlm.nih.gov/]. *Drosophila* sequences were obtained from whole genome shotgun and clone-based data and annotated by the FlyBase Consortium [http://www.flybase.org] (Refseq NZ_AABU00000000.1).

Gene sequences were scanned for appropriate primer locations using PerlPrimer [perlprimer.sourceforge.net]. The parameters set for primer design

were as follows: primer Tm between 58-62°C, amplicon size between 75-100 base pairs, and primer length of 20-24 nucleotides. Primer pairs that met these parameters were compared and a single pair was chosen generally on the basis of the dimer ΔG, or how likely they were to pair up with each other.

To validate the efficiency of each primer set, standard curves were constructed using genomic DNA from DSR, DSRT, or a combination of both. DNA was diluted to 50ng/µl, 5ng/ µl, 0.5ng/µl, 0.05ng/µl, 0.005ng/µl, and 0.0005ng/µl. Quantitative PCR was used to measure the cycle thresholds (CTs) of the primer during 40 cycles for each dilution. The CT vs. concentration of DNA was plotted and the slope of the line was calculated. The efficiency, or, in other words, how close to an exact doubling of DNA every cycle occurred, of each primer set was determined by the equation:

$$E = 10^{(-1/slope)}$$

Primers that exhibited efficiencies that ranged between 90-110% were deemed suitable for future analyses. Primer sequences are displayed in Table 1.

Table 1 – Primers used in this study

Target Gene	Species	Sequence 5'-3'
CuZnSOD	*D. melanogaster*	F – GTC GAC GAG AAT CGT CAC CT
		R – GGA GTC GGT GAT GTT GAC CT
ATPase	*D. melanogaster*	F – AAC CAC AAT TGG AGC CAT TC
		R – GAC GAG GCC AAA GTT CAA AG
WSP	*w*Alb (*Aedes albopictus*)	F – AAC ATT TGC TCC AAC AAC TG
		R – TAG GCA TAT CTT CAA TCG CT
WSP	*w*Ri (*D. simulans*)	F – ATC AGG GTT GAT GTT GAA GG
		R – CAG TAT CTG GGT TAA ATG CTG

FtsZ	*w*Ri (*D. simulans*)	F – TGT CTA TTG ATC TTA GTC TGC C
		R – GTT ATT CAC AGC ATT TCC AC
FtsZ	*w*Mel (*D. melanogaster*)	F – CAT CTA CTT CTT CAC GCA CTC
		R – TAA TTA ACA TTA CTG GTG GCG G
Lysozyme	WORiA(*w*Ri)	F – GAC TTT ATG CGA GTA TAC CGA
		R – TCT TCC GTT GAA TTT GTT CC
Adenine Methyltransferase	WORiB (*w*Ri)	F – CTT AAA TGA CCA TCA ACC ACA G
		R – GCT TCA ATC AGG GAA TTT GG
Ankyrin (*w*Ri_005629)	WO (*w*Ri)	F – AGG GAC TAA TGT TAA TGA CGA
		R – TCT ACT ATT TGT TCA TGC CCA G
Holliday Junction Resolvase	WORiB(*w*Ri)	F – TTG TTC TCT TCA CAC CAA GC
		R – GAA GAC ATT TAG GAA CTG ATG C
Terminase	WO (*w*Ri)	F – CCT TGA TGA CCT CTT ACC CA
		R – TAC ATG ATA AGT ATG ATG GCG G
Contractile Tail Tube protein	WORiC (*w*Ri)	F- GTT GAT GGT AGA GGT TAT GCA G
		R – GAA TAT CCA TAC CAC CAG CTC
ORF7 (minor capsid protein C)	WO (*w*Ri)	F – CCCACATGAGCCAATGACGTCTG
		R-CGTTCGCTCTGCAAGTAACTCCATTAAAAC

2.7 Quantitative PCR – *Wolbachia* and WO phage density

Relative copy numbers of *Wolbachia* and WO phage in *D. simulans* were obtained using the MiniOpticon System (Bio-Rad) or the Applied Biosystems 7500 Fast Real Time PCR System. The relative *Wolbachia* infection level was measured by comparing the copy number of the gene for *Wolbachia* surface protein, *wsp,* to a single copy gene in the *Drosophila* genome, CuZn superoxide dismutase (*sod*). Phage copy numbers were measured by comparing the adenine methyltransferase (*wMTase*) (WORiB*), lyzozyme* (WORiA), and *tail tube protein* (WORiC) genes to *wsp* in *w*Ri (see Table 1 for locus tags and primer sequences).

Reactions were performed in low profile 48-well white plates with flat cap strips (Bio-Rad). Ten microliter reactions included 400nM of each forward and reverse primer, 5µl of 2x Dynamite qPCR mastermix (Molecular Biology Service

Unit – University of Alberta) which included SYBR green (Molecular Probes) and Platinum Taq (Invitrogen), and 125ng of DNA. The thermal cycling conditions were 95ºC for 2 minutes, 40 cycles of 95ºC, 55ºC, and 72ºC for 30 seconds each, and a final 2 minute 72ºC extension. Fluorescent data were acquired after every 72ºC extension. A 60-95ºC melting curve was performed to confirm the specificity of the products. No template controls were included to account for DNA contamination. All samples were analyzed in technical and biological triplicates.

Data were analyzed by the Opticon Monitor 3 software (Bio-Rad) which uses the ΔCT method. The average copy number of integrated phage was compared to the expected number based on published sequence data and the difference was statistically analyzed with a two-tailed t-test. The correlation tests between the three WO phages and *w*Ri were performed using the Pearson Product Moment Correlation test. When determining the relative copy number for each of the phage types, it was assumed that integrated prophage sequences would amplify with the same efficiency as sequences from mature virus particles.

2.8 Isolation of *Wolbachia* from overnight *Drosophila* embryos

Several hundred adults were placed on yeast-coated egg laying dishes, containing 2.2% agar in fruit juice, overnight. The next morning, the embryos were collected with a fine paintbrush and washed briefly in sterile 0.7% NaCl with 1% Triton X-100 in a fine mesh basket. The embryos were soaked in a 50% bleach solution for 2-3 minutes, or until the white chorion was visibly shed.

Following dechorionation, embryos were rinsed 2 x 5 minutes in sterile H_2O and then transferred to 1ml of sterile PBS in a dounce homogenizer where they were crushed thoroughly.

The egg homogenate was transferred to a 1.5ml centrifuge tube and centrifuged at 3000 rpm for 2 minutes. The supernatant was removed and kept in a fresh tube. Subsequent supernatants were pooled in this new tube. The pellet was re-suspended in 200µl sterile PBS and centrifuged at 3000 rpm for two minutes. Again, the supernatant was removed, transferred to the pool and the pellet was discarded.

The pooled sample was centrifuged at 3000 rpm for 3 minutes, the supernatant was transferred to a new centrifuge tube, and the pellet was discarded. This was repeated 4 more times. The final supernatant was filtered through a 5µm syringe filter into a fresh 1.5ml centrifuge tube. This final product was centrifuged at 13 000 rpm for 7 minutes and the supernatant was discarded. The pellet (containing *Wolbachia*) was re-suspended in 200µl PBS (0.01 M phosphate buffer, 0.0027 M potassium chloride, and 0.137 M sodium chloride, pH 7.4) and frozen at -80°C overnight.

DNA from the isolated *Wolbachia* cells was extracted the following day using Qiagen's DNeasy Kit and following the modifications for Gram negative bacteria.

2.9 Drosophila feeding experiments

In general, adult males and females (10-20 males and females) were placed together in medium vials containing 5 ml of either experimental or control media, (see Table 2) which contained an equal concentration of the solvent used to dissolve the treatment of interest. Control medium was prepared using a standard yeast/cornmeal recipe. One liter of fly media contained 34g sucrose, 42g cornmeal, 4.5g agar, and 12-15g yeast extract in tap water. Experimental media were prepared in the same batch as the control and, to this, the chemical of interest was added. Flies were allowed to lay eggs for 5 days and then they were removed. Newly eclosed F1 males and females were aged to 0 - 3 days and frozen at -80°C for further analysis.

Table 2 – Chemicals used in feeding experiments

Chemical Name	Description	Solubility	Concentration	Manufacturer
L – Glutathione	Antioxidant	ddH_2O	0.22mM(Bonilla et al., 2006)	Sigma Aldrich
Glycine	Amino Acid	ddH_2O	0.15 mM	Bioshop Canada Inc.
L-Cysteine	Amino Acid	ddH_2O	0.15 – 0.3 mM	Sigma Aldrich
Glutamic Acid	Amino Acid	ddH_2O	0.15 mM	Sigma Aldrich
Ascorbic Acid	Antioxidant	ddH_2O	50mM(Sem and Rhen, 2012)	Sigma Aldrich
Ferric Ammonium Citrate (FAC)	Oxidizer	ddH_2O	5mM (Kremer et al., 2009a)	Sigma Aldrich
Apocynin	NADPH Oxidase inhibitor	DMSO	10mM	Abcam

Diphenyleneio-donium Chloride (DPI)	NADPH Oxidase inhibitor	DMSO	50μM	Sigma Aldrich
VAS2870	NADPH Oxidase inhibitor	DMSO	20μM	Sigma Aldrich

2.10 *Drosophila* pupation and eclosion monitoring

DSR or DSRT males and females (10 each) were seeded into vials containing either control medium or experimental medium and allowed to lay eggs for 5 days before being removed from vials. Vials were monitored daily for the following 5 days and the number of puparia was recorded. Following pupal monitoring, vials were monitored an additional 5 days for eclosion. Newly eclosed flies were removed daily and frozen at -80°C until further testing.

2.11 *Drosophila* egg production

DSR or DSRT males and females (10 each) were seeded into vials containing either control medium or experimental medium and allowed to lay eggs for 5 days before removal. Vials were monitored daily and newly eclosed F1 females were seeded into fresh vials (containing either the control or experimental medium) and allowed to mature 6 more days. On day 6, females were cold anaesthetized and dissected in a drop of sterile PBS. The ovaries were removed and oocytes at stage 10 or older were counted.

2.12 Immunocytochemistry

The fixation of testes and ovaries was adapted from Bonaccorsi et al (2011). Testes or ovaries were carefully dissected from several 0 - 5 day old males and females in a drop of sterile TB buffer [1 mM EDTA, 183 mM KCl, 47mM NaCl, 1mM Phenylmethylsulfonyl fluoride (PMSF), 10mM Tris-HCl, pH 6.8] under the dissecting microscope and transferred to a 20 x 20 slide (Fisherbrand Superfrost Plus Microscope Slides, 1 oz.; # 12-550-15) in 2µl of TB buffer. A clean coverslip was placed over the tissue and slight pressure was applied to squash the tissues. Slides were immersed in liquid nitrogen for approximately 30 seconds and the coverslips were removed using a razor blade. The slides were immediately incubated in ice-cold methanol for 5 minutes then transferred to ice-cold acetone for 1-2 minutes. Following acetone incubation, the slides were transferred to a PATX solution (0.5% *v/v* acetic acid and 1% *v/v* Triton X-100 in PBS) for 10 minutes at room temperature.

Following fixation, slides were washed in PBS twice for 5 minutes each wash. Approximately 200µl of primary antibody was added and slides were allowed to incubate for 1-2 hours at room temperature in a humidity chamber. Rabbit Anti-Nox5 (human NADPH Oxidase 5, Assay Biotech # c16867, 1mg/ml) was used at a dilution of 1:200; guinea pig anti-dDuox was a gift from K. Kamei (Kyoto Institute of Technology, Japan) and was used at a dilution of 1:1000. The slides were washed in PBS 3 times for 5 minutes each to remove the excess primary antibody and then incubated in approximately 200µl of secondary

antibody for 1 hour at room temperature in the dark. Goat anti-rabbit IgG conjugated with Alexa Fluor® 488 (Invitrogen #A-11034, 2mg/ml) was prepared with a dilution of 1:50 and goat anti-guinea pig IgG conjugated with Alexa Fluor® 555 (Invitrogen #A-21435, 2mg/ml) was prepared at a dilution of 1:500 Following secondary antibody incubation, the slides were washed twice for 5 minutes each with PBS. The excess moisture was removed from the slides and 2 µl of Vectashield (mounting medium for fluorescence with DAPI to visualize the DNA, Vector Laboratories, Burlingame, CA, cat # H-1200) was dropped onto the tissue. Slides were visualized using a Leica DMRXA fluorescent microscope equipped with a Nikon DXM1200 digital camera. Images were processed and merged using Adobe Photoshop CS5.

2.13 DCFDA assay for total ROS

Males ≤ 5 days post eclosion were cold anesthetized and homogenized in 100µl of PBS with approximately 30 strokes of a sterile plastic pestle. 700 additional microlitres of PBS was added and the samples were centrifuged at 750g for 2 minutes to pellet the cell debris. 147µl of supernatant was removed from each tube and added to a clear 96-well plate. 3µl of 2,7-dichlorodihydrofluorescein diacetate (DCFDA) was added to bring each well to a final concentration of 10µM of DCFDA. The NADPH oxidase inhibitors DPI, VAS2870, and apocynin were added to a final concentration of 100µg/ml, 50µg/ml, and 2mM, respectively. The samples were incubated at room

temperature for 10 minutes and the fluorescent data were acquired at 485nm using a FLUOSTAR Ultima fluorescent spectrophotometer.

3. Results

3.1 *Wolbachia* heavily infect testes in DSR

A quantitative PCR approach was employed to determine the baseline density of *w*Ri in whole animals and gonads. Relative abundances of the *Wolbachia wsp* gene were compared to the single copy *D. simulans* gene *superoxide dismutase* (*sod*) (Figure 1). Young males 2 – 6 days post eclosion contain approximately 6.5 *Wolbachia* per host cell. Females have a slightly higher overall infection rate; whole young females have ~ 10.5 *Wolbachia* per cell. The abundance of *Wolbachia* in the ovaries does not differ significantly from the density in whole animals. Testes in young males, however, show a significantly higher *Wolbachia* density ($p < 0.001$) when compared to whole males and females and ovaries; approximately 35 bacteria are found per host cell.

To determine the localization of *Wolbachia* in the testes of DSR males, testes squashes were fixed and labelled with DAPI, a fluorescent probe that strongly binds A-T rich regions of DNA and can be used to identify both host genomic DNA and bacterial presence. Figure 2 displays *Wolbachia* presence in A) the stem cell precursor cells, B) primary spermatocytes and C) elongating spermatids. *Wolbachia* cells are indicated by arrows in A-C and within the dashed area in D and appear to be irregular or rod shaped.

3.2 *w*Ri contains extrachromosomal phage DNA

In order to determine which WO phage is capable of extra-chromosomal replication, bacterial lysates isolated from overnight embryos were passed through 0.22µm filters and the DNA was extracted from the filtrate. PCR was performed on the resulting DNA to look for amplification of phage genes in the absence of the bacterial chromosome. In both *D. melanogaster* (infected with *w*Mel) and DSR, amplification of *orf7* (present in WO-A, WO-B, and WO-C) occurred without amplification of *wsp* (*Wolbachia* chromosomal gene; Figure 3).

3.3 WORiC is the active phage in *w*Ri

Quantitative PCR was used to test whether *Wolbachia* prophages were replicating extrachromosomally. Specific primers that differentiate between the prophage types in *w*Ri were designed (Table 1) and *Wolbachia* titer was determined by comparing the *wsp* gene copy number to the *Drosophila* nuclear *sod* gene. Integrated and extrachromosomal viral copy numbers were determined using primers specific to *Wolbachia* genes *lysozyme* (WORiA), *MTase* (WORiB), and *tail tube protein* (WORiC). The amplification of the WO-specific primers was compared to *Wolbachia* copy number using *wsp* (*w*Ri-specific primers).Values reported are the combination of integrated plus extrachromosomal phages.

WORiA is found once in the *w*Ri genome. The relative copy number of the ORF which encodes a putative *lyzozyme* [WRi _012650] was measured in young males and females (three replicates of 15 flies each), testes and ovaries, and 15 minute AEL embryos. The relative lyzozyme (WORiA) copy number in these tissues ranged from 0.94 – 1.16 per *Wolbachia* cell (Figure 4A). This is consistent with the single integrated copy in the genome and indicates no extrachromosomal WORiA (all p values > 0.05; two-tailed t-test)

In *w*Ri, there are two integrated copies of the WORiB prophage and each contains one copy of the *MTase* gene [WRi_005640; WRi_010300] (Klasson et al., 2009). In DSR males, females, testes, ovaries, and two-hour embryos, the relative *MTase* copy number ranged from 1.83-2.10 and was not significantly different than two per *Wolbachia* genome (all p values > 0.05, two-tailed t-test) (Figure 4B). There is no evidence of extrachromosomal WORiB phage genomes.

The gene encoding the phage tail tube protein is present once in the *w*Ri genome on the WORiC insert. In males, females, testes, ovaries, and 15 minute after egg laying (AEL) embryos, the relative tail tube protein copy number was significantly greater than the expected one copy per *Wolbachia* genome ($p < 0.05$ in all cases, two- tailed t-test; Figure 4C). Therefore, WORiC is the extrachromosomal phage in *w*Ri. The average density of all samples tested ranged from 1.29 – 1.61 copies of WORiC per *wsp* copy.

3.4 WORiC replication does not correlate with *Wolbachia* density

Occasionally, a DNA sample showed no evidence of extra-chromosomal WORiC DNA (data not shown). This indicates that DNA extracted from groups of flies may mask variation with respect to the amount of replicating phage per individual. Thus, third instar larvae were synchronized to a 1 hour age difference and *w*Ri, WORiA, WORiB, and WORiC numbers were measured for each individual to determine whether the WO copy number varied between individuals (Figure 5). Relative phage densities were also compared to *Wolbachia* densities to determine whether variations in phage copy numbers were related to the bacterial density as observed by Bordenstein *et al* (Bordenstein et al., 2006) in *N. vitripennis*. Among 16 third instar larvae tested, the *Wolbachia* densities ranged from 6.67 to 19.21 copies per host *sod* gene, with the exception of one outlier at 34.88. WORiA relative numbers averaged 0.97 and varied from 0.86 to 1.13 copies per *Wolbachia* (Figure 5A). WORiB densities for the larvae averaged 2.02 copies per *w*Ri and ranged between 1.56 and 2.78 (Figure 5B). Finally, WORiC copy numbers averaged 1.17 and ranged between 0.91 and 1.50 per *wsp* (Figure 5C). None of the densities of the three phage types correlated significantly with the *Wolbachia* density (Pearson correlation; $p = 0.256$, 0.12, and 0.16 for WORiA, WORiB, and WORiC, respectively) among the 16 samples tested. Removing the outlier individual (34.88 *Wolbachia* per host cell) from the analyses did not change the statistical outcome of the correlation test in WORiC (Pearson correlation; $p > 0.7$)

3.5 *Wolbachia*-infected males contain higher amounts of cellular ROS

Total ROS in DSR and DSRT was measured in a 96 well assay using the fluorescent probe 2'-7'-dichlorodihydrofluorescein diacetate (DCFDA), which fluoresces upon interaction with ROS. A total of three independent biological replicates were tested in triplicate and each well contained the homogenate from 10 flies in a solution containing 10μM DCFDA. Figure 6 depicts the relative difference in DSR DCFDA fluorescence when compared to DSRT. DSR had a 1.39 fold increase in total ROS when compared to DSRT.

3.6 Glutathione increases *Wolbachia* density in DSR

Previously it was reported that *Wolbachia* infection leads to a high amount of oxidative stress in DSR flies and a mosquito cell line (Aa23) when compared to their uninfected counterparts (Brennan et al., 2012, 2008). Glutathione was added to the diet of DSR in an attempt to lower the amount of general ROS that these flies were experiencing. Adults were placed on a yeast/cornmeal medium with or without 0.22mM glutathione (Bonilla et al., 2006) added and allowed to lay eggs for several days at which point they were removed. The resulting F1 flies were collected <5 days post eclosion and analyzed by quantitative PCR for *Wolbachia* copy number. When raised on medium containing glutathione, both males and females had a significant increase in *Wolbachia* density when compared to flies fed the standard yeast/cornmeal diet (Kruskal-Wallis Test $p < 0.001$; Figure 7). Males fed glutathione had a 2.11-fold increase (17.4 ± 0.4 vs. 6.6 ± 0.6) in

Wolbachia over males fed a standard diet. Females fed glutathione had a 2.14-fold increase in *Wolbachia* density (26.8 ± 0.8 vs. 10.5 ± 2.1) when compared to the flies fed the control diet.

3.7 Increased *w*Ri density from glutathione is not a factor of increased fly fitness

To determine if the increase in *Wolbachia* density could be attributed to an increase in host fitness when fed glutathione, several measurements of fitness were taken and compared between glutathione-fed and control flies. The timing of eclosion and the number of adults eclosed was determined (Figure 8)

The difference between glutathione-fed and control in the cumulative number of flies eclosed is not significant (ANOVA; $p = 0.198$) and after day 17, the pupae had all eclosed. Each vial ($n = 3$) yielded approximately 40 adults.

F1 females that were removed from the treatment and control vials during eclosion monitoring were transferred to new vials which had the same medium components and allowed to reach 6 days of age. 6 day old females were dissected and the number of stage 11 or older eggs present was counted (Figure 9). DSR females raised on a control diet contained an average of 8.3 ± 1.8 stage 10 eggs ($n = 10$) while DSR flies fed glutathione had 7.7 ± 2.9 eggs ($n = 24$). These differences were not significantly different (ANOVA $p = 0.593$).

DSRT flies were also subjected to the feeding treatments and stage 11 or greater eggs were counted (Figure 9) from 6 day post eclosion females. DSRT

females fed a control diet had 8.7 ± 3.9 eggs (n = 35). Females raised on the glutathione diet had significantly more eggs (t-test $p < 0.001$); they contained an average of 13.7 ± 4.7 eggs (n = 31).

3.8 Feeding L-glycine, L-cysteine, or glutamic acid alone do not increase *Wolbachia* density

In order to determine the singular effects of the three amino acids that comprise glutathione, flies were housed on medium containing 0.15mM of L-glycine, glutamic acid, or L-cysteine and allowed to lay eggs. After 4 days of egg laying, the adults were removed and the resulting F1 progeny were collected 0-3 days post eclosion. DNA was isolated from whole F1 flies and the relative copy number of the *Wolbachia* gene *wsp* was compared to the host gene *sod* using quantitative PCR. For each bar, n = 3 groups of 15 individuals each.

Males fed a control diet had 7.3 ± 0.3 *Wolbachia.* When diet was supplemented with amino acids there was no significant change in the relative abundance of *Wolbachia* present in the flies ($p = 0.112$; ANOVA; Figure 10A). Adding 0.15mM L-glycine resulted in 9.6 ± 1.8 *Wolbachia*, 0.15mM glutamic acid resulted in 7.1 ± 0.5 *Wolbachia*, 0.15mM L-cysteine resulted in 9.1 ± 2.6 *Wolbachia*, and 0.30mM L-cysteine resulted in 6.7 ± 0.2 *Wolbachia*.

Females fed a control diet contained 12.9 ± 1.6 *Wolbachia*. When fed 0.15mM L-glycine, 0.15mM glutamic acid, 0.15mM L-cysteine, and 0.30mM L-cysteine, females contained 8.6 ± 1.6, 12.3 ± 0.2, 12.7 ± 4.2, and 14.4 ± 3.0

Wolbachia, respectively. There was no significant differences between any of the treatment groups ($p = 0.181$; ANOVA; Figure 10B).

3.9 Effect of redox-altering dietary supplements is varied

Because glutathione had a significant effect on *Wolbachia* density, flies were subjected to other redox compounds to determine whether decreasing or increasing the total amount of ROS in the flies had a general effect on *Wolbachia* titer. Adult flies were placed on medium containing 50mM ascorbic acid (antioxidant), or 5mM ferric ammonium citrate (FAC; oxidizer via the Fenton reaction, see equation 1), allowed to lay eggs for several days, and removed. The F1 flies were taken 0-3 days post eclosion and quantitative PCR was used to determine the relative *Wolbachia* densities (Figure 7).

Figure 8 depicts the quantitative PCR results; males experienced an increase in *Wolbachia* density when fed ascorbic acid and FAC. Ascorbic acid-fed males contained 17.2 ± 0.9 *Wolbachia* per host cell and males fed FAC contained 19.3 ± 1.0 *Wolbachia* per host cell. The difference between the ascorbic acid and FAC treatments when compared to males grown on the control medium was significant (ANOVA; $p < 0.001$).

Females experienced a significant increase in *Wolbachia* density only when grown on ascorbic acid-containing medium; they contained 22.3 ± 1.2 *Wolbachia* per host cell (ANOVA; $p < 0.05$; Figure 7). Females grown on FAC

had 10.2 ± 0.2 *Wolbachia* per host cell, which is not significantly different from the *Wolbachia* density in flies fed a control diet (ANOVA; $p > 0.05$).

3.10 *w*Mel does not increase density following antioxidant treatment

Because *D. melanogaster* is a more amenable system to manipulate compared to *D. simulans* (i.e. genetic manipulations and a fully annotated genome), a test was performed to determine if glutathione feeding increased the *w*Mel density in *D. melanogaster*. *D. melanogaster* (containing *w*Mel) were seeded into vials containing either 0.22mM glutathione in standard yeast/cornmeal or a control diet lacking glutathione and allowed to lay eggs for several days. F1 flies were collected 2-5 days post eclosion and, from these flies, DNA was extracted and the relative abundance of *w*Mel was determined by qPCR using the host gene *RpoS* and the *Wolbachia* gene *FtsZ*. Flies reared on the control diet had an average of 8.8 ± 1.9 *Wolbachia* per host cell and flies reared on 0.22mM glutathione contained 7.6 ± 0.1 *Wolbachia* per host cell (Figure 11). The *Wolbachia* density between flies reared on glutathione and a standard yeast cornmeal diet is not significantly different in *D. melanogaster* ($p = 0.451$; ANOVA).

3.11 Nox5 is primarily nuclear in DSR testes

Immunofluorescence was used to determine the localization of Nox and Duox in developing sperm in DSR and DSRT. Nox can be found in the nuclei of

primary spermatocytes and elongating spermatids in both DSR and DSRT (Figure 12 and 13). There is no obvious difference in the patterns of antibody localization in primary spermatocytes between DSR and DSRT; fluorescent signals occur in the nucleus but do not appear to overlap with the DNA. In elongating spermatids, there does not appear to be difference between DSR and DSRT dNox localization, however, there is clear overlap of Nox with the host DNA. Nox does not appear to be located in proximity to *Wolbachia* in any of the cell types observed.

3.12 Dual oxidase localizes to *Wolbachia* in developing sperm cells

Anti-dDuox antiserum was used to determine localization of dDuox in DSR and DSRT testes squashes. In the apical end of the testes, where the germline stem cell population resides, there is a distinct clustering of *Wolbachia* along the peripheral edges. Duox strongly localizes to these clusters in young DSR males (Figure 14). In DSR primary spermatocytes, duox appears as concentrated points that co-localize to the *Wolbachia* present in the cell (Figure 15). In uninfected primary spermatocytes, there is a small amount of Duox in the nuclear area but no obvious punctiform staining is present (Figure 15). Duox localization is most obvious in elongating spermatids (Figure 16) where the *Wolbachia* density is the greatest.

3.13 Apocynin, DPI, and VAS2870 have varying effects on total ROS in whole flies

Whole fly homogenates were added to solutions containing 10μM DCFDA and one of the Nox/Duox inhibitors apocynin (2mM), DPI (100μg/ml), or VAS2870 (50ng/μl) to determine the relative reduction in total ROS. Figure 17 depicts the relative decrease in ROS in whole males when compared to the DMSO control (no inhibitor) in DSR and DSRT.

In DSR and DSRT, the three inhibitors tested had the same pattern of effect on the amount of ROS measured by DCFDA fluorescence; DPI had the least amount of ROS inhibition and VAS2870 had the greatest ROS inhibition. DSR homogenates treated with DPI had a 25.15% ± 0.09% reduction in ROS and DSRT had a 16.44% ± 0.12% reduction in ROS when compared to the control samples. When treated with apocynin, DSR displayed a 47.49% ± 0.03% reduction and DSRT had a 33.71% ± 0.08% reduction in total ROS when compared to the control samples. VAS2870 proved to have the greatest effect on total ROS within the homogenates (Figure 17B); DSR had a 64.75% ± 0.08% reduction in ROS and DSRT had 64.52% ± 0.05% reduction in the total ROS when compared to the control samples. All of the inhibitors tested were able to significantly decrease the amount of total ROS when compared to the control treatment (2-way ANOVA; $p < 0.001$).

3.14 Inhibition of NOX and DUOX do not change *Wolbachia* density

Flies were grown on media containing the 10mM apocynin or 20mM VAS2870 and the resulting F1 generation was analyzed by quantitative PCR for *Wolbachia* density and compared to flies grown on a control medium containing DMSO. Young males grown on the control diet had 5.1 ± 3.7 *Wolbachia* per host cell. Males raised on 20mM apocynin and 10mM VAS2870 had 5.2 ± 2.0 ($p = 0.950$) and 3.9 ± 1.3 ($p = 0.500$) *Wolbachia* per host cell, respectively (Figure 18). The differences between flies grown on the control and the treatment diets were not significant (Control vs. apocynin - ANOVA; $p = 0.950$. control vs. VAS2870 – ANOVA; $p = 0.500$).

F1 females grown on the control diet had 8.0 ± 4.7 *Wolbachia* per cell. Grown on 20mM apocynin, females had 8.0 ± 3.5 *Wolbachia.* VAS2870-treated females had 6.3 ± 0.8 *Wolbachia* per host cell (Figure 18). When the *Wolbachia* density in the control group was compared to the apocynin and VAS2870-treated flies, the differences were not significant (Control vs. apocynin - ANOVA; $p = 0.963$. Control vs. VAS2870 - Kruskal-Wallis one way ANOVA on ranks; $p = 0.352$).

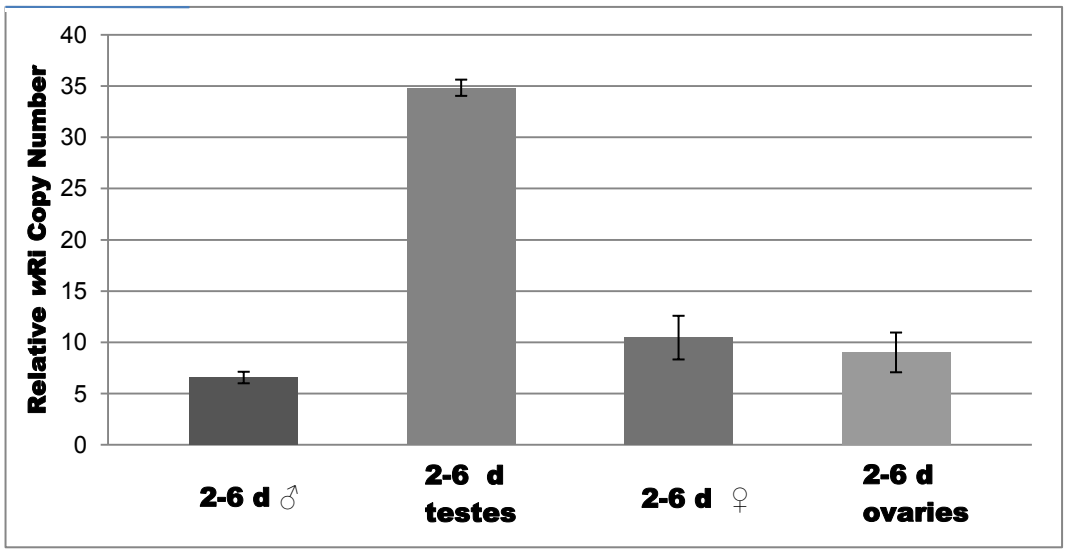
Relative wRi Copy Number
40
35
30
25
20
15
10
5
0
2-6 d ♂
2-6 d testes
2-6 d ♀
2-6 d ovaries

Figure 1 – Relative *Wolbachia* densities in 2-6 day post-eclosion males, females, testes and ovaries. Values are the relative abundance of *Wolbachia wsp* copy number compared with host *sod* measured by quantitative PCR. Error bars represent standard deviation.

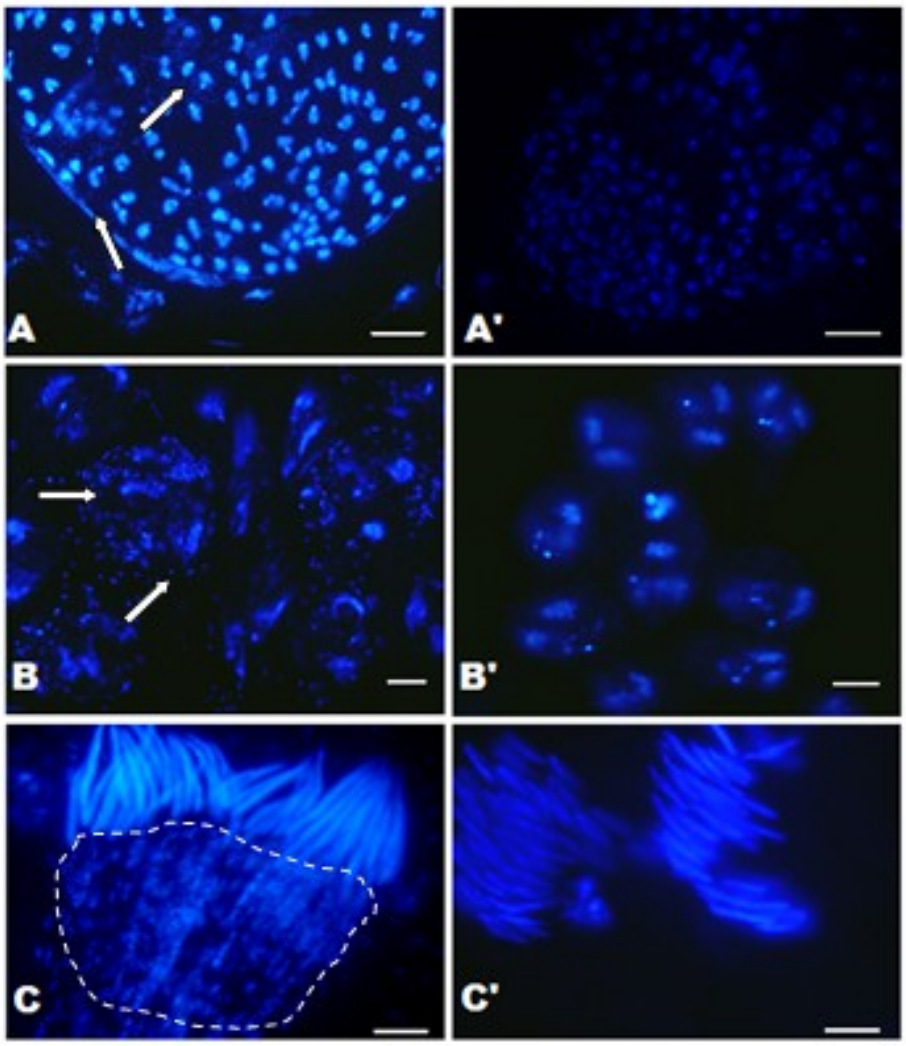
A
A'
B
B'
C
C'

Figure 2 – DAPI stained cells within young male testes. A), A') stem cell precursor cells, B), B') primary spermatocytes, C),C') elongating sperm cysts in DSR. *Wolbachia* are indicated by arrows in A and B. A', B', and C' are the equivalent cell types in DSRT. Scale bars: A, and A' = 20µm, B, B', C, and C' = 10um.

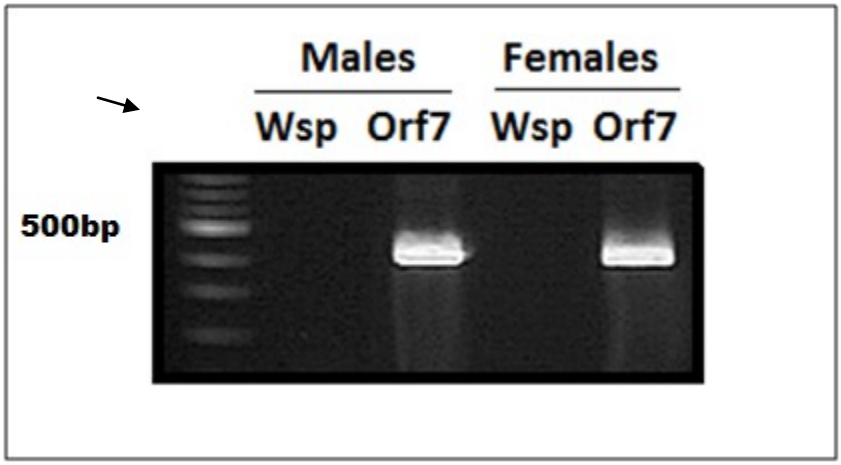
Males
Females
Wsp
Orf7
Wsp
Orf7
500bp

Figure 3 – PCR amplification of *Wolbachia*-free embryonic cytoplasmic extracts to detect the presence of mature viral particles in DSR. Isolated *Wolbachia* were passed through a 0.22μm filter and DNA from the filtrate was amplified with primers specific for the *ORF7* gene, which is found in all four copies of the WO phage, and *Wsp*, which is found in the *w*Ri genome.

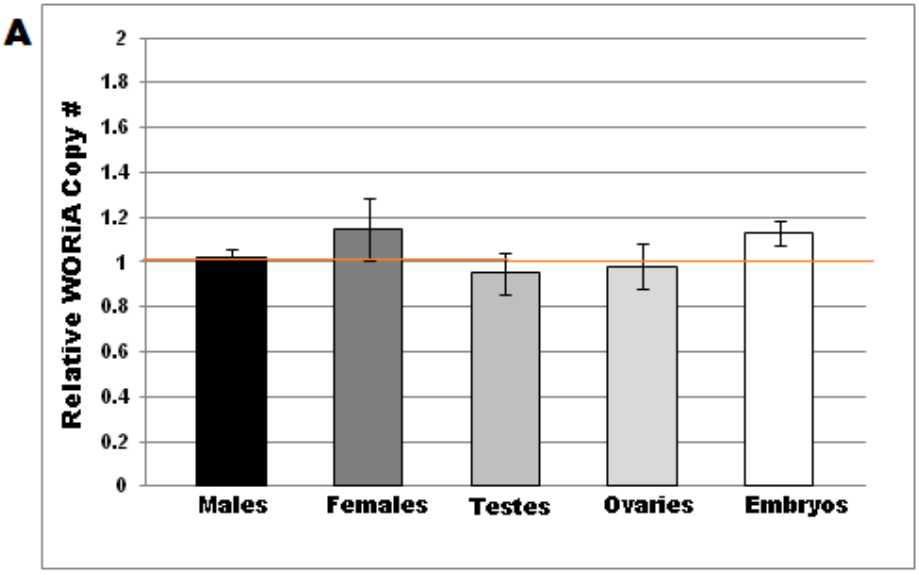
A
Relative WORiA Copy #
2
1.8
1.6
1.4
1.2
1
0.8
0.6
0.4
0.2
0
Males
Females
Testes
Ovaries
Embryos

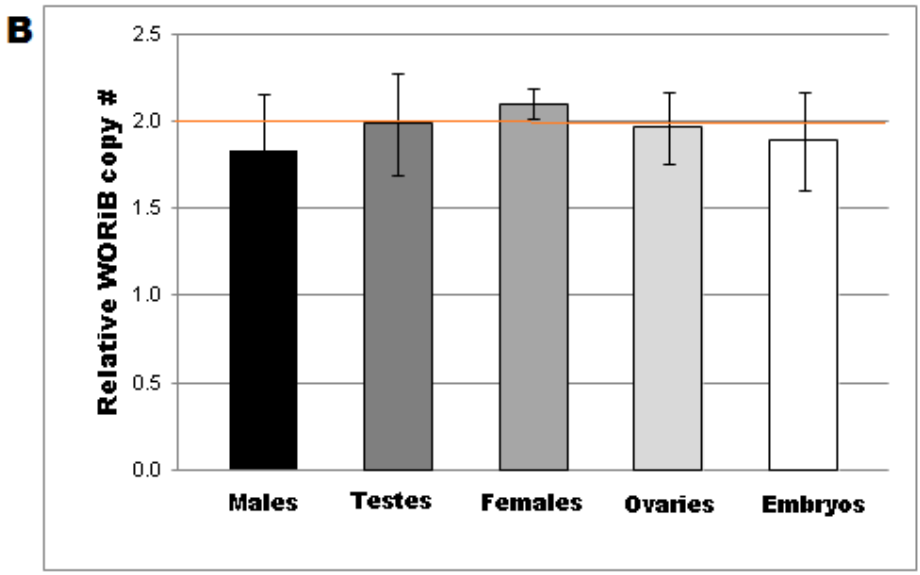
B
Relative WORiB copy #
2.5
2.0
1.5
1.0
0.5
0.0
Males
Testes
Females
Ovaries
Embryos

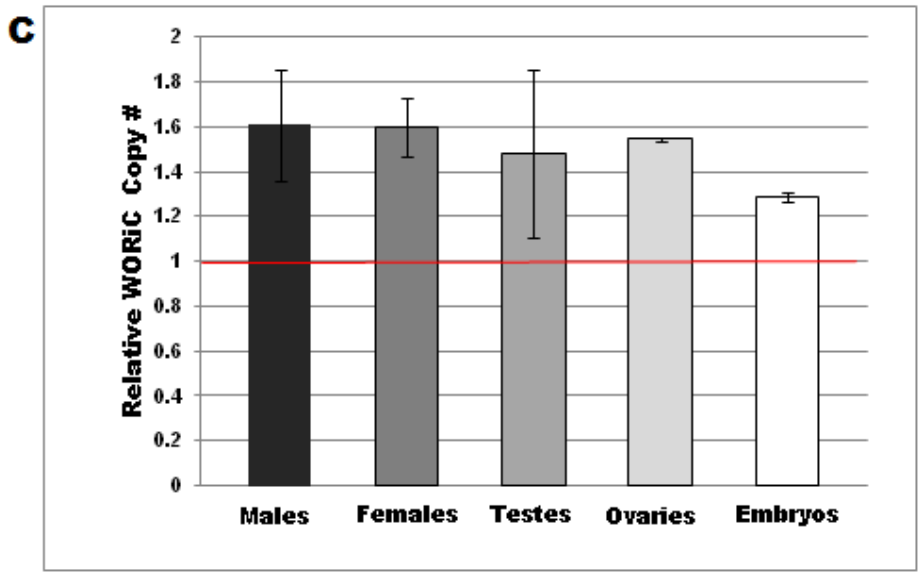
C
Relative WORiC Copy #
2
1.8
1.6
1.4
1.2
1
0.8
0.6
0.4
0.2
0
Males
Females
Testes
Ovaries
Embryos

Figure 4 – Quantitative PCR to determine the density of WORiA, WORiB, and WORiC (4A, 4B, and4C, respectively) in young males, females, testes, ovaries, and overnight embryos. The relative copy number of WORiA, WORiB, and WORiC were determined by comparing the phage *lysozyme* gene, the phage *MTase* gene, and the phage *Tail tube protein* gene, respectively, to the *Wolbachia wsp* gene. The black line indicates the expected number of phage particles present due to the integrated copy in the *w*Ri genome. Error bars represent standard deviation.

A

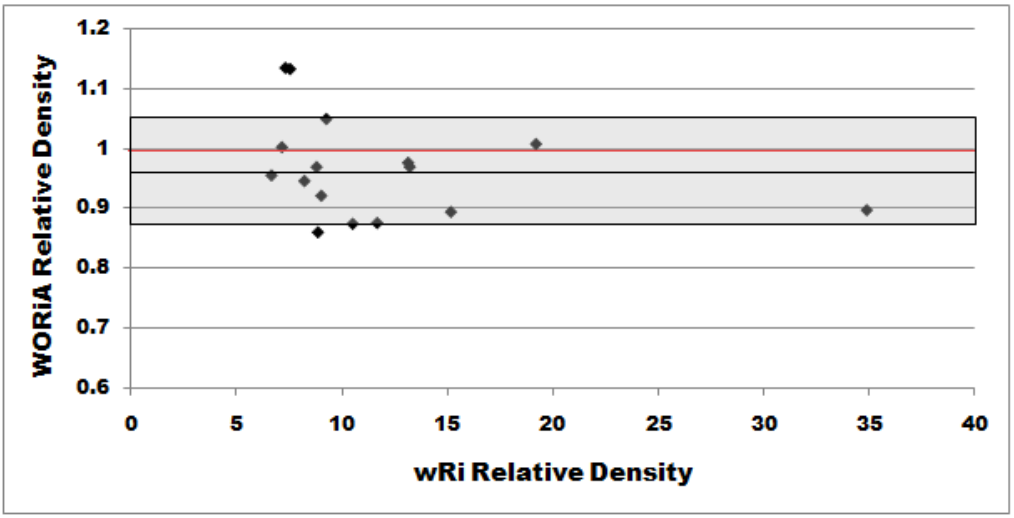
WORiA Relative Density
1.2
1.1
1
0.9
0.8
0.7
0.6
0
5
10
15
20
25
30
35
40
wRi Relative Density

B

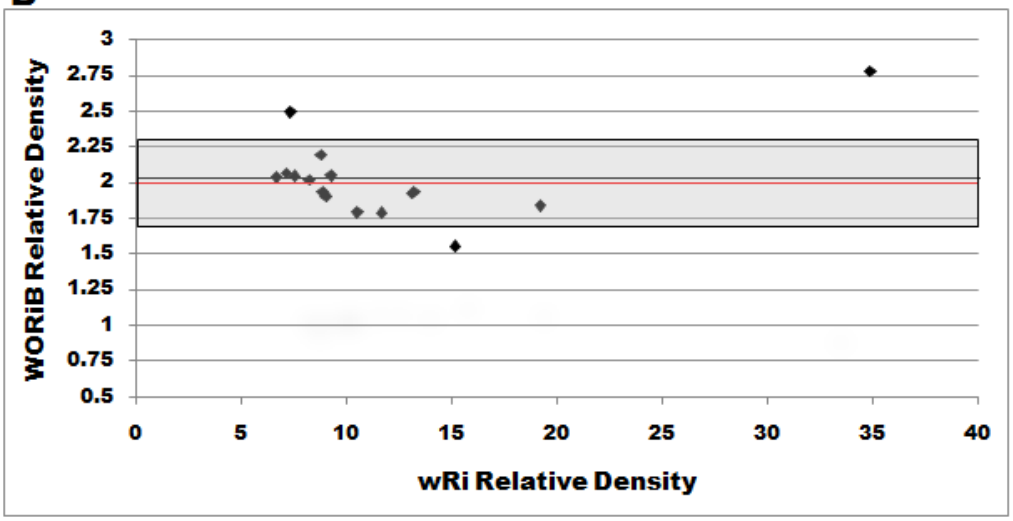
WORiB Relative Density
3
2.75
2.5
2.25
2
1.75
1.5
1.25
1
0.75
0.5
0
5
10
15
20
25
30
35
40
wRi Relative Density

C

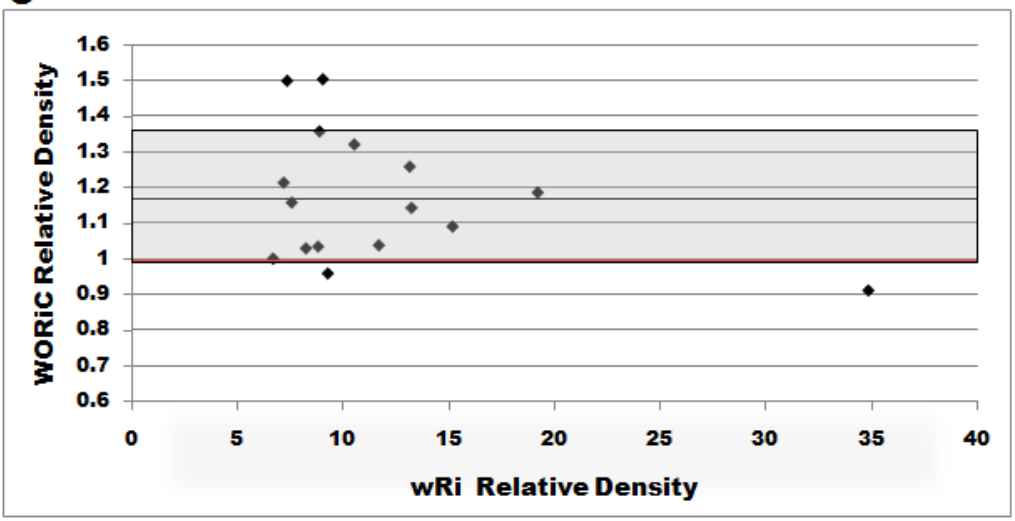
WORiC Relative Density
1.6
1.5
1.4
1.3
1.2
1.1
1
0.9
0.8
0.7
0.6
0
5
10
15
20
25
30
35
40
wRi Relative Density

Figure 5 – Quantitative PCR of DNA extracted from third instar DSR larvae. The relative copy number of WORiA (A), WORiB (B), and WORiC (C) were determined by comparing the phage *lysozyme* gene, the phage *MTase* gene, and the phage *Tail tube protein* gene, respectively, to the *Wolbachia wsp* gene. Each point represents one individual. The red line represents the number of integrated phage copies that occur in the *w*Ri genome and the shaded area represents the standard deviation of the points.

Table 3 – Genes comprising the tail morphogenesis region and the DNA packaging and head assembly region, the two necessary components for WORiC replication.

Locus Tag	Open Reading Frame	
WRi_006910	tail protein D, putative CDS	Tail Morphogenesis
WRi_006920	tail protein X, putative CDS	
WRi_006930	tail protein U, putative CDS	
WRi_006940	tail tape measure protein CDS	
WRi_006950	hypothetical protein CDS	
WRi_006960	hypothetical protein CDS	
WRi_006970	contractile tail tube protein CDS	
WRi_006980	phage tail sheath protein CDS	
WRi_006990	hypothetical protein CDS	
WRi_007000	hypothetical protein CDS	
WRi_007010	hypothetical protein CDS	
WRi_007020	VrlC.2 CDS	
WRi_07030	VrlC.1 CDS	
WRi_007040	transposase, IS5 family CDS	
WRi_07030	VrlC.1 CDS	
WRi_007060	hypothetical protein CDS	
WRi_007070	Tail protein I, putative CDS	
WRi_007080	baseplate assembly protein J, putative CDS	
WRi_007090	baseplate assembly protein W, putative CDS	
WRi_007100	hypothetical protein CDS	
WRi_007110	baseplate assembly protein V CDS	
WRi_007120	hypothetical protein CDS	
WRi_007130	minor tail protein Z, putative CDS	
WRi_007140	hypothetical protein CDS	DNA Packaging and Head Assembly
WRi_007150	hypothetical protein CDS	
WRi_007160	hypothetical protein CDS	
WRi_007170	minor capsid protein C, putative CDS	
WRi_007180	portal protein, lambda family CDS	
WRi_007190	phage uncharacterized protein CDS	
WRi_007200	hypothetical protein CDS	
WRi_007210	terminase large subunit, putative CDS	

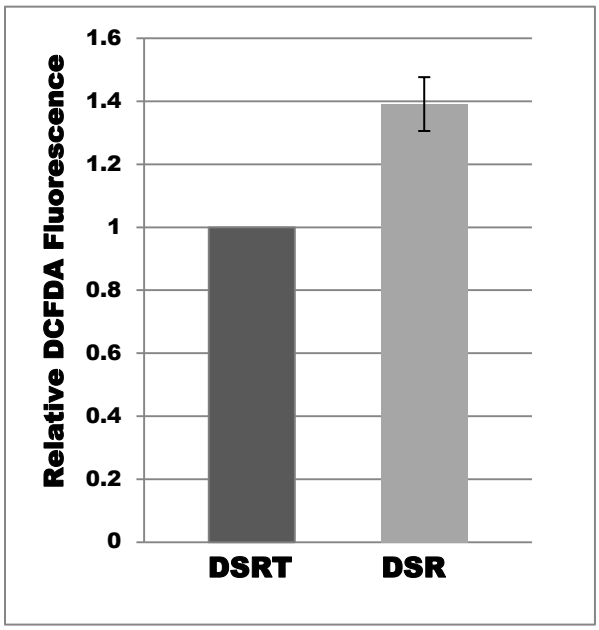
Relative DCFDA Fluorescence
1.6
1.4
1.2
1
0.8
0.6
0.4
0.2
0
DSRT
DSR

Figure 6 – DCFDA assay to determine the relative difference of total ROS between whole DSRT males when compared to whole DSR males. Total homogenate from 1 – 5 day post eclosion males was incubated with DCFDA, a fluorescent indicator of total ROS, and fluorescent data were acquired at 485nm for the next 30 minutes. Data represented here is the result of three independent experiments, with samples run in triplicate.

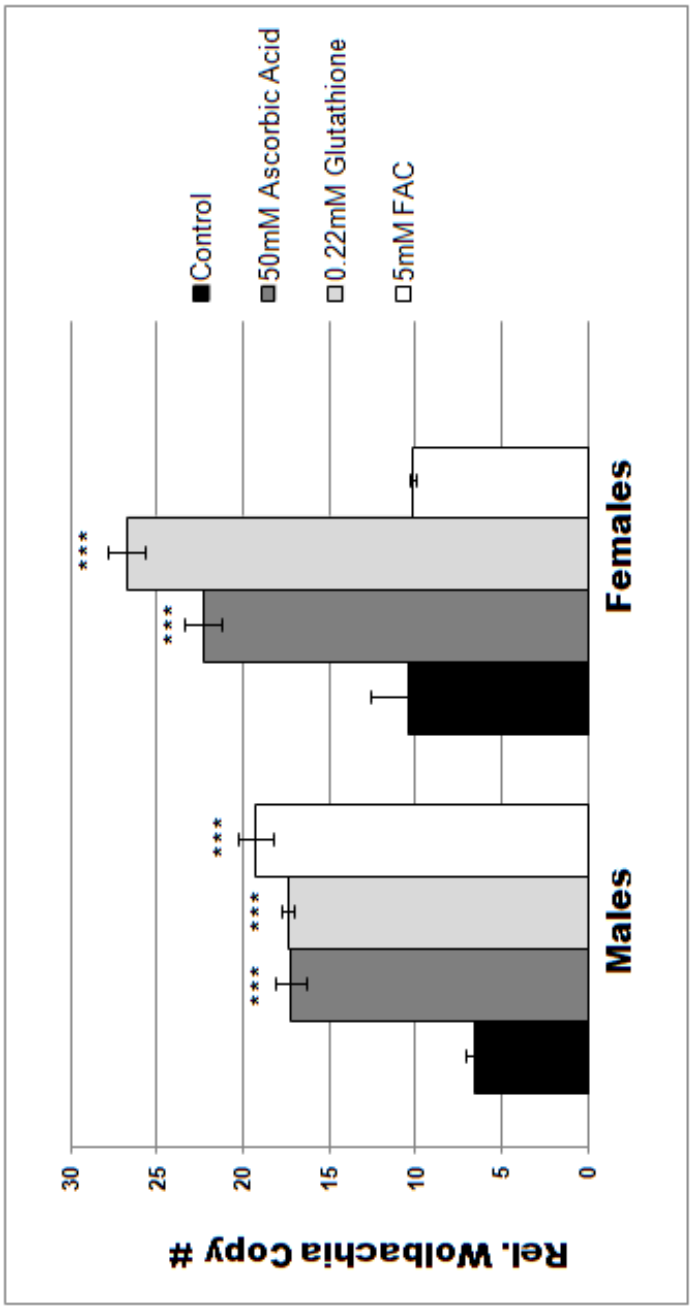
Rel. Wolbachia Copy #
30
25
20
15
10
5
0
Control
50mM Ascorbic Acid
0.22mM Glutathione
5mM FAC
Females
Males
***
***
***
***
***

Figure 7 – Quantitative PCR of DNA taken from young males and females grown on a standard control diet, 50mM ascorbic acid, 0.22mM glutathione, or 5mM ferric ammonium citrate (FAC). Bars represent the relative *Wolbachia wsp* copy number in relation to the host *sod* copy number. Three independent trials were performed and error bars depict standard deviation. *** = $p < 0.001$ (Kruskal-Wallis Test) relative to control.

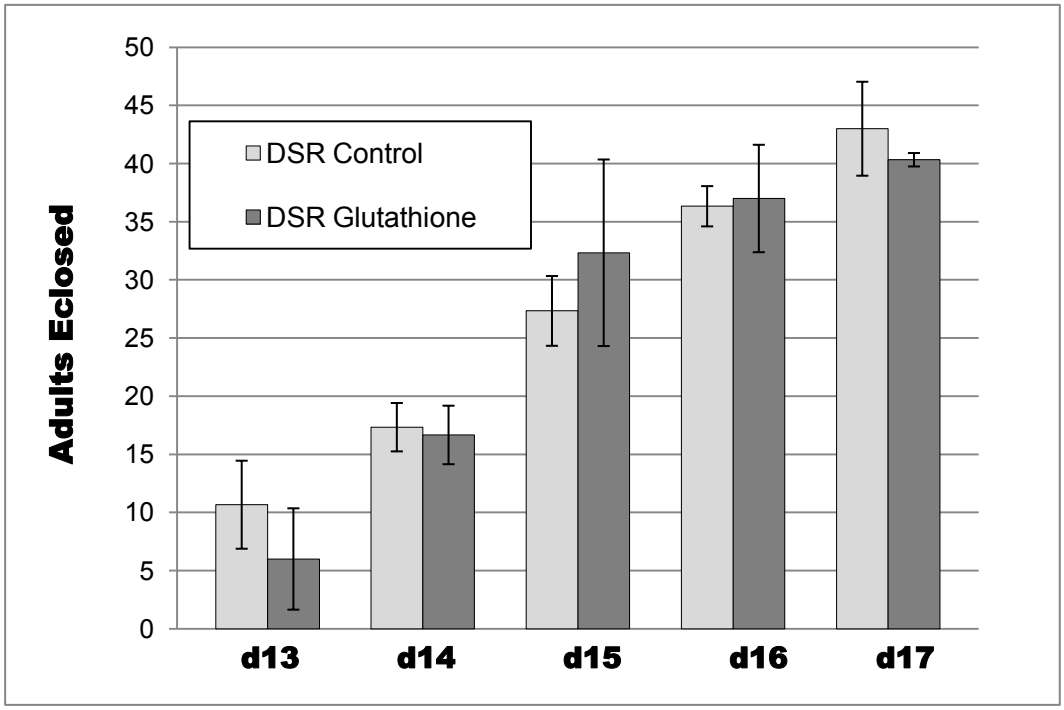
Adults Eclosed
50
45
40
35
30
25
20
15
10
5
0
DSR Control
DSR Glutathione
d13
d14
d15
d16
d17

Figure 8 – Comparison of total eclosion between F1 flies grown on control and media containing 0.22mM glutathione. Adults were placed on control or glutathione-containing medium and allowed to lay eggs for 5 days before removal; 13 days later, the number of flies eclosed was monitored for an additional 5 days. Error bars represent standard deviation between the 3 replicates.

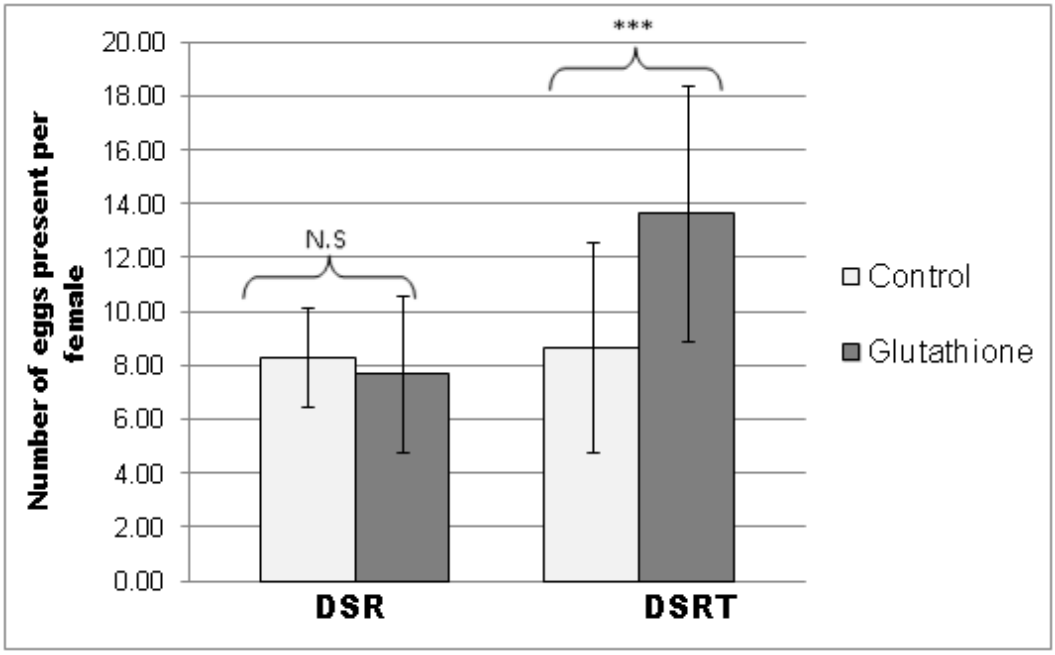
Number of eggs present per female
20.00
18.00
16.00
14.00
12.00
10.00
8.00
6.00
4.00
2.00
0.00
N.S
***
DSR
DSRT
Control
Glutathione

Figure 9 – The number of stage 10 or later oocytes found within individual 6 day old females following growth and maturation on a standard yeast/cornmeal diet (light grey) or a diet containing 0.22mM glutathione (dark grey) in DSR and DSRT. Error bars depict standard deviation and *** represents $p < 0.001$ (t-test).

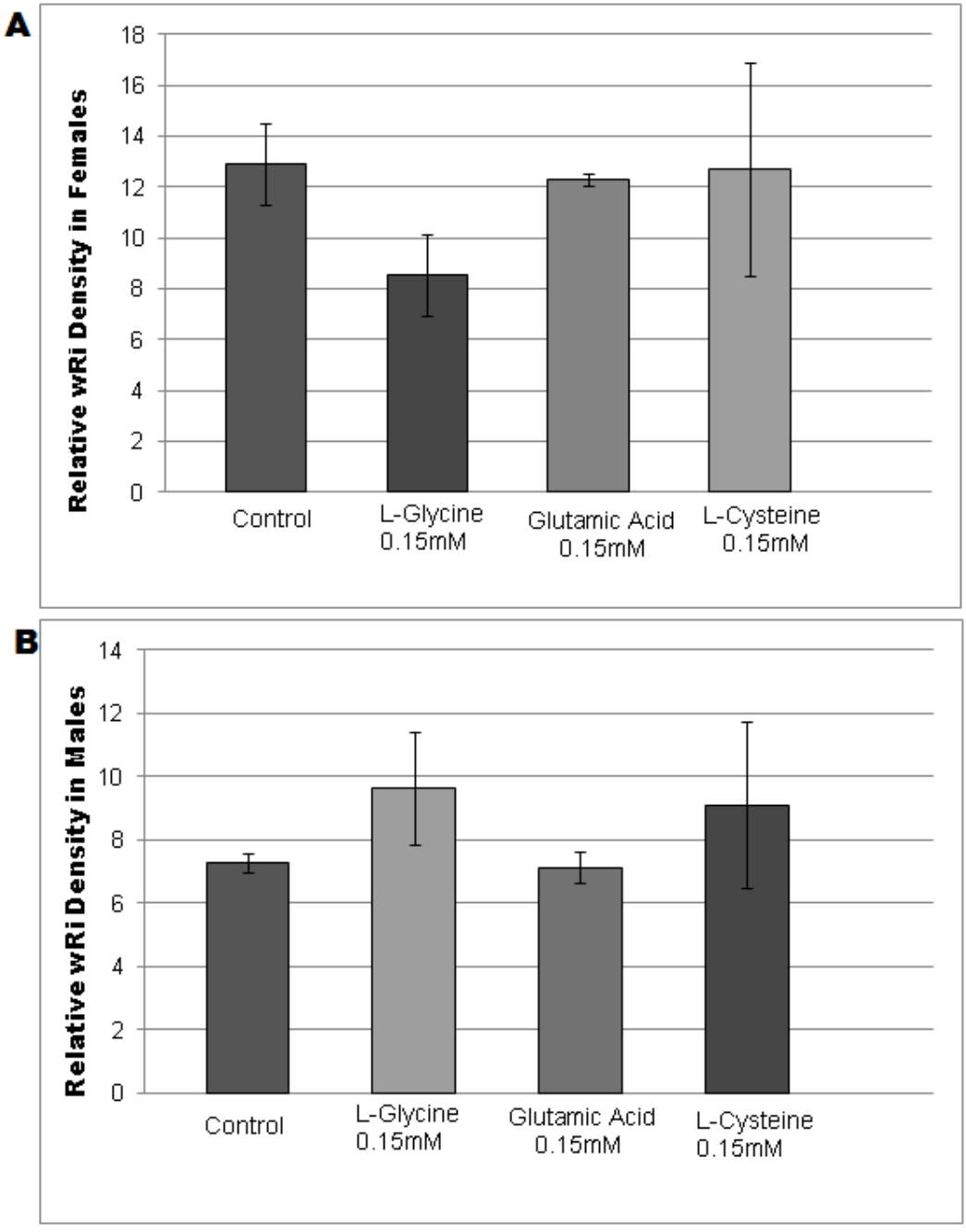
A
Relative wRi Density in Females
18
16
14
12
10
8
6
4
2
0
Control
L-Glycine 0.15mM
Glutamic Acid 0.15mM
L-Cysteine 0.15mM
B
Relative wRi Density in Males
14
12
10
8
6
4
2
0
Control
L-Glycine 0.15mM
Glutamic Acid 0.15mM
L-Cysteine 0.15mM

Figure 10 – Quantitative PCR of DNA taken from newly eclosed females A) and males (B) grown on 0.15mM of L-glycine, glutamic acid, or L-cysteine. Bars represent the relative *Wolbachia* copy number which was determined by comparing *Wolbachia wsp* to host *sod.* Error bars depict the standard deviation for each group. None of the amino acid treatments resulted in a difference in *Wolbachia* density (ANOVA; $p > 0.05$)

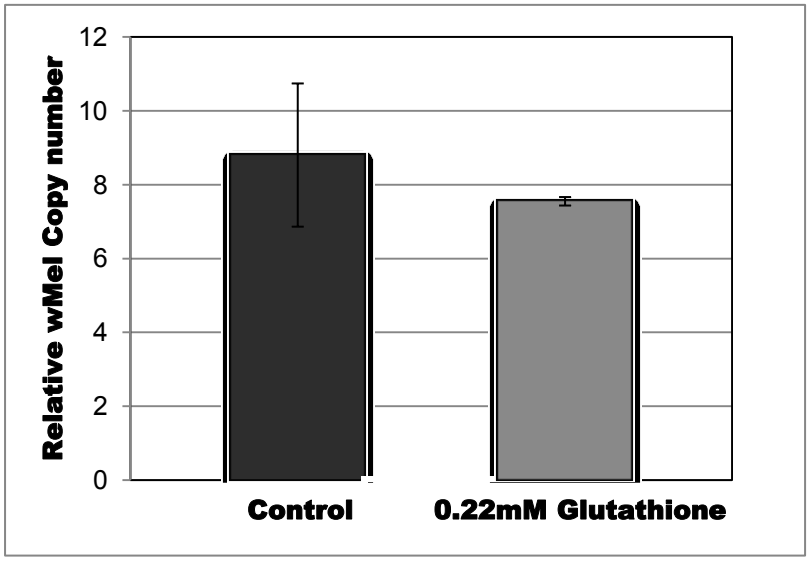
Relative wMel Copy number
12
10
8
6
4
2
0
Control
0.22mM Glutathione

Figure 11 – Relative *w*Mel copy number in groups of young males and females (pooled) fed either a control diet (dark grey) or a control diet plus 0.22mM glutathione (light grey). The bars represent the relative copy number of the *w*Mel *ftsZ* gene compared to *D. melanogaster rpoS.* Error bars represent the standard deviation (ANOVA; $p > 0.05$).

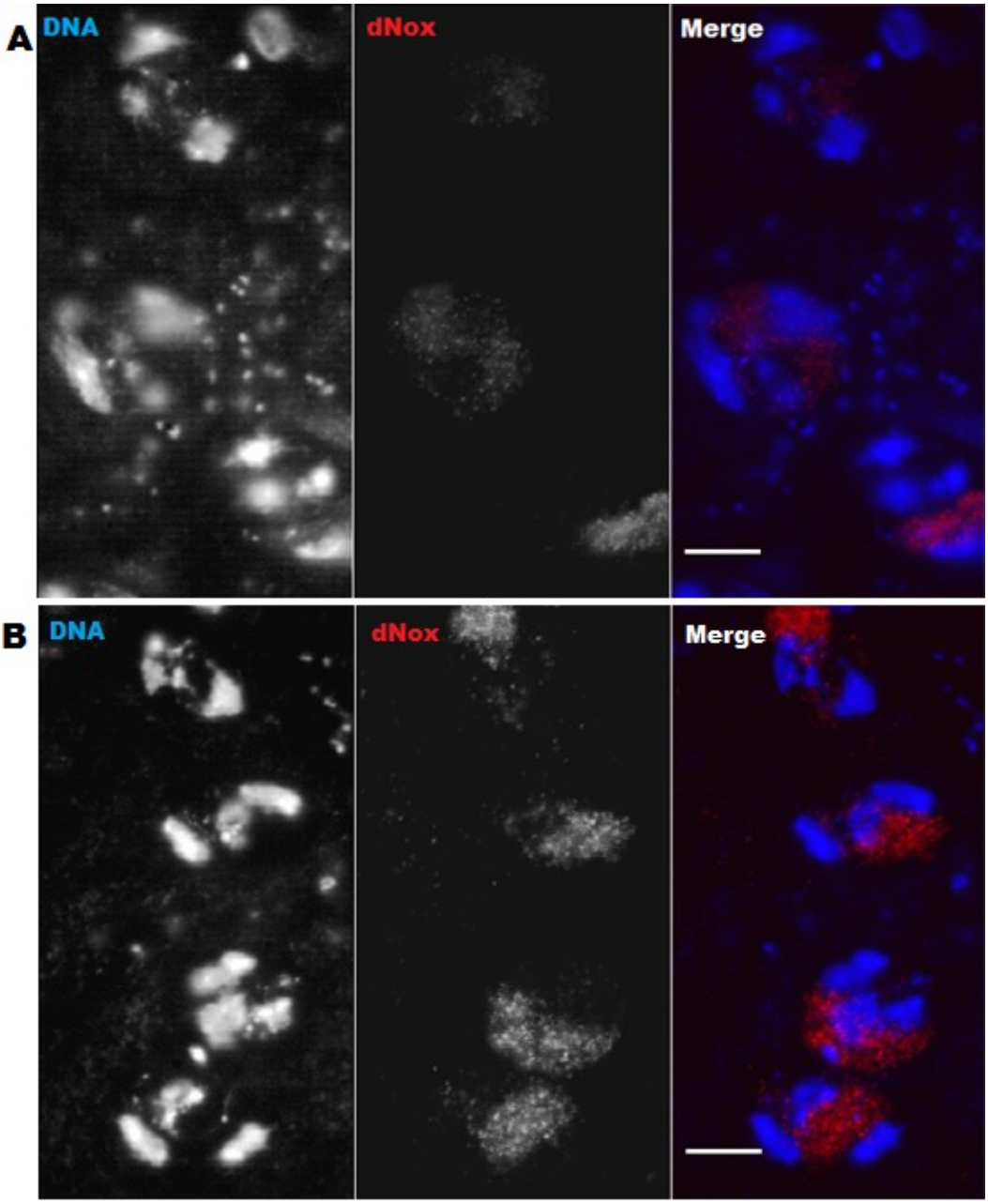
A
DNA
dNox
Merge
B
DNA
dNox
Merge

Figure 12 –Primary spermatocytes in DSR (A) and DSRT (B). In (A) the chromosomes of the three cells shown are visible as large brightly concentrated DAPI signals. The *Wolbachia* is visible within the cytoplasm of the bottom two cells as small, punctuate spots. Anti-Nox5 appears to localize adjacent to the chromosomes. In (B) four cells are visible in the first panel and their chromosomes are brightly stained with DAPI (the small spots in the top right corner are DNA from an adjacent cell not shown, not from *Wolbachia*). Nox localization in DSRT appears adjacent to the chromosomes, as in DSR. Anti-Nox5 was used at a concentration of 5µg/ml and the scale bar = 10µm.

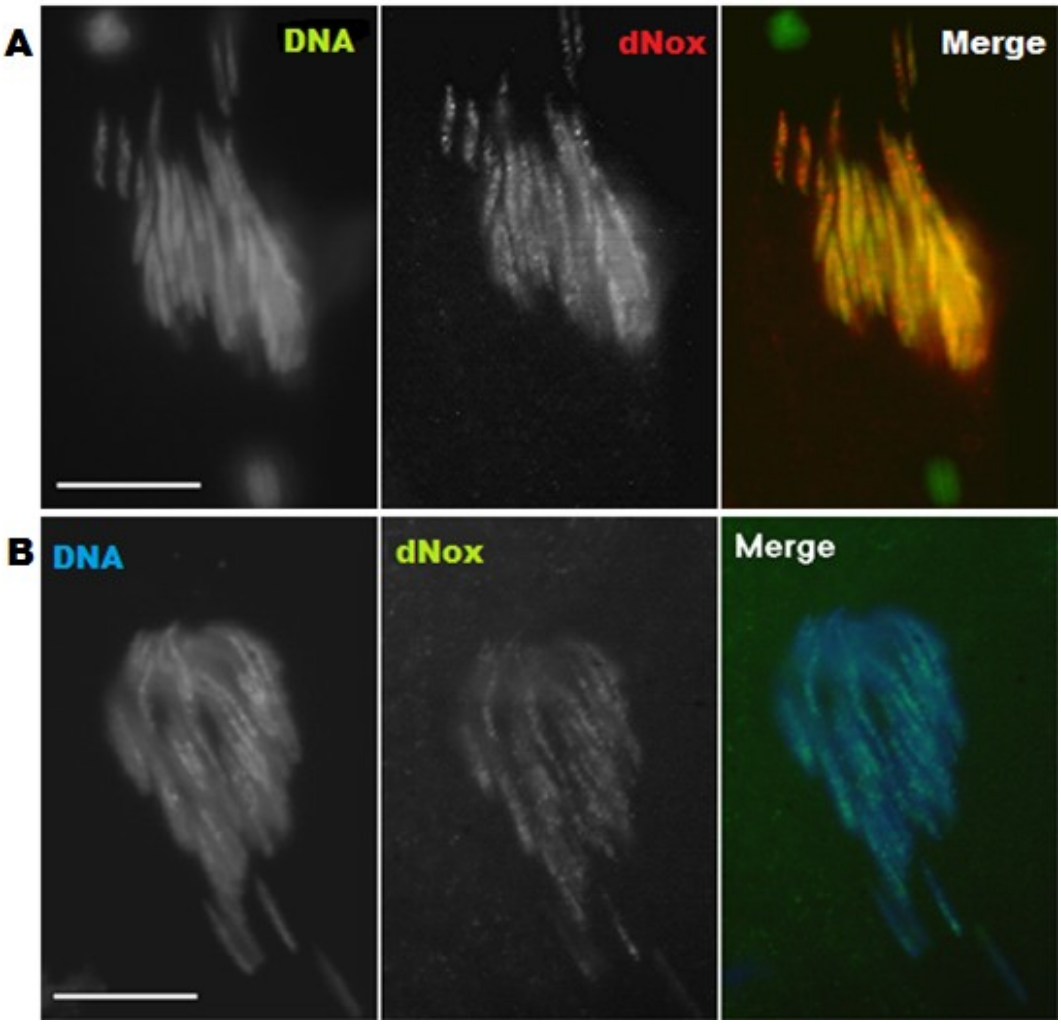
A
DNA
dNox
Merge
B
DNA
dNox
Merge

Figure 13 – Representative elongating spermatid bundles in DSR (A) and DSRT (B). In (A), the elongating nuclei of the spermatids are stained with DAPI. *Wolbachia* are not visible in this image due to migration away from the nuclei in the waste bag at this stage. Nox5 is found in the slender nuclei here. In (B) DNA DAPI staining is shown in the first panel and Nox5 localization is shown in the second panel. Like (A), Nox appears to be present only within the compact nuclei of these cells. Anti-Nox5 was used at a concentration of 5µg/ml and the scale bar represents 10µm.

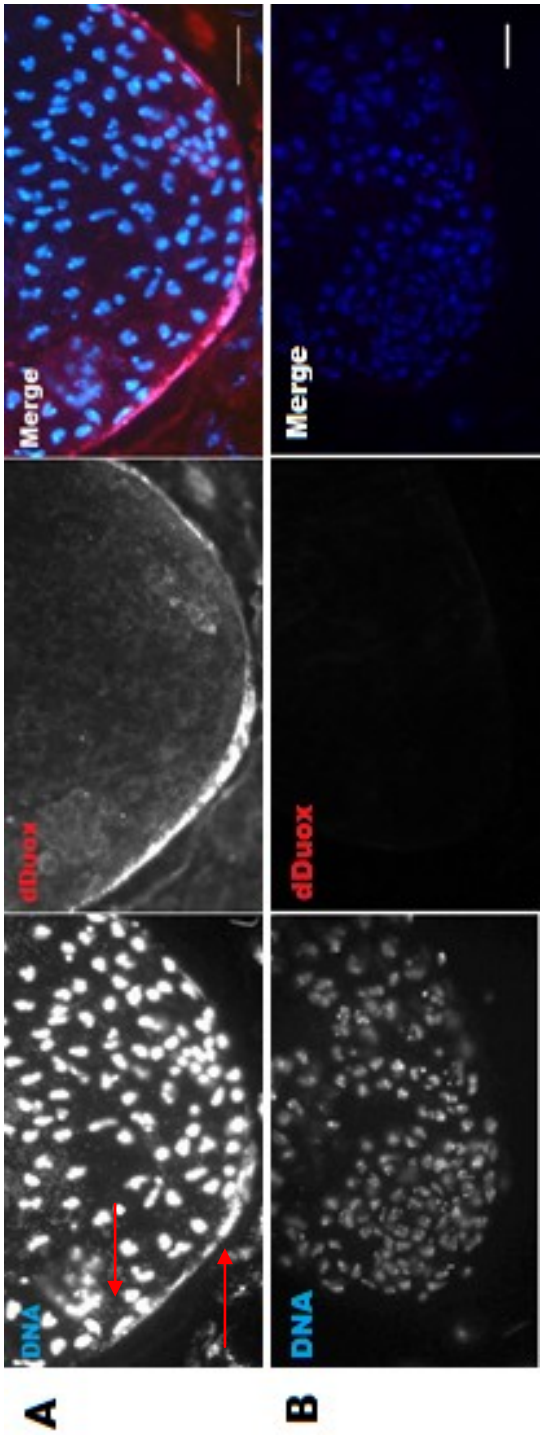
A
DNA
dDuox
Merge
B
DNA
dDuox
Merge

Figure 14 – The apical tip of the testis containing stem cell precursor cells in DSR (A) and DSRT (B). In the first panel of (A), precursor cell nuclei are visible as round bright spots and the *Wolbachia* are lighter haze of fluorescence between nuclei and along the periphery of the apical tip (red arrows). dDuox, in the second panel, appears along the periphery of the apical tip, which appears to co-localize with the *Wolbachia* (see merge). There is also cytoplasmic localization of dDuox. In (B), precursor cell nuclei are stained with DAPI and appear as irregular fluorescent spots. In the second panel of (B), the dDuox signal is too weak to confirm any specific localization patterns. The Mander's overlap coefficient (R) is 0.194 and the Pearson's correlation coefficient (Rr) is 0.743. dDuox was used at a dilution of 1:1000 and the scale bar represents 10μm.

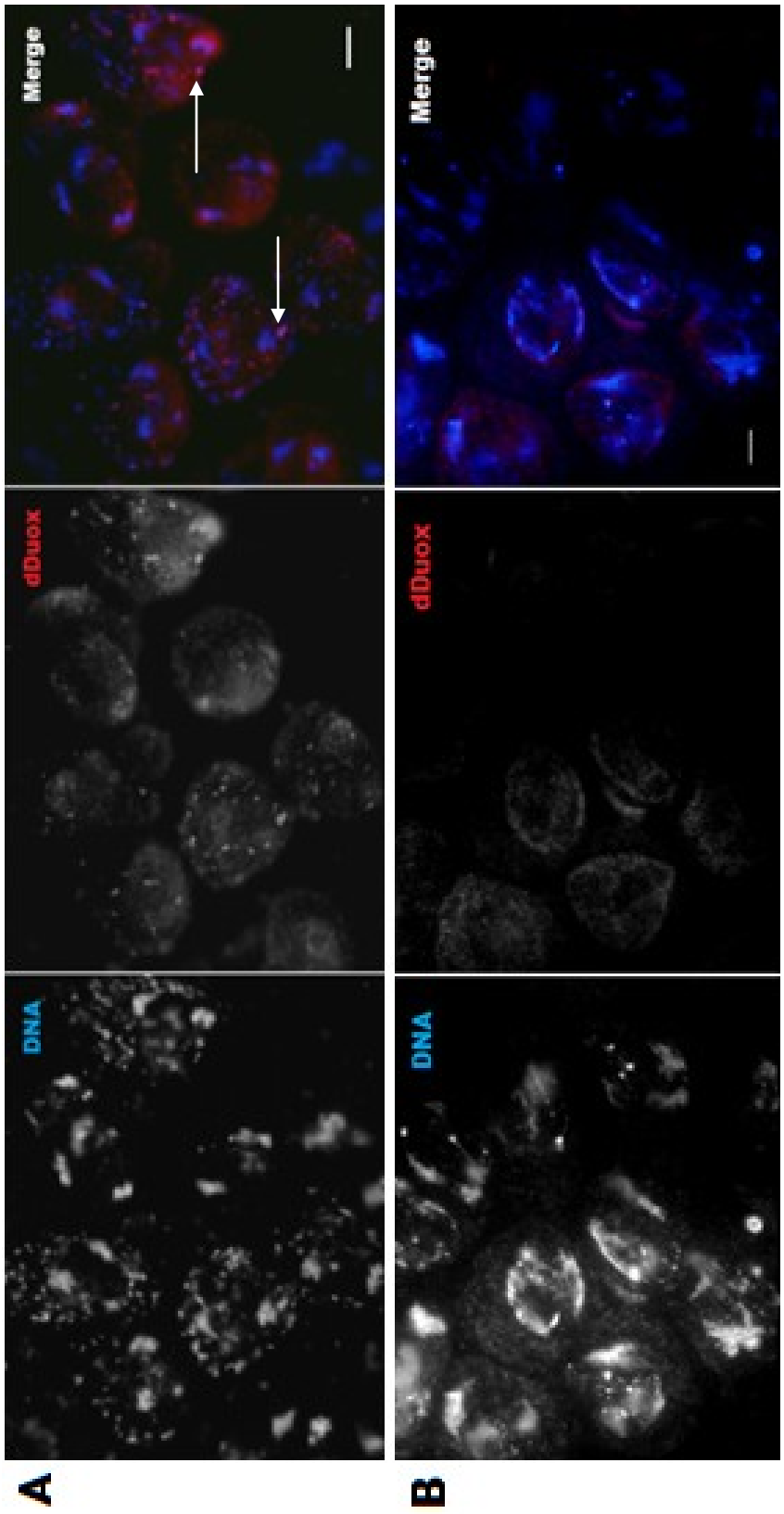
A
DNA
dDuox
Merge
B
DNA
dDuox
Merge

Figure 15 – Primary spermatocytes in DSR (A) and DSRT (B) labeled with anti-dDuox (1:1000, red) and DAPI (blue). In (A) several cells are shown and in the first panel, chromosomes and *Wolbachia* are labeled with DAPI. The chromosomes are identifiable as three large, irregular spots and the *Wolbachia* are the smaller, punctate spots that spread away from the nuclei. dDuox localization in the second panel of (A) appears weakly adjacent to the nucleus and throughout the cytoplasm; bright, concentrated spots also occur within the cytoplasm. In the merge, overlapping of *Wolbachia* and the cytoplasmic punctuate dDuox signal can be seen. In (B), chromosomes are stained with DAPI and are visible as large, irregular shapes. Localization of dDuox appears mostly adjacent to the nucleus with no punctate aggregation within the cytoplasm. Analysis of co-localization between dDuox and DNA fluorescence in DSR produces an R of 0.715, and an Rr of 0.471 which indicates a significant co-localization event. The scale bar represents 10μm.

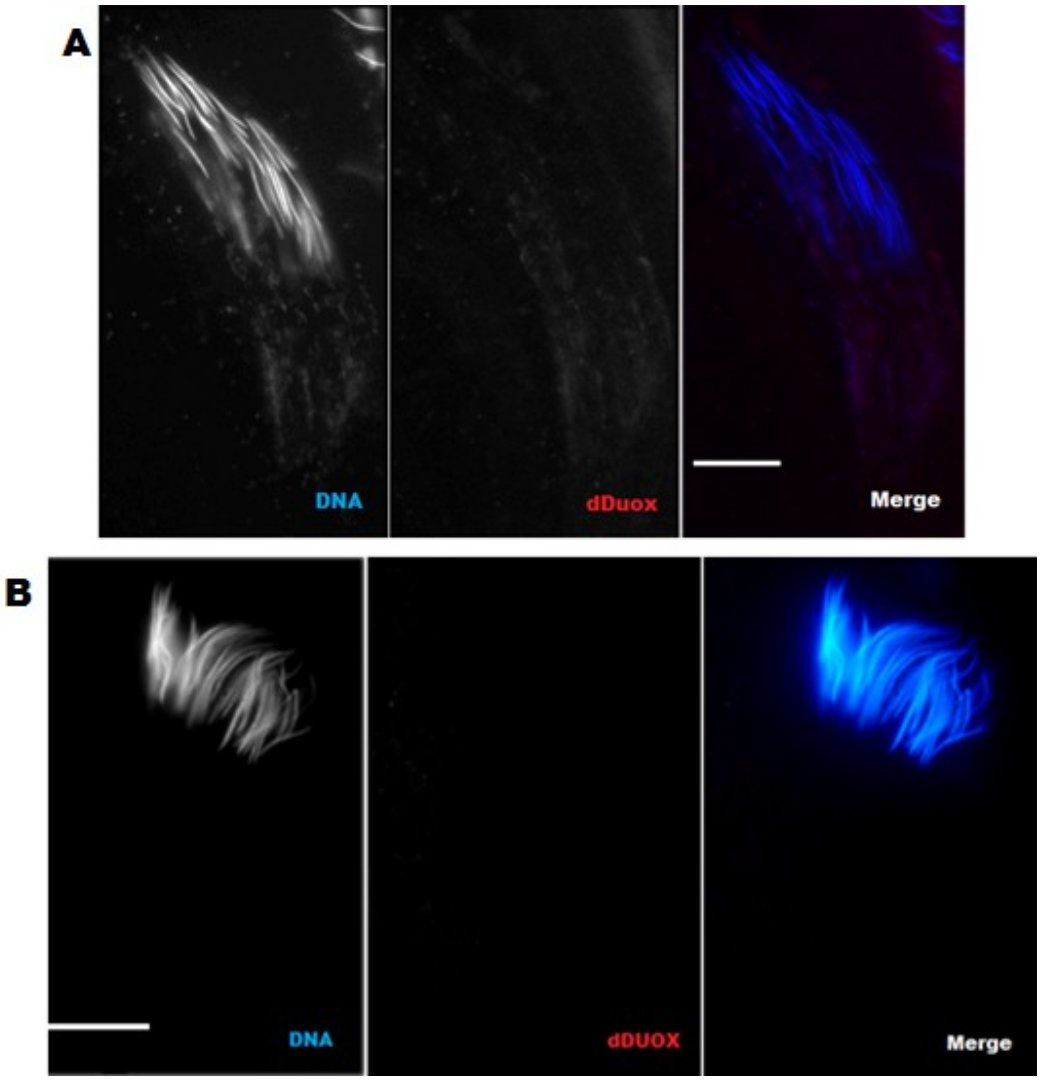
A
DNA
dDuox
Merge
B
DNA
dDUOX
Merge

Figure 16 – Elongating spermatids labeled with anti-dDuox (1:1000, red) and DAPI (blue) in DSR (A) and DSRT (B). In (A) the nuclei of this sperm bundle are thin, needle-like structures. The small spots are *Wolbachia*, which are present immediately below the nuclei and excess *Wolbachia*, likely from another cell, is also visible surrounding the nuclei. dDuox appears adjacent to the thin nuclei and also in punctate spots surrounding the nuclei. In (B) the nuclei appear as thin, needle-like structures and no *Wolbachia* is present. There appears to be no dDuox present in these cells. Analysis of co-localization between dDuox and DNA fluorescence in DSR produces an R of 0.81, and a Rr of 0.71 which indicates a significant co-localization event. The scale bar indicates 10μm.

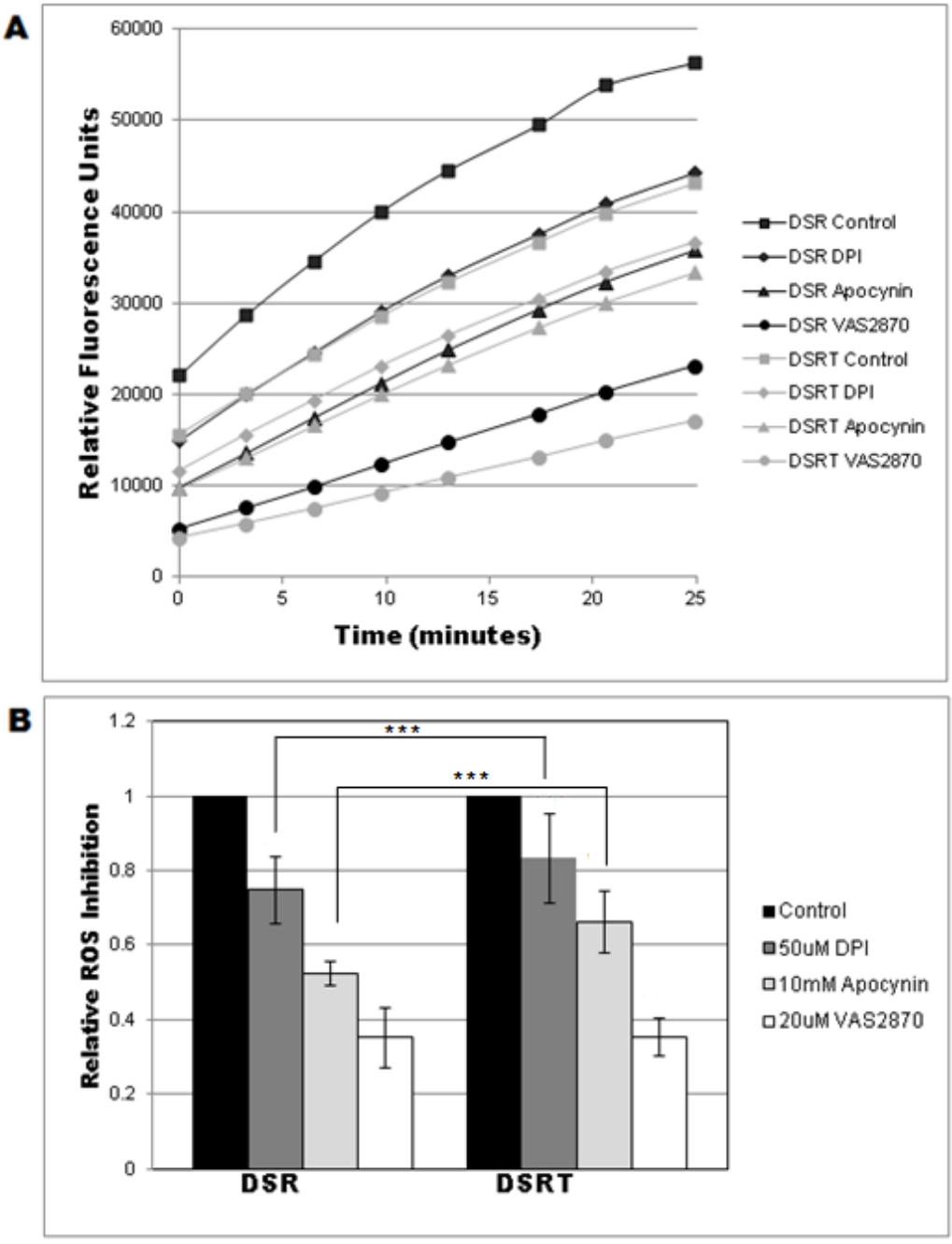
A
Relative Fluorescence Units
60000
50000
40000
30000
20000
10000
0
0
5
10
15
20
25
Time (minutes)
DSR Control
DSR DPI
DSR Apocynin
DSR VAS2870
DSRT Control
DSRT DPI
DSRT Apocynin
DSRT VAS2870
B
Relative ROS Inhibition
1.2
1
0.8
0.6
0.4
0.2
0
***
***
DSR
DSRT
Control
50uM DPI
10mM Apocynin
20uM VAS2870

Figure 17 – (A) DCFDA fluorescence in homogenates from whole DSR (black) and DSRT (grey) males by three NADPH oxidase inhibitors, DPI (50μM, diamond), apocynin (20mM, triangle), and VAS2870 (10μM, circle) over a period of 25 minutes. The control (EDTA) samples are depicted by a square. (B) is derived from the same data set, but shows average of the difference at all time points between the relative amount of inhibition DPI, apocynin, and VAS2870 confer to DSR and DSRT when compared to the control samples. All three inhibitors in DSR and DSRT significantly reduce the total ROS (2 way ANOVA $p < 0.001$).

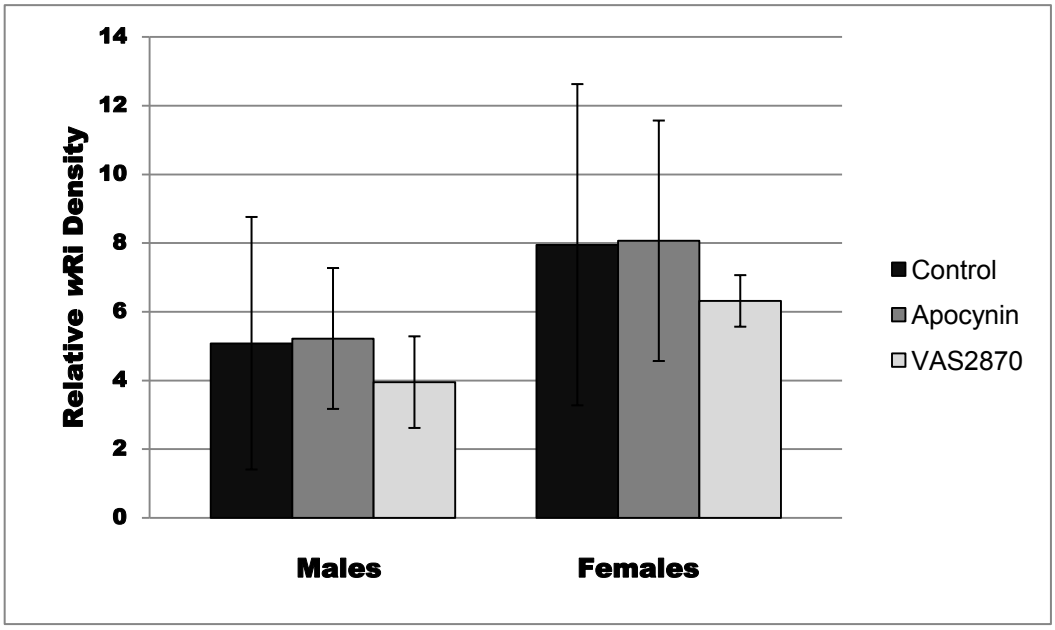
14
12
10
8
6
4
2
0
Relative nRi Density
Males
Females
Control
Apocynin
VAS2870

Figure 18 – Quantitative PCR to determine *Wolbachia* density from 0 – 4 day post eclosion males and females after rearing on control media (black bar), 5µg/ml apocynin (dark grey bar), or 20µg/ml VAS2870 (light grey bar). Error bars reflect the standard deviations of the samples. Treatments are not significantly different from one another (ANOVA $p = 0.654$)

4. Discussion

Turelli and Hoffman (1991) originally described *Wolbachia* and CI in *D. simulans* Riverside in the late 1980s and DSR continues to be an excellent model for studying the cell biology of *Wolbachia* endosymbiosis. The relationship between DSR, *Wolbachia*, and the WO phage is complex; the purpose of this study was to investigate different aspects of this tripartite association with respect to how *Wolbachia* density is regulated as a means to explain the biology of CI. The relationship between the WO phage and *w*Ri was examined to determine whether *Wolbachia* density was regulated by phage activity in DSR and thus, could contribute to CI. Intracellular bacteria can be sensitive to redox stress and the possibility that the DSR antioxidant and innate immune system contributes to the maintenance of *Wolbachia* density in a redox-dependent manner was also explored.

4.1 *wRi* is a type I infection in DSR testes

Wolbachia density in the testes is thought to be a significant factor in the strength of CI penetrance in host populations. Clark *et al* describe the basic cellular unit of CI as WISS (*Wolbachia* Infected Spermatocyst/Spermatid); CI intensity depends on the number of WISS+ cysts (Clark et al., 2003). Consistent with previous data described by others (Clark and Karr, 2002; Clark et al., 2003; Riparbelli et al., 2012), quantitative PCR and fluorescent microscopy indicate that *w*Ri heavily infected the testes (Figure 1) and is present in stem cell precursor cells, primary spermatocytes, elongating sperm cysts, and mature sperm just prior

to individualization (Figure 2). This is consistent with a type I WISS strain, which has been defined by infected spermatocysts and spermatids. Type II WISS+ cysts contain *Wolbachia* in the somatic components of the spermatocyst and type II WISS+ cells do not contain any detectable *Wolbachia* in the developing spermatocysts. It has been previously reported that *w*Ri has a higher CI rate than other *Wolbachia* strains found in *D. simulans* and *D. melanogaster* because *w*Ri infection produces more WISS+ cysts; each cyst does not necessarily contain a greater number of *Wolbachia* (Clark et al., 2003; Veneti et al., 2004). Analysis of genomic DNA from whole males shows that there are significantly fewer *Wolbachia* present per cell than is found in the testes (Figure 1). Correa and Ballard (Correa and Ballard, 2012) measured *w*Ha density in 50 isofemale lines derived from field-caught *D. simulans* and the lines varied in density between <1 and 10 *Wolbachia* per cell. The value reported here for *Wolbachia* density in the whole flies in somatic cells is overrepresented because the contribution of *Wolbachia* from the testes is included in this analysis.

In contrast to testes, it is not entirely clear what effect *Wolbachia* density has in developing oocytes. It appears, however, that *Wolbachia* density in *Drosophila* females is strictly regulated; density in the ovaries has shown to be between approximately 5 and 15 *Wolbachia* per cell and does not significantly change after immune challenge, changes in temperature, increases in yeast and sugar in diet, or as the flies age (Correa and Ballard, 2012). In contrast to males, DSR females do not appear to have any differences in *Wolbachia* density between

their ovaries and their whole bodies when measured by qPCR (Figure 1). All groups of females tested in this study had an average of between 8 and 10 *Wolbachia* per cell. The spider mite *Tetranychus urticae* has between 1 and 3 copies of the *Wolbachia wsp* gene per host *β-actin* gene (Zhao et al., 2013). *N. vitripennis*, in contrast to *D. simulans*, carries a much lower *Wolbachia* load; (Bordenstein et al., 2006; Bordenstein and Bordenstein, 2011) *w*VitA has a density of less than one *Wolbachia* per host cell. This low density, however, is partially related to the activity of the WO phage.

4.2 Phage control of *Wolbachia* density

4.2.1 WORiC is the active phage within *w*Ri

The phage density model predicts that high titers of mature phage particles within *Wolbachia* will lead to disruption and death of the bacterial cell (Bordenstein et al., 2006). In *N. vitripennis*, this modulation of *w*VitA density by phage replication leads to a reduction of cytoplasmic incompatibility when compared to the CI caused by the closely related *w*VitB, which has a low level of replicating phage. In *w*Ri, there have been no previous studies that have addressed the replication and titers of WORiA, WORiB, or WORiC and, furthermore, it was not clear which, if any, of the prophage genomes were active within *w*Ri.

Gavotte *et al* used a filtration-based purification method accompanied by TEM and ORF7-specific PCR to show that mature phage particles form in *Wolbachia*-infected tissues in both *D. simulans* and *D. melanogaster*, but the specific identity

of these virus particles and the regulation of their induction was not addressed (Gavotte et al., 2004).

In order to determine the identity of mature phages in *D.* simulans, the activity of the three distinct prophages found in *w*Ri infecting DSR was measured using quantitative PCR. Phage type-specific primers were used to determine how many copies of the phage genomes were present in addition to the integrated forms. The only phage chromosome to appear in excess of the integrated copy number was WORiC (Figure 4C). The average number of copies of WORiC in all tissues tested ranged from 1.29 – 1.61 copies per *Wolbachia* cell, consistently above the one copy integrated into the *w*Ri genome. Thus, WORiC appears to be the only actively replicating phage in *D. simulans*. An *in silico* analysis of the WORiC genome confirmed that, of the three WO phages in *w*Ri, WORiC was the most similar to the two known replicating WO phages in other *Wolbachia* strains, WOVitA and WOCauB (Biliske et al., 2011).

*w*Ri is considered to be a high CI strain of *Wolbachia* in *D. simulans* with embryonic lethality resulting from crosses between infected males and uninfected females typically between 90 – 100% [(Hoffmann and Turelli, 1988; Veneti et al., 2003), and in our laboratory, H. Harris, personal communication)]. In *N. vitripennis* infected with *w*VitB, which is also a high CI-inducing strain of *Wolbachia*, Bordenstein *et al* reported an average WOVitB copy number of 1.6 ± 0.12 per *Wolbachia* (Bordenstein et al., 2006). In the present study, a similar relative density of WORiC suggests that this phage is the active virus observed in

past TEM micrographs of *Drosophila* tissues (Masui, et al. 2000; Gavotte et al. 2004). WORiC genes have been reported as actively transcribed in previous literature. Specifically, the three ankyrin related genes found in WORiC are expressed in males, females, ovaries, testes, early (2 hour AEL) and late (overnight) embryos (Klasson et al., 2009).

In silico analysis of the WORiC genome in comparison to known active WO phages revealed two core components of the phage genome that must be present in order for replication (Biliske et al., 2011). WORiC contains 27 open reading frames (ORFs) that comprise the tail morphogenesis component and 9 ORFs that make up the DNA packaging and head assembly component (Table 3).

4.2.2 WORiA and WORiB are phage remnants

WORiA and WORiB did not show any evidence of extrachromosomal DNA beyond the one and two copies, respectively, found within the *w*Ri genome. Alignments to WOCauB and WOVitA1 show that both WORiA and WORiB lack the core structural components necessary for virion assembly (Table 3) (Biliske et al., 2011). The persistence of WORiA and WORiB within the *w*Ri genome suggests that there may be selective pressures maintaining these two prophages. There is evidence that an adenine methyltransferase found in WORiB is actively transcribed from the prophage genome (Saridaki et al., 2011) and so this region may be necessary for another, unrelated, aspect of *Wolbachia* biology.

4.2.3 WO phage density does not correlate with *w*Ri density

The average density of WORiC derived from pooled samples of multiple individuals and tissues is shown in Figure 5C. When 16 third instar larvae were individually measured for phage density, WORiA and WORiB did not significantly deviate from the expected means of one and two copies, respectively. Individual larva, however, had a much wider distribution of WORiC copy numbers, ranging from individuals that appeared to have no extrachromosomal viruses to individuals having more than 1.5 WORiC per *Wolbachia* (Figure 5C). This indicates that not every individual within the larval population is experiencing viral replication, although most are. Currently, the signals which induce viral replication within the confines of an endosymbiotic bacterium are unknown. Attempts to increase viral replication by exposing larvae to heat shock, mitomycin C, or hydrogen peroxide did not increase the amount of phage DNA present (data not shown).

The relative *Wolbachia w*Ri density per *D. simulans* larval host cell was also measured (Figure 5). In these cells, the *w*Ri density did not significantly correlate with WORiA, WORiB, or WORiC relative densities. However, the WORiC density trended toward a weakly inverse association with *w*Ri density (Figure 5C). This lack of correlation does not agree with the phage density model postulated by Bordenstein *et al* (Bordenstein et al., 2006), whereby the *Wolbachia* copy number and CI in *N. vitripennis* was found to be inversely related to phage activity. It raises the notion that phage density is a population and strain-specific

factor and that phage density and *Wolbachia* density in DSR may not be related. Low levels of replicating phage, as seen here for WORiC, do not impact *Wolbachia w*Ri density and are unlikely to have an effect on CI.

4.3 Redox Control of *Wolbachia* density

4.3.1 DSR Males contain more ROS than DSRT males

Previously it had been shown that DSR testes contain a higher amount of the antioxidant superoxide dismutase (SOD) than DSRT (Brennan et al., 2012); SOD activity is an indirect measure of total superoxide (ROS). Additionally, it had been shown that the embryonic mosquito cell line, Aa23, contained higher amounts of total ROS than an uninfected, parallel line, Aa23T (Brennan et al., 2008).

Using the fluorescent compound DCFDA, which fluoresces in the presence of all reactive oxygen intermediates including hydroxyl, superoxide, and hydrogen peroxide (Eruslanov and Kusmartsev, 2010), total ROS in homogenates of whole males was significantly higher in DSR when compared to DSRT (Figure 6). Therefore DSR flies experience greater amounts of oxidative stress when compared to DSRT, in agreement with (Brennan et al., 2008).

4.3.2 Glutathione increases *Wolbachia* titer in DSR

The abundance of reactive oxygen species has deleterious effects on spermatocyte chromatin (Brennan et al., 2012). Excess ROS induces DNA

damage by many mechanisms; a common result is the formation of 8-oxoguanine lesions (reviewed in (Dizdaroglu, 2012). In CI crosses, replication of the paternal chromatin following fertilization is incomplete and this delays the deposition of maternal histones onto the chromatin (Landmann et al., 2009). It has been suggested that the poor fidelity of paternal chromatin replication could be a result of DNA damage (Brennan et al., 2012). In this study, an attempt was made to lower the oxidative stress that DSR flies experience through an antioxidant-rich diet. Flies were fed a diet containing 0.22mM glutathione (Bonilla et al., 2006), allowed to lay eggs, and the F1 generation was analyzed by quantitative PCR. Glutathione is a powerful antioxidant that is recycled within cells between reduced GSH and oxidized GSSG. Previous studies that examined the protective effect of glutathione to the oxidizing agent, paraquat, determined that 0.22mM was an optimal concentration to grant the greatest antioxidant capacity; higher concentrations (0.43mM) were detrimental to the survivability of the flies (Bonilla et al., 2006).

While CI penetrance remained at 100% following glutathione treatments, (H. Harris, personal communication) *Wolbachia* density doubled in both males and females (Figure 7). This indicates that *Wolbachia* titer is sensitive to the redox environment; when the cellular ROS levels are reduced, *Wolbachia* are able to divide more freely or are not inhibited in growth. A similar phenomenon has been shown previously in the tsetse fly, *Glossina morsitans morsitans*, infected with *Trypanosoma brucei*, the protozoan agent of human sleeping sickness. The

oral administration of non-enzymatic antioxidants such as glutathione, N-acetyl-cysteine, ascorbic acid, and uric acid to the tsetse flies resulted in a marked increase in trypanosome infection within the fly midgut and this is likely due to a mitigation of the host ROS produced by an innate immune response (MacLeod et al., 2007). These conclusions could be confirmed by the DCFDA assay to determine that amount of total ROS in the flies was reduced.

Another possibility in determining how glutathione increases *Wolbachia* density is that glutathione may be acting as a signaling factor to increase bacterial cell division. In contrast to Gram positive bacteria, which often lack the enzymes for glutathione synthesis, glutathione is commonly found in Gram negative bacteria and is most abundant during the stationary phase in *Escherichia coli* (Fahey et al., 1978), Apontoweil & Berends 1975). Glutathione is not only an antioxidant, it is responsible for mitigating a wide variety of stressors such as osmotic stress, low pH, and toxic chlorine compounds [reviewed in (Masip et al., 2006)]. It is not clear whether *Wolbachia* are subjected to these other forms of stress inside their host cells and it is difficult to compare the stressors that a free living bacterium experiences with an intracellular symbiont that may rely on host signals for replication (Ruang-areerate et al., 2004).

4.3.3 L-glycine, L-cysteine, or glutamic acid supplementation is not sufficient to increase *w*Ri density in DSR

The possibility that *Wolbachia* may use excess glutathione in a redox-independent manner was explored. Glutathione is a tripeptide composed of L-glycine, L-cysteine, and glutamic acid. The closely related α-proteobacterium *Francisella tularensis* requires L-cysteine for growth and obtains this amino acid from glutathione using the enzyme γ-glutamyl transpeptidase (Alkhuder et al., 2009). *Legionella pneumophila*, the causative agent of Legionnaire's disease in humans, scavenges L-cysteine, L-glutamine, and L-serine by upregulating a host amino acid transporter; bacteria lacking these amino acids have severely reduced replication (Wieland et al., 2005).

Currently it is unknown whether *Wolbachia* is able to scavenge amino acids from its host; attempts to recreate the cellular environment that *Wolbachia* requires to replicate have so far proved unsuccessful. To this end, DSR was grown on media containing one of L-cysteine, L-glycine, or glutamic acid in twice the molar concentration that was present in 0.22mM glutathione and analyzed by qPCR for changes in bacterial titer. There was no statistical difference in the *Wolbachia* density in flies fed the control diets when compared to the flies fed any of the three amino acids (Figure 10). This indicates that the increase in *Wolbachia* density is due to the glutathione and not one of its constituents.

4.3.4 Ascorbic acid increases *Wolbachia* density in DSR males and females

Ascorbic acid (Vitamin C) is a water soluble reducing agent that is often acquired from the environment; it cannot be synthesized by insects and higher mammals (Chatterjee, 2013). Like glutathione, ascorbic acid exists in a reduced (AA) state and an oxidized (dihydroascorbic acid; DHA) state. AA/DHA ratios reflect the amount of ROS in a system; high AA/DHA indicates a strongly reducing environment. GSH is also able to recycle DHA back into AA(Meister, 1994). Ascorbic acid can also act as an oxidizing agent and high doses of orally administered ascorbic acid in *Drosophila* have a negative impact on longevity (Massie et al., 1976)

When males and females were allowed to develop on medium containing 50mM of ascorbic acid, their *Wolbachia* density increased by 2.63 and 2.14 fold, respectively, compared to flies raised on control diet (Figure 7). This concentration was chosen based on studies in *Caenorhabditis elegans* that determined that 50mM ascorbic acid administered to nematodes decreases the ability to mount a ROS response to pathogenic bacteria (Sem and Rhen, 2012). An overall lowering of the total ROS in *Drosophila* hosts allows *Wolbachia* to increase replication.

4.3.5 Glutathione does not increase fitness in DSR

D. melanogaster lacking the *indy* (I'm not dead yet; a mitochondrial dicarboxylate cotransporter) gene have an extended lifespan without a reduction or gain in fertility and fecundity (Rogina et al., 2000). A possible cause of this extended lifespan was revealed when it was found that *indy* mutants have less total ROS and less accumulated oxidative damage throughout their lifespan (Neretti et al., 2009). Similarly, DSR flies fed exogenous glutathione do not appear to be more or less fit; there is no significant difference in eclosion rates and egg production between control and treated flies (Figure 8 and 9) in spite of twice the normal *Wolbachia* titer and increased ROS present. What this indicates is that increased *Wolbachia* replication in the presence of glutathione is likely due to the antioxidant properties of glutathione (reviewed in Meister 1994) and not the general increase in host fitness and, thus, resources that would stimulate *Wolbachia* replication. The total ROS present in glutathione-fed flies was not measured, however, and this would provide confirmation that of the effects of glutathione on *Wolbachia* density.

Interestingly, DSRT females had a significant increase in egg production when grown on glutathione media (Figure 9). This increase may be caused by an increase in bioavailable glutathione since DSRT flies are not under considerable oxidative stress. Higher concentrations of glutathione (0.33, 0.44, 0.55mM, data not shown) did not increase the *Wolbachia* density in DSR more than the 0.22mM

treatment and, therefore, DSR egg production at higher concentrations was not monitored.

4.3.6 Iron supplementation increases *Wolbachia* density in males only

Iron is of limited bioavailability and most organisms require iron to control the redox environment for enzymatic reactions (Andrews et al., 2003). An abundance of iron, however, can be toxic to cells because it reacts with H_2O_2 to produce dangerous hydroxyl radicals by what is known as the Fenton reaction ($Fe^{2+} + H_2O_2 \rightarrow Fe^{3+} + OH^- + HO^{\cdot}$) (Fenton, 1894). Pathogenic and symbiotic bacteria must sequester iron from their hosts to ensure that enough is available for growth and to avoid free iron within the system. Low levels of iron can inhibit cellular processes and, in the case of enterohaemorrhagetic *E. coli*, can induce production of the Shiga toxin (Calderwood and Mekalanos, 1987). Bacteria generally rely on ferritins (*ftnA*; iron storage), bacterioferritins (*bfr*; haem-containing), and siderophores (low molecular weight iron scavengers) to accomplish sequestration [Reviewed in (Andrews et al., 2003)]. The bacterial plant pathogen *Agrobacterium tuminfaciens* relies on a membrane bound ferritin *mbfA* to confer protection against plant-generated H_2O_2 (Ruangkiattikul et al., 2012). Upon treatment with 5mM ferric ammonium citrate, the *Wolbachia* density in males increased 2.94 fold (Figure 7).

Asobara tabida is a parasitoid infected with *w*At and has a lowered expression of both the heavy and light chains of ferritin, which is involved in iron storage, when compared with uninfected individuals (Kremer et al., 2009b). Excess iron treatment through diet increases the expression of *w*At bacterioferritin and induces apoptosis in the ovaries of *A. tabida* (Kremer et al., 2009b). Maintenance of mitochondrial iron metabolism is essential for spermatogenesis in *Wolbachia*-free *D. melanogaster* and mutants in the iron transporter gene, *mitoferrin,* render flies sterile (Metzendorf and Lind, 2010). Other studies have shown that *w*Mel confers a fecundity benefit to *D. melanogaster* that have been exposed to either iron starvation or iron overload (Brownlie et al., 2009).

Interestingly, 5mM iron supplementation did not change the *Wolbachia* density in infected female DSR; these infected females contained 10.17 ± 0.18 *Wolbachia* per host cell compared with 10.45 ± 2.13 *Wolbachia* per cell in the control females (Figure 7). In infected *A. tabida*, 20mM iron overload increases apoptosis in the ovaries (Kremer et al., 2009b). When *Wolbachia* levels rise due to exogenous redox-affecting compounds such as iron, ascorbic acid, and glutathione, it is not clear if the density increases are tissue specific or global. Heavy and light chain ferritin expression in *A. tabida* in the ovaries is much lower than in whole females or males (Kremer et al., 2009b). If the assumption is made from Figure 7 that iron is limited in males, and increases in *Wolbachia* density are a result of more free iron, then these results show that iron may be the limiting factor for *Wolbachia* growth in males but not in females. Another possibility is

that the ovaries are more susceptible to the reactive oxygen generated via the Fenton reaction as a result of excess iron. *Wolbachia* density in females may remain stable due to increased replication in response to the addition of free iron but that excess replication is eliminated by the high amount of ROS generated by the free iron in the tissues.

4.3.7 Glutathione does not increase *w*Mel density in *D. melanogaster*

In laboratory populations, *D. melanogaster* infected with *w*Mel experiences less CI mortality than *D. simulans* infected with *w*Ri, approximately 25% in *D. melanogaster* compared to 95-100% in *D. simulans* (Bourtzis et al., 1996). To date, there have been no reports of artificially increasing or decreasing *Wolbachia* density or CI levels via the addition of exogenous molecules. *D. simulans* and *w*Ri are commonly examined to elucidate the cytogenetics of CI, however, since CI is nearly 100% complete in *D. simulans* infected with *w*Ri, only experimental modifications that decrease CI levels can be analyzed effectively. *D. melanogaster* and *w*Mel provide an excellent model to study the effects of *Wolbachia* density on CI levels because, theoretically, CI could be raised or lowered. *D. melanogaster* also has the advantage of an easily manipulated genetic composition.

*w*Mel density in whole males is similar to that of *w*Ri; approximately 8 *Wolbachia* are found per host cell throughout *D. melanogaster* (Figure 11) compared to approximately 6 *w*Ri per host cell in *D. simulans*. Previous reports of

Wolbachia titer in *D. melanogaster* testes have shown that there are significantly less bacteria present compared to DSR testes (Veneti et al., 2003); DSR testes contain approximately 35 *Wolbachia* per host cell. When newly eclosed *D. melanogaster* males grown on 0.22mM glutathione were analyzed for *Wolbachia* density, there was no statistical difference in titer between the treated and control flies (Figure 11). This is in contrast to the 2.94 fold increase in *w*Ri density when *D. simulans* was subjected to the same feeding treatment.

The relationship between *w*Mel and reactive oxygen species generation has never been investigated. High CI strains such as *w*Ri and *w*Alb (which infects the Asian tiger mosquito, *Aedes albopictus*) induce the generation of ROS and the corresponding antioxidant repertoire in their hosts (Brennan et al., 2012, 2008). *w*Mel in *D. melanogaster* does not appear to induce a sperm modification that results in high CI levels and it is possible that this system is in oxidative equilibrium, such that the cellular redox environment of its host may permit the optimal growth of the symbiont at the greatest density that is permitted. On the contrary, perhaps *D. melanogaster* mounts a more successful ROS response that is able to control *w*Mel replication and, therefore, results in a lowered level of CI. It is not currently known what factors contribute to the capacities of different hosts and/or different strains of *Wolbachia* to control bacterial density, but these factors could include host nutrient availability, *Wolbachia* scavenging abilities, or induction of the host innate immune response in the form of antimicrobial peptides.

4.3.8 Nox distribution is nuclear in developing sperm

The NADPH oxidase family is responsible for the NADPH-dependent reduction of molecular oxygen to superoxide or hydrogen peroxide. In humans, Nox 1 through 5 generate ROS in response to invading microbes through a phenomenon called an "oxidative burst." This ROS plays a large role in determining the total redox environment of the organism, which can lead to pathology in some instances (Choi and Ou, 2006). The role of Nox may be somewhat plastic; deletions and substitutions of the Nox genes occur through a wide variety of organisms. *C. elegans* and budding yeasts lack all Nox genes, *Anopheles gambiae*, the mosquito vector of malaria, contains an extra Nox (NoxM), *D. melanogaster* only contains Nox5, rodents lack Nox5, *Xenopus tropicalis* lacks Nox3, and several species of fungi contain NoxA and NoxB, which are phylogenetically distinct from Nox1-5 (Kawahara et al., 2007)

Drosophila NADPH oxidase (dNox) is the ortholog of human Nox5 (Ritsick et al., 2007) and has not previously been studied in *Wolbachia*-infected flies. In both DSR and DSRT, dNox was found exclusively in the nuclei of primary spermatocytes, canoe spermatids and late elongating spermatids. dNox was not found in pre-meiotic cells or in mature sperm. Nuclear localization of Nox is common in other organisms; in human endocardial endothelial cells, Nox5 is primarily found in the nucleus (Ahmarani et al., 2013). Bánfi et al. (2001b) established that hNox5 was primarily expressed in human pachytene

spermatocytes and suggested that hNox5 might have a role in cell division, apoptosis, or DNA compaction during spermatogenesis.

There was no observable difference between the localization patterns of dNox between DSR and DSRT (Figures 12 and 13). This suggests that the role of dNox in *Drosophila* is likely unrelated to *Wolbachia*-mediated changes in sperm chromatin and the mechanism of CI.

4.3.9 Duox co-localizes with *Wolbachia* in developing sperm

Dual oxidase (duox) is a member of the NADPH oxidase family and has much of the same function as Nox in immunity and generation of the oxidative burst. The duox protein contains a Nox domain, an EF hand motif domain, and a unique peroxidase domain that has homology to a heme-containing peroxidase (Kawahara et al., 2007). Humans have Duox1 and Duox2 but many lower organisms such as teleost fish and insects only contain one ortholog of this enzyme (Kawahara et al., 2007).

In the *Drosophila* gut, fine control over *dDuox* expression is maintained in order to avoid the deleterious effects of an overproduction of ROS (Anh et al., 2011; Ha et al., 2009a, 2009b). Flies that have reduced expression of *dDuox* easily succumb to opportunistic bacteria however. In 2009, Ha *et al.* discovered that there are two separate regulatory pathways in the gut that lead to the expression of *dDuox* during times of minimal and heavy infections with pathogenic gut microbes. When normal gut flora is present in *Drosophila*, dDuox

is activated by the PLC-β pathway in a calcium-dependent manner (Ha et al., 2009a). When bacterial load becomes heavy with infectious bacteria, *dDuox* expression is upregulated by the p38 pathway by activation of ATF2 (Ha et al., 2009b). In order to minimize the damage done by the oxidative burst, *Drosophila* dDuox activation also activates Peroxiredoxin V (dPrxV), an antioxidant, through the transcription factor FOXO (Ahn et al., 2012). A mosquito Prx that shares 58% identity with human PrxV was found to be upregulated in the Aa23 *Ae. albopictus* cell line infected with *Wolbachia* (Brennan et al., 2008).

In Figures 14, 15, and 16, Duox can be seen in close association with *Wolbachia* in DSR primary spermatocytes and elongating spermatids. It was also found in the apical region of the testes amongst the *Wolbachia* in the primary germ cells (Figures 14A, 15A, and 16A). The close proximity of dDuox to the *Wolbachia*-containing vesicles and the increase in ROS previously reported in the germ line (Brennan et al., 2012) of DSR males suggests that the host may be treating *Wolbachia* as foreign and the cells infected with *Wolbachia* are experiencing oxidative bursts through dDuox. This would account for the high levels of ROS and the subsequent DNA damage found in testes and primary spermatocytes, respectively (Brennan et al., 2012).

Recently it was reported that dDuox distinguishes pathogenic from commensal bacteria in the *Drosophila* gut by the production of uracil by pathogenic bacteria. Uracil acts as a ligand for Duox and enables the generation of the oxidative burst (Lee et al., 2013). It is not currently known if *Wolbachia* is a

"uracil producer" in natural infections, but trans-infection of *Wolbachia* from one host into another results in an upregulation of innate immunity, including the production of AMPs (Xi et al., 2008). This upregulation of innate immunity has applicable uses in eradicating vector-borne human diseases. For example, *Aedes aegypti* WB1 (an uninfected strain transinfected with *Ae. albopictus w*Alb) is resistant to Dengue virus. Upon viral infection, *Wolbachia*-infected mosquitoes launch a robust innate defense. Duox expression and ROS levels are increased and this leads to an up-regulation of the Toll pathway, which produces antimicrobial peptides (Pan et al., 2012).

4.3.10 VAS2870 is a potent inhibitor of ROS in *D. simulans*

VAS2870 remains the most effective specific inhibitor of Nox/Duox-derived ROS and does not have antioxidant properties (Wind et al., 2010). DSR and DSRT whole fly homogenates subjected to VAS2870 treatment experienced the greatest reduction in DCFDA fluorescence; both infected and uninfected flies had 64% less ROS than the control groups (Figure 17). While the reduction of ROS was not significantly different between DSR and DSRT, the DSR samples had 26% more total ROS than DSRT at the end of the experiment. As shown previously, DSR flies naturally deal with higher concentrations of ROS than DSRT (Figure 6) and have an upregulated repertoire of antioxidants that prevent oxidative stress in most tissues (Brennan et al., 2008). If VAS2870 is effectively inhibiting only Nox/Duox-generated ROS, the 26% difference in total ROS between DSR and DSRT may be accounted for by an unknown factor; the

contribution by *Wolbachia* to the total ROS in DSR is still a possibility and has not yet been explored.

4.3.11 *Wolbachia* infection increases the effectiveness of apocynin

Apocynin (4-hydroxy-3-methoxyacetophenone) was originally extracted from the herb *Picrorhiza kurroa* from the Himalayan Mountains and has been used as an NADPH oxidase inhibitor for the past 20 years. Recently, however, the effectiveness of this compound has been questioned and new data indicate that apocynin may have additional targets in a cell. To be fully effective as a Nox inhibitor, apocynin must be oxidized by H_2O_2 using peroxidase as a catalyst and the single apocynin radicals must dimerize or trimerize (Heumüller et al., 2008; Ximenes et al., 2007). Once dimerized, apocynin is thought to inhibit the translocation of the p^{47} subunit to the membrane where the NADPH oxidase complex is assembled (Barbieri et al., 2004).

When apocynin was added to the DSR and DSRT homogenates, there was a significant decrease in DCFDA fluorescence when compared to control samples (Figure 18). DSR had a 47.49% reduction and DSRT had 33.71% reduction in ROS. The presence of *Wolbachia* in DSR accounted for 13.8% more inhibition of ROS when compared with DSRT ($p > 0.05$).

Non-dimerized apocynin radicals can act as oxidants within cells; Apocynin reduces the GSH/GSSG ratio in human adherent monocyte cultures (Barbieri et al., 2004). *In vitro*, apocynin is able to increase oxidization of GSH to

GSSG and cysteine seven fold and this leads to GSH depletion over time (Castor et al., 2010). Most importantly, apocynin can oxidize NADPH, which is the substrate for all NADPH oxidase family members to produce ROS; oxidation and consumption of the NADPH substrate could affect the ability of all NADPH oxidases to generate superoxide or hydrogen peroxide (Castor et al., 2010). DSR flies contain significantly more ROS than DSRT flies [Figure 6 and (Brennan et al., 2012, 2008)]; once exposed to apocynin, the excess H_2O_2 may be responsible for the formation of excess apocynin radicals followed by oxidation of the of NADPH substrate and reduction in total ROS produced. Alternatively, the excess H_2O_2 may be responsible for an increase in apocynin dimerization and activity as an NADPH oxidase inhibitor.

4.3.12 DPI weakly inhibits ROS generation in *D. simulans*

DPI is now described as a general flavoprotein (contains a nucleotide derivative of riboflavin) inhibitor; xanthine oxidase, nitric oxide synthase, and NADPH oxidase are all flavoproteins and DPI strongly inhibits the superoxide generated by these two proteins (Wind et al., 2010). Alternatively, Chang *et al* (Chang et al., 2013) used DPI, in combination with *duoxA* (*duox* maturation factor) knockout mice, to determine that Duox is responsible for the excess H_2O_2 that contributes to the pathogenesis of allergic asthma. It is not currently known how DPI interacts with and inhibits flavoproteins.

In the *D. simulans* system, only a modest reduction in ROS occurred when DPI was added to cell extracts. DPI decreased total ROS in DSR by 25.15% and in DSRT by 16.44% (Figure 18). It is possible that the target of DPI inhibition does not exist in *D. simulans* or *D. melanogaster* and the reduction of ROS was a result of the antioxidant properties of the molecule (Wind et al., 2010).

4.3.13 Oral administration of apocynin and VAS2870 is not sufficient to influence *Wolbachia* density

Wolbachia infection in *D. simulans* leads to an increase in reactive oxygen species and oxidative stress in the form of DNA damage to the host (Brennan et al., 2012, 2008). Since dDuox was found in close proximity to *Wolbachia* in testes (Figure 14, 15, and 16), it became a good candidate as the agent responsible for generating the excess ROS. To this end, flies were seeded onto media supplemented with either apocynin or VAS2870 (Nox/Duox inhibitors) and the resulting F1 generation was analyzed to determine whether inhibition of dNox/dDuox could influence *Wolbachia* density. Unlike glutathione and ascorbic acid, however, neither apocynin nor VAS2870 had a significant influence on *Wolbachia* density in young whole males and females (Figure 18).

While an increase in *Wolbachia* following treatment with NADPH oxidase inhibitors, combined with the potent effect of these two compounds on total ROS in flies may have firmly established the role of dDuox as a modulator of *Wolbachia* titer in *D. simulans*, the failure to affect *Wolbachia* replication after

treatment does not necessarily rule out dDuox as a key factor in the regulation of *Wolbachia* density. Artificially colored fly media ensured that the developing larvae were ingesting the medium, but it is possible that VAS2870 was not distributed systemically throughout the flies and was impeded by the gut epithelium. VAS2870 is known to have poor solubility and is not ideal for *in vivo* studies (Wind et al., 2010), however, it is the only compound available that is known to specifically inhibit Duox function (Niethammer et al., 2009). A VAS2870 derivative, VAS3947 has very recently been developed and retains all of the same properties as VAS2870 except that the solubility is four times greater (Wind et al. 2010; Tegtmeier et al. 2005). Unfortunately, VAS3947 is not currently commercially available.

5. Conclusions

Understanding how *Wolbachia* density is regulated is an important aspect of *Wolbachia*-host biology; how *Wolbachia* density relates to the mechanisms of CI is still not fully understood. This study looked at two different aspects of the *w*Ri – *D. simulans* relationship to elucidate what factors are contributing to the regulation of *Wolbachia* density.

It was determined that, unlike other *Wolbachia*-host systems, the WO phage does not play a role in the maintenance of *w*Ri copy numbers within flies. This study did reveal, however, that two out of the three integrated prophages in the *w*Ri genome are phage remnants and that only WORiC is actively replicating. The redox control of *Wolbachia* density appears to be a more likely mechanism for

maintaining an optimal symbiont titer. DSR has adapted to tolerate a high amount of oxidative stress when *Wolbachia* is present and when the excess ROS is neutralized by the addition of exogenous antioxidants, *Wolbachia* is able to multiply without strict restriction. A likely candidate for the production of the high amount of ROS seen in DSR when compared to DSRT is dDuox, which is known to function as a professional ROS producer and is found in close association with *Wolbachia* in developing spermatocytes.

This study takes a unique approach at contributing to knowledge surrounding the factors that contribute to CI. While the effector molecules that are directly involved in modification of sperm chromatin were not investigated, a "step-back" approach was taken; *Wolbachia* density undoubtedly contributes to the concentration and delivery of the specific factors that elicit the CI phenotype. More work in this field is clearly necessary in order to understand the entire mechanism of CI as a whole.

6. Notes

[1] *A version of this chapter has been published. Biliske et al. 2011. BMC Microbiology 11:251.*

7. Literature Cited

Ahmarani, L., Avedanian, L., Al-Khoury, J., Perreault, C., Jacques, D., Bkaily, G., 2013. Whole-cell and nuclear NADPH oxidases levels and distribution in human endocardial endothelial, vascular smooth muscle, and vascular endothelial cells. Canadian Journal of Physiology and Pharmacology 91, 71–9.

Ahn, H.-M., Lee, K.-S., Lee, D.-S., Yu, K., 2012. JNK/FOXO mediated PeroxiredoxinV expression regulates redox homeostasis during Drosophila melanogaster gut infection. Developmental and Comparative Immunology 38, 466–73.

Alkhuder, K., Meibom, K.L., Dubail, I., Dupuis, M., Charbit, A., 2009. Glutathione provides a source of cysteine essential for intracellular multiplication of Francisella tularensis. PLoS Pathogens 5, e1000284.

Ameziane-El-Hassani, R., Morand, S., Boucher, J.-L., Frapart, Y.-M., ADupuypostolou, D., Agnandji, D., Gnidehou, S., Ohayon, R., Noël-Hudson, M.-S., Francon, J., Lalaoui, K., Virion, A., 2005. Dual oxidase-2 has an intrinsic Ca2+-dependent H2O2-generating activity. The Journal of Biological Chemistry 280, 30046–54.

Andrews, S.C., Robinson, A.K., Rodriguez-Quiñones, F., 2003. Bacterial iron homeostasis. FEMS Microbiology Reviews 27, 215–237.

Anh, N.T.T., Nishitani, M., Harada, S., Yamaguchi, M., Kamei, K., 2011. Essential role of Duox in stabilization of Drosophila wing. The Journal of Biological Chemistry 286, 33244–51.

Apontoweil, P., Berends, W., 1975. Glutathione biosynthesis in Escherichia coli K 12. Properties of the enzymes and regulation. Biochimica et Biophysica Acta 399, 1–9.

Aussel, L., Zhao, W., Hébrard, M., Guilhon, A.-A., Viala, J.P.M., Henri, S., Chasson, L., Gorvel, J.-P., Barras, F., Méresse, S., 2011. Salmonella detoxifying enzymes are sufficient to cope with the host oxidative burst. Molecular Microbiology 80, 628–40.

Aylward, F.O., Burnum, K.E., Scott, J.J., Suen, G., Tringe, S.G., Adams, S.M., Barry, K.W., Nicora, C.D., Piehowski, P.D., Purvine, S.O., Starrett, G.J., Goodwin, L. a, Smith, R.D., Lipton, M.S., Currie, C.R., 2012. Metagenomic and metaproteomic insights into bacterial communities in leaf-cutter ant fungus gardens. The ISME Journal 6, 1688–701.

Baldo, L., Werren, J.H., 2007. Revisiting Wolbachia supergroup typing based on WSP: spurious lineages and discordance with MLST. Current Microbiology 55, 81–7.

Bánfi, B., Molnár, G., Maturana, a, Steger, K., Hegedûs, B., Demaurex, N., Krause, K.H., 2001a. A Ca(2+)-activated NADPH oxidase in testis, spleen, and lymph nodes. The Journal of biological chemistry 276, 37594–601.

Bánfi, B., Molnár, G., Maturana, A., Steger, K., Hegedûs, B., Demaurex, N., Krause, K.H., 2001b. A Ca(2+)-activated NADPH oxidase in testis, spleen, and lymph nodes. The Journal of Biological Chemistry 276, 37594–601.

Bánfi, B., Tirone, F., Durussel, I., Knisz, J., Moskwa, P., Molnár, G.Z., Krause, K.-H., Cox, J.A., 2004. Mechanism of Ca2+ Activation of the NADPH Oxidase 5 (NOX5). Journal of Biological Chemistry 279 , 18583–18591.

Barbieri, S.S., Cavalca, V., Eligini, S., Brambilla, M., Caiani, A., Tremoli, E., Colli, S., 2004. Apocynin prevents cyclooxygenase 2 expression in human monocytes through NADPH oxidase and glutathione redox-dependent mechanisms. Free Radical Biology & Medicine 37, 156–65.

Barreau, C., Benson, E., Gudmannsdottir, E., Newton, F., White-Cooper, H., 2008. Post-meiotic transcription in Drosophila testes. Development 135, 1897–902.

Beckmann, J.F., Markowski, T.W., Witthuhn, B. a, Fallon, A.M., 2013. Detection of the Wolbachia-encoded DNA binding protein, HU beta, in mosquito gonads. Insect Biochemistry and Molecular Biology 43, 272–9.

Biliske, J. a, Batista, P.D., Grant, C.L., Harris, H.L., 2011. The bacteriophage WORiC is the active phage element in wRi of Drosophila simulans and represents a conserved class of WO phages. BMC Microbiology 11, 251.

Biterova, E.I., Barycki, J.J., 2009. Mechanistic details of glutathione biosynthesis revealed by crystal structures of Saccharomyces cerevisiae glutamate cysteine ligase. The Journal of Biological Chemistry 284, 32700–8.

Bonilla, E., Medina-Leendertz, S., Villalobos, V., Molero, L., Bohórquez, A., 2006. Paraquat-induced oxidative stress in drosophila melanogaster: effects of melatonin, glutathione, serotonin, minocycline, lipoic acid and ascorbic acid. Neurochemical Research 31, 1425–32.

Bonnefoy, E., Orsi, G. a, Couble, P., Loppin, B., 2007. The essential role of Drosophila HIRA for de novo assembly of paternal chromatin at fertilization. PLoS Genetics 3, 1991–2006.

Bordenstein, S.R., Marshall, M.L., Fry, A.J., Kim, U., Wernegreen, J.J., 2006. The tripartite associations between bacteriophage, Wolbachia, and arthropods. PLoS Pathogens 2, e43.

Bordenstein, S.R., Wernegreen, J.J., 2004. Bacteriophage flux in endosymbionts (Wolbachia): infection frequency, lateral transfer, and recombination rates. Molecular Biology and Evolution 21, 1981–91.

Bordenstein, S.R., Werren, J.H., 2000. Do Wolbachia influence fecundity in Nasonia vitripennis? Heredity 84 (Pt 1), 54–62.

Bordenstein, Sarah R, Bordenstein, Seth R, 2011. Temperature affects the tripartite interactions between bacteriophage WO, Wolbachia, and cytoplasmic incompatibility. PloS One 6, e29106.

Bossan, B., Koehncke, A., Hammerstein, P., 2011. A new model and method for understanding Wolbachia-induced cytoplasmic incompatibility. PloS One 6, e19757.

Bouchon, D., Rigaud, T., Juchault, P., 1998. Evidence for widespread Wolbachia infection in isopod crustaceans: molecular identification and host feminization. Proceedings. Biological sciences / The Royal Society 265, 1081–90.

Bourtzis, K., Nirgianaki, A., Markakis, G., Savakis, C., 1996. Wolbachia Infection and Cytoplasmic Incompatibility in Drosophila Species. Genetics 144, 1063–1073.

Brennan, L.J., Haukedal, J. a, Earle, J.C., Keddie, B., Harris, H.L., 2012. Disruption of redox homeostasis leads to oxidative DNA damage in spermatocytes of Wolbachia-infected Drosophila simulans. Insect Molecular Biology 21, 510–20.

Brennan, L.J., Keddie, B.A., Braig, H.R., Harris, H.L., 2008. The endosymbiont Wolbachia pipientis induces the expression of host antioxidant proteins in an Aedes albopictus cell line. PloS One 3, e2083.

Brownlie, J.C., Cass, B.N., Riegler, M., Witsenburg, J.J., Iturbe-Ormaetxe, I., McGraw, E. a, O'Neill, S.L., 2009. Evidence for metabolic provisioning by a common invertebrate endosymbiont, Wolbachia pipientis, during periods of nutritional stress. PLoS Pathogens 5, e1000368.

Caldera, E.J., Poulsen, M., Suen, G., Currie, C.R., 2009. Insect Symbioses: A Case Study of Past, Present, and Future Fungus-Growing Ant Research. Environmental Entomology 38, 78–92.

Calderwood, S.B., Mekalanos, J.J., 1987. Iron regulation of Shiga-like toxin expression in Escherichia coli is mediated by the fur locus. Journal of Bacteriology 169, 4759–64.

Callaini, G., Dallai, R., Riparbelli, M.G., 1997. Wolbachia-induced delay of paternal chromatin condensation does not prevent maternal chromosomes from entering anaphase in incompatible crosses of Drosophila simulans. Journal of Cell Science 110, 271–80.

Canchaya, C., Proux, C., Fournous, G., Bruttin, A., Brussow, H., 2003. Prophage Genomics. Microbiology and Molecular Biology Reviews 67, 238–276.

Casiraghi, M., Bordenstein, S.R., Baldo, L., Lo, N., Beninati, T., Wernegreen, J.J., Werren, J.H., Bandi, C., 2005. Phylogeny of Wolbachia pipientis based on gltA, groEL and ftsZ gene sequences: clustering of arthropod and nematode symbionts in the F supergroup, and evidence for further diversity in the Wolbachia tree. Microbiology 151, 4015–22.

Casjens, S., 2003. Prophages and bacterial genomics: what have we learned so far? Molecular Microbiology 49, 277–300.

Castor, L.R.G., Locatelli, K.A., Ximenes, V.F., 2010. Pro-oxidant activity of apocynin radical. Free Radical Biology & Medicine 48, 1636–43.

Caturegli, P., Asanovich, K.M., Walls, J.J., Bakken, J.S., Madigan, J.E., Popov, V.L., Dumler, J.S., 2000. ankA: an Ehrlichia phagocytophilia group gene encoding a cytoplasmic protein antigen with ankyrin repeats. Infection and Immunity 68, 5277–5283.

Chang, S., Linderholm, A., Franzi, L., Kenyon, N., Grasberger, H., Harper, R., 2013. Dual oxidase regulates neutrophil recruitment in allergic airways. Free Radical Biology & Medicine 65, 38–46.

Chatterjee, I.B., 2013. Evolution and the Biosynthesis of Ascorbic Acid. Science 182, 1271–1272.

Cheng, Z., Arscott, L.D., Ballou, D.P., Williams, C.H., 2007. The relationship of the redox potentials of thioredoxin and thioredoxin reductase from Drosophila melanogaster to the enzymatic mechanism: reduced thioredoxin is the reductant of glutathione in Drosophila. Biochemistry 46, 7875–85.

Cho, K.-O., Kim, G.-W., Lee, O.-K., 2011. Wolbachia bacteria reside in host Golgi-related vesicles whose position is regulated by polarity proteins. PloS One 6, e22703.

Choi, J., Ou, J.-H.J., 2006. Mechanisms of liver injury. III. Oxidative stress in the pathogenesis of hepatitis C virus. American Journal of Physiology. Gastrointestinal and Liver Physiology 290, G847–51.

Clark, M. a, Moran, N. a, Baumann, P., 1999. Sequence evolution in bacterial endosymbionts having extreme base compositions. Molecular bBology and Evolution 16, 1586–98.

Clark, M.E., Karr, T.L., 2002. Distribution of Wolbachia Within Drosophila Reproductive Tissue: Implications for the Expression of Cytoplasmic Incompatibility. Integrated and Comparative Biology 339, 332–339.

Clark, M.E., Veneti, Z., Bourtzis, K., Karr, T.L., 2003. Wolbachia distribution and cytoplasmic incompatibility during sperm development : the cyst as the basic cellular unit of CI expression. Mechanisms of Development 120, 185–198.

Correa, C.C., Ballard, J.W.O., 2012. Wolbachia gonadal density in female and male Drosophila vary with laboratory adaptation and respond differently to physiological and environmental challenges. Journal of Invertebrate Pathology 111, 197–204.

Covacin, C., Barker, S.C., 2007. Supergroup F Wolbachia bacteria parasitise lice (Insecta: Phthiraptera). Parasitology Research 100, 479–85.

Dale, C., Moran, N. a, 2006. Molecular interactions between bacterial symbionts and their hosts. Cell 126, 453–65.

De Cuevas, M., Matunis, E.L., 2011. The stem cell niche: lessons from the Drosophila testis. Development 138 , 2861–2869.

Dedeine, F., Vavre, F., Fleury, F., Loppin, B., Hochberg, M.E., Bouletreau, M., 2001. Removing symbiotic Wolbachia bacteria specifically inhibits oogenesis in a parasitic wasp. Proceedings of the National Academy of Sciences of the United States of America 98, 6247–52.

Dizdaroglu, M., 2012. Oxidatively induced DNA damage: mechanisms, repair and disease. Cancer Letters 327, 26–47.

Dobson, S.L., Rattanadechakul, W., Marsland, E.J., 2004. Fitness advantage and cytoplasmic incompatibility in Wolbachia single- and superinfected Aedes albopictus. Heredity 93, 135–42.

Drancourt, M., Raoult, D., 1994. Taxonomic position of the Rickettsiae: current knowledge. FEMS Microbiology Reviews 13, 13–24.

Dudkina, N. V, Kiseleva, E. V, 2005. Structural organization and distribution of the symbiotic bacteria Wolbachia during spermatogenesis of Drosophila simulans. Ontogenez 36, 41–50.

Dumler, J.S., Choi, K., Garcia-garcia, J.C., Barat, N.S., Scorpio, D.G., Garyu, J.W., Grab, D.J., Bakken, J.S., 2005. Human Granulocytic Anaplasmosis and Anaplasma phagocytophilum. Emerging Infectious Diseases 11, 1828–1834.

Duplouy, A., Iturbe-Ormaetxe, I., Beatson, S. a, Szubert, J.M., Brownlie, J.C., McMeniman, C.J., McGraw, E. a, Hurst, G.D., Charlat, S., O Neill, S.L., Woolfit, M., 2013. Draft genome sequence of the male-killing Wolbachia strain wBol1 reveals recent horizontal gene transfers from diverse sources. BMC Genomics 14, 20.

Eruslanov, E., Kusmartsev, S., 2010. Identification of ROS Using Oxidized DCFDA and Flow-Cytometry, in: Armstrong, D. (Ed.), Advanced Protocols in Oxidative Stress II SE - 4. Humana Press, pp. 57–72.

Fabrizio, J.J., Hime, G., Lemmon, S.K., Bazinet, C., 1998. Genetic dissection of sperm individualization in Drosophila melanogaster. Development 125, 1833–43.

Fahey, R.C., Brown, W.C., Adams, W.B., Worsham, M.B., 1978. Occurrence of glutathione in bacteria. Journal of bacteriology 133, 1126–9.

Fenn, K., Conlon, C., Jones, M., Quail, M. a, Holroyd, N.E., Parkhill, J., Blaxter, M., 2006. Phylogenetic relationships of the Wolbachia of nematodes and arthropods. PLoS pathogens 2, e94.

Fenton, H.J.H., 1894. LXXIII.-Oxidation of tartaric acid in presence of iron. Journal of the Chemical Society, Transactions 65, 899–910.

Ferree, P.M., Sullivan, W., 2006. A genetic test of the role of the maternal pronucleus in Wolbachia-induced cytoplasmic incompatibility in Drosophila melanogaster. Genetics 173, 839–47.

Ferri, E., Bain, O., Barbuto, M., Martin, C., Lo, N., Uni, S., Landmann, F., Baccei, S.G., Guerrero, R., de Souza Lima, S., Bandi, C., Wanji, S., Diagne, M., Casiraghi, M., 2011. New insights into the evolution of Wolbachia infections in filarial nematodes inferred from a large range of screened species. PloS One 6, e20843.

Foster, J., Ganatra, M., Kamal, I., Ware, J., Makarova, K., Ivanova, N., Bhattacharyya, A., Kapatral, V., Kumar, S., Posfai, J., Vincze, T., Ingram, J., Moran, L., Lapidus, A., Omelchenko, M., Kyrpides, N., Ghedin, E., Wang,

S., Goltsman, E., Joukov, V., Ostrovskaya, O., Tsukerman, K., Mazur, M., Comb, D., Koonin, E., Slatko, B., 2005. The Wolbachia genome of Brugia malayi: endosymbiont evolution within a human pathogenic nematode. PLoS bBology 3, e121.

Fujii, Y., Kubo, T., Ishikawa, H., Sasaki, T., 2004. Isolation and characterization of the bacteriophage WO from Wolbachia, an arthropod endosymbiont. Biochemical and biophysical research communications 317, 1183–8.

Gamston, C., Rasgon, J., 2007. Maintaining Wolbachia in cell-free medium. Journal of visualized experiments : JoVE 223.

Garcia-Garcia, J.C., Rennoll-Bankert, K.E., Pelly, S., Milstone, A.M., Dumler, J.S., 2009. Silencing of host cell CYBB gene expression by the nuclear effector AnkA of the intracellular pathogen Anaplasma phagocytophilum. Infection and Immunity 77, 2385–91.

Gatto, G.J., Ao, Z., Kearse, M.G., Zhou, M., Morales, C.R., Daniels, E., Bradley, B.T., Goserud, M.T., Goodman, K.B., Douglas, S. a, Harpel, M.R., Johns, D.G., 2013a. NADPH oxidase-dependent and -independent mechanisms of reported inhibitors of reactive oxygen generation. Journal of enzyme inhibition and medicinal chemistry 28, 95–104.

Gatto, G.J., Ao, Z., Kearse, M.G., Zhou, M., Morales, C.R., Daniels, E., Bradley, B.T., Goserud, M.T., Goodman, K.B., Douglas, S. a, Harpel, M.R., Johns, D.G., 2013b. NADPH oxidase-dependent and -independent mechanisms of reported inhibitors of reactive oxygen generation. Journal of enzyme inhibition and medicinal chemistry 28, 95–104.

Gavotte, L., Vavre, F., Henri, H., Ravallec, M., Stouthamer, R., Boulétreau, M., 2004. Diversity, distribution and specificity of WO phage infection in Wolbachia of four insect species. Insect molecular biology 13, 147–53.

Gönczy, P., DiNardo, S., 1996. The germ line regulates somatic cyst cell proliferation and fate during Drosophila spermatogenesis. Development (Cambridge, England) 122, 2437–47.

Gottlieb, Y., Zchori-fein, E., Werren, J.H., Karr, T.L., 2011. Diploidy restoration in Wolbachia-infected Muscidifurax uniraptor (Hymenoptera : Pteromalidae). Journal of Invertebrate Pathology 81, 166–174.

Graveley, B.R., Brooks, A.N., Carlson, J.W., Duff, M.O., Landolin, J.M., Yang, L., Artieri, C.G., van Baren, M.J., Boley, N., Booth, B.W., Brown, J.B., Cherbas, L., Davis, C.A., Dobin, A., Li, R., Lin, W., Malone, J.H., Mattiuzzo, N.R., Miller, D., Sturgill, D., Tuch, B.B., Zaleski, C., Zhang, D., Blanchette,

M., Dudoit, S., Eads, B., Green, R.E., Hammonds, A., Jiang, L., Kapranov, P., Langton, L., Perrimon, N., Sandler, J.E., Wan, K.H., Willingham, A., Zhang, Y., Zou, Y., Andrews, J., Bickel, P.J., Brenner, S.E., Brent, M.R., Cherbas, P., Gingeras, T.R., Hoskins, R.A., Kaufman, T.C., Oliver, B., Celniker, S.E., 2011. The developmental transcriptome of Drosophila melanogaster. Nature 471, 473–479.

Gunduz, E.A., Douglas, A.E., 2009. Symbiotic bacteria enable insect to use a nutritionally inadequate diet. Proceedings of the Royal Society B 276, 987–991.

Ha, E.-M., Lee, K.-A., Park, S.H., Kim, S.-H., Nam, H.-J., Lee, H.-Y., Kang, D., Lee, W.-J., 2009a. Regulation of DUOX by the Galphaq-phospholipase Cbeta-Ca2+ pathway in Drosophila gut immunity. Developmental cell 16, 386–97.

Ha, E.-M., Lee, K.-A., Seo, Y.Y., Kim, S.-H., Lim, J.-H., Oh, B.-H., Kim, J., Lee, W.-J., 2009b. Coordination of multiple dual oxidase-regulatory pathways in responses to commensal and infectious microbes in drosophila gut. Nature immunology 10, 949–57.

Ha, E.-M., Oh, C.-T., Bae, Y.S., Lee, W.-J., 2005. A direct role for dual oxidase in Drosophila gut immunity. Science (New York, N.Y.) 310, 847–50.

Haegeman, A., Vanholme, B., Jacob, J., Vandekerckhove, T.T.M., Claeys, M., Borgonie, G., Gheysen, G., 2009. An endosymbiotic bacterium in a plant-parasitic nematode: member of a new Wolbachia supergroup. International Journal for Parasitology 39, 1045–54.

Harris, H.L., Brennan, L.J., Keddie, B.A., Braig, H.R., 2010. Bacterial symbionts in insects: balancing life and death. Symbiosis 51, 37–53.

Hertig, M., Wolbach, S.B., 1924. Studies on Rickettsia-Like Micro-Organisms in Insects. The Journal of medical research 44, 329–374.7.

Heumüller, S., Wind, S., Barbosa-Sicard, E., Schmidt, H.H.H.W., Busse, R., Schröder, K., Brandes, R.P., 2008. Apocynin is not an inhibitor of vascular NADPH oxidases but an antioxidant. Hypertension 51, 211–7.

Hilgenboecker, K., Hammerstein, P., Schlattmann, P., Telschow, A., Werren, J.H., 2008. How many species are infected with Wolbachia?--A statistical analysis of current data. FEMS microbiology letters 281, 215–20.

Hoerauf, A., Mand, S., Volkmann, L., Büttner, M., Marfo-Debrekyei, Y., Taylor, M., Adjei, O., Büttner, D.W., 2003. Doxycycline in the treatment of human

onchocerciasis: Kinetics of Wolbachia endobacteria reduction and of inhibition of embryogenesis in female Onchocerca worms. Microbes and infection / Institut Pasteur 5, 261–73.

Hoffmann, A.A., Turelli, M., 1988. Unidirectional Incompatibility in Drosophila simulans: Inheritance, Geographic Variation and Fitness Effects. Genetics 119, 435–444.

Hosokawa, T., Koga, R., Kikuchi, Y., Meng, X.-Y., Fukatsu, T., 2010. Wolbachia as a bacteriocyte-associated nutritional mutualist. Proceedings of the National Academy of Sciences of the United States of America 107, 769–74.

Hoste, C., Dumont, J.E., Miot, F., De Deken, X., 2012. The type of DUOX-dependent ROS production is dictated by defined sequences in DUOXA. Experimental cell research 318, 2353–64.

Hurst, G.D.D., Jiggins, F.M., Schulenburg, J.H.G. Von Der, Bertrand, D., West, S.A., Goriacheva, I.I., Zakharov, I.A., Werren, J.H., Stouthamer, R., Majerus, M.E.N., Hurstl, G.D.D., London, J.W., 2013. Male-killing Wolbachia in two species of insects. Proceedings. Biological sciences / The Royal Society 266, 735–740.

Ikeda, T., Ishikawa, H., Sasaki, T., 2003. Infection density of Wolbachia and level of cytoplasmic incompatibility in the Mediterranean flour moth, Ephestia kuehniella. Journal of Invertebrate Pathology 84, 1–5.

Inaba, M., Yuan, H., Salzmann, V., Fuller, M.T., Yamashita, Y.M., 2010. E-cadherin is required for centrosome and spindle orientation in Drosophila male germline stem cells. PloS one 5, e12473.

Ishmael, N., Dunning Hotopp, J.C., Ioannidis, P., Biber, S., Sakamoto, J., Siozios, S., Nene, V., Werren, J., Bourtzis, K., Bordenstein, S.R., Tettelin, H., 2009. Extensive genomic diversity of closely related Wolbachia strains. Microbiology 155, 2211–22.

Jaenike, J., Unckless, R., Cockburn, S.N., Boelio, L.M., Perlman, S.J., 2010. Adaptation via symbiosis: recent spread of a Drosophila defensive symbiont. Science (New York, N.Y.) 329, 212–5.

Kawahara, T., Quinn, M.T., Lambeth, J.D., 2007. Molecular evolution of the reactive oxygen-generating NADPH oxidase (Nox/Duox) family of enzymes. BMC evolutionary biology 7, 109.

KC Binnington and AA Hoffmann, 1989. Wolbachia-like Organisms and Cytoplasmic Incompatibility in Drosophila simulans. Journal of Invertebrate Pathology 352, 344–352.

Kent, B.N., Bordenstein, S.R., 2011. Phage WO of Wolbachia: lambda of the endosymbiont world 18, 173–181.

Kimura, K., Kidwell, M.G., 1994. Differences in P element population dynamics between the sibling species Drosophila melanogaster and Drosophila simulans. Genetics Research 63, 27–38.

Klasson, L., Walker, T., Sebaihia, M., Sanders, M.J., Quail, M. a, Lord, A., Sanders, S., Earl, J., O'Neill, S.L., Thomson, N., Sinkins, S.P., Parkhill, J., 2008. Genome evolution of Wolbachia strain wPip from the Culex pipiens group. Molecular bBology and Evolution 25, 1877–87.

Klasson, L., Westberg, J., Sapountzis, P., Näslund, K., Lutnaes, Y., Darby, A.C., Veneti, Z., Chen, L., Braig, H.R., Garrett, R., Bourtzis, K., Andersson, S.G.E., 2009. The mosaic genome structure of the Wolbachia wRi strain infecting Drosophila simulans. Proceedings of the National Academy of Sciences of the United States of America 106, 5725–30.

Korshunov, S.S., Imlay, J. a, 2002. A potential role for periplasmic superoxide dismutase in blocking the penetration of external superoxide into the cytosol of Gram-negative bacteria. Molecular microbiology 43, 95–106.

Kremer, N., Voronin, D., Charif, D., Mavingui, P., Mollereau, B., Vavre, F., 2009a. Wolbachia interferes with ferritin expression and iron metabolism in insects. PLoS pathogens 5, e1000630.

Kremer, N., Voronin, D., Charif, D., Mavingui, P., Mollereau, B., Vavre, F., 2009b. Wolbachia interferes with ferritin expression and iron metabolism in insects. PLoS pathogens 5, e1000630.

Landmann, F., Orsi, G. a, Loppin, B., Sullivan, W., 2009. Wolbachia-mediated cytoplasmic incompatibility is associated with impaired histone deposition in the male pronucleus. PLoS pathogens 5, e1000343.

Lassya, C.W., Karr, T.L., 1996. Cytological analysis of fertilization and early embryonic development incompatible crosses of. Mechanisms of development 57, 47–58.

Lattorff, H.M.G., Moritz, R.F. a, Crewe, R.M., Solignac, M., 2007. Control of reproductive dominance by the thelytoky gene in honeybees. Biology letters 3, 292–5.

Lee, K.-A., Kim, S.-H., Kim, E.-K., Ha, E.-M., You, H., Kim, B., Kim, M.-J., Kwon, Y., Ryu, J.-H., Lee, W.-J., 2013. Bacterial-Derived Uracil as a Modulator of Mucosal Immunity and Gut-Microbe Homeostasis in Drosophila. Cell 153, 797–811.

Lefoulon, E., Gavotte, L., Junker, K., Barbuto, M., Uni, S., Landmann, F., Laaksonen, S., Saari, S., Nikander, S., de Souza Lima, S., Casiraghi, M., Bain, O., Martin, C., 2012. A new type F Wolbachia from Splendidofilariinae (Onchocercidae) supports the recent emergence of this supergroup. International Journal for Parasitology 42, 1025–36.

Lin, M., den Dulk-Ras, A., Hooykaas, P.J.J., Rikihisa, Y., 2007. Anaplasma phagocytophilum AnkA secreted by type IV secretion system is tyrosine phosphorylated by Abl-1 to facilitate infection. Cellular Microbiology 9, 2644–57.

Lin, T.Y., Viswanathan, S., Wood, C., Wilson, P.G., Wolf, N., Fuller, M.T., 1996. Coordinate developmental control of the meiotic cell cycle and spermatid differentiation in Drosophila males. Development 122, 1331–41.

Little, J.W., Michalowski, C.B., 2010. Stability and instability in the lysogenic state of phage lambda. Journal of bacteriology 192, 6064–76.

Lo, N., Paraskevopoulos, C., Bourtzis, K., O'Neill, S.L., Werren, J.H., Bordenstein, S.R., Bandi, C., 2007. Taxonomic status of the intracellular bacterium Wolbachia pipientis. International Journal of Systematic and Evolutionary Microbiology 57, 654–7.

Loppin, B., Bonnefoy, E., Anselme, C., Laurençon, A., Karr, T.L., Couble, P., 2005. The histone H3.3 chaperone HIRA is essential for chromatin assembly in the male pronucleus. Nature 437, 1386–90.

MacLeod, E.T., Maudlin, I., Darby, a C., Welburn, S.C., 2007. Antioxidants promote establishment of trypanosome infections in tsetse. Parasitology 134, 827–31.

Maiorino, M., Ursini, F., Bosello, V., Toppo, S., Tosatto, S.C.E., Mauri, P., Becker, K., Roveri, A., Bulato, C., Benazzi, L., De Palma, A., Flohé, L., 2007. The thioredoxin specificity of Drosophila GPx: a paradigm for a peroxiredoxin-like mechanism of many glutathione peroxidases. Journal of molecular biology 365, 1033–46.

Martin, G., Sorokine, O., Moniatte, M., Bulet, P., Hetru, C., Van Dorsselaer, A., 1999. The structure of a glycosylated protein hormone responsible for sex

determination in the isopod, Armadillidium vulgare. The European Journal of Biochemistry 262, 727–736.

Masip, L., Veeravalli, K., Georgiou, G., 2006. The Many Faces of Glutathione in Bacteria. Antioxidants & redox signaling 8, 753–762.

Massie, H.R., Baird, M.B., Piekielniak, M.J., 1976. Ascorbic acid and longevity in Drosophila. Experimental gerontology 11, 37–41.

Masui, S., Kamoda, S., Sasaki, T., Ishikawa, H., 2000a. Distribution and Evolution of Bacteriophage WO in Wolbachia , the Endosymbiont Causing Sexual Alterations in Arthropods. Journal of molecular evolution 035513, 491–497.

Masui, S., Kuroiwa, H., Sasaki, T., Inui, M., Kuroiwa, T., Ishikawa, H., 2001. Bacteriophage WO and virus-like particles in Wolbachia, an endosymbiont of arthropods. Biochemical and biophysical research communications 283, 1099–104.

Masui, S., Sasaki, T., Ishikawa, H., 2000b. Genes for the Type IV Secretion System in an Intracellular Symbiont , Wolbachia , a Causative Agent of Various Sexual Alterations in Arthropods Genes for the Type IV Secretion System in an Intracellular Symbiont , Wolbachia , a Causative Agent of Various. The Journal of Bacteriology 182, 6529–6531.

Mathers, J., Fraser, J.A., Mcmahon, M., Saunders, R.D.C., Hayes, J.D., Mclellan, L.I., 2004. Antioxidant and cytoprotective responses to redox stress. Biochemical Society Symposia 176, 157–176.

Mavingui, P., Valiente Moro, C., Tran-Van, V., Wisniewski-Dyé, F., Raquin, V., Minard, G., Tran, F.-H., Voronin, D., Rouy, Z., Bustos, P., Lozano, L., Barbe, V., González, V., 2012. Whole-genome sequence of Wolbachia strain wAlbB, an endosymbiont of tiger mosquito vector Aedes albopictus. Journal of Bacteriology 194, 1840.

McGraw, E. a, Merritt, D.J., Droller, J.N., O'Neill, S.L., 2001. Wolbachia-mediated sperm modification is dependent on the host genotype in Drosophila. Proceedings. Biological sciences / The Royal Society 268, 2565–70.

Meister, A., 1994. Minireview: Glutathione-Ascorbic Acid Antioxidant System in Animals. The Journal of Biological Chemistry 13, 9397–9400.

Metzendorf, C., Lind, M.I., 2010. Drosophila mitoferrin is essential for male fertility: evidence for a role of mitochondrial iron metabolism during spermatogenesis. BMC developmental biology 10, 68.

Min, K.T., Benzer, S., 1997. Wolbachia, normally a symbiont of Drosophila, can be virulent, causing degeneration and early death. Proceedings of the National Academy of Sciences of the United States of America 94, 10792–6.

Morand, S., Ueyama, T., Tsujibe, S., Saito, N., Korzeniowska, A., Leto, T.L., 2009. Duox maturation factors form cell surface complexes with Duox affecting the specificity of reactive oxygen species generation. FASEB journal : official publication of the Federation of American Societies for Experimental Biology 23, 1205–18.

Moreira, S., Stramer, B., Evans, I., Wood, W., Martin, P., 2010. Prioritization of Competing Damage and Developmental Signals by Migrating Macrophages in the Drosophila Embryo. Current Biology 20, 464–470.

Musset, B., Clark, R. a, DeCoursey, T.E., Petheo, G.L., Geiszt, M., Chen, Y., Cornell, J.E., Eddy, C. a, Brzyski, R.G., El Jamali, A., 2012. NOX5 in human spermatozoa: expression, function, and regulation. The Journal of biological chemistry 287, 9376–88.

Neretti, N., Wang, P.-Y., Brodsky, A.S., Nyguyen, H.H., White, K.P., Rogina, B., Helfand, S.L., 2009. Long-lived Indy induces reduced mitochondrial reactive oxygen species production and oxidative damage. Proceedings of the National Academy of Sciences of the United States of America 106, 2277–82.

Niethammer, P., Grabher, C., Look, a T., Mitchison, T.J., 2009. A tissue-scale gradient of hydrogen peroxide mediates rapid wound detection in zebrafish. Nature 459, 996–9.

Nigro L. and Louis C., 1989. Ultrastructural Evidence of Wolbachia Rickettsiales in Drosophila simulans and Their Relationships with Unidirectional Cross-Incompatibility. Journal of Invertebrate Pathology 44, 39–44.

Noda, H., Koizumi, Y., Zhang, Q., Deng, K., 2001. Infection density of Wolbachia and incompatibility level in two planthopper species, Laodelphax striatellus and Sogatella furcifera. Insect biochemistry and molecular biology 31, 727–37.

O'Neill, S.L., Giordano, R., Colbert, a M., Karr, T.L., Robertson, H.M., 1992. 16S rRNA phylogenetic analysis of the bacterial endosymbionts associated

with cytoplasmic incompatibility in insects. Proceedings of the National Academy of Sciences of the United States of America 89, 2699–702.

Oh, H.W., Kim, M.G., Shin, S.W., Bae, K.S., Ahn, Y.J., Park, H.Y., 2000. Ultrastructural and molecular identification of a Wolbachia endosymbiont in a spider, Nephila clavata. Insect molecular biology 9, 539–43.

Ohsako, T., Hirai, K., Yamamoto, M.-T., 2003. The Drosophila misfire gene has an essential role in sperm activation during fertilization. Genes & genetic systems 78, 253–66.

Oliveira, G.D.A., Lieberman, J., Barillas-Mury, C., 2012. Epithelial nitration by a peroxidase/NOX5 system mediates mosquito antiplasmodial immunity. Science (New York, N.Y.) 335, 856–9.

Oliver, K.M., Russell, J. a, Moran, N. a, Hunter, M.S., 2003. Facultative bacterial symbionts in aphids confer resistance to parasitic wasps. Proceedings of the National Academy of Sciences of the United States of America 100, 1803–7.

Orr, W.C., Radyuk, S.N., Prabhudesai, L., Toroser, D., Benes, J.J., Luchak, J.M., Mockett, R.J., Rebrin, I., Hubbard, J.G., Sohal, R.S., 2005. Overexpression of glutamate-cysteine ligase extends life span in Drosophila melanogaster. The Journal of biological chemistry 280, 37331–8.

Paddock, C.D., Childs, J.E., 2003. Ehrlichia chaffeensis : a Prototypical Emerging Pathogen Ehrlichia chaffeensis : a Prototypical Emerging Pathogen 16.

Pan, X., Zhou, G., Wu, J., Bian, G., Lu, P., Raikhel, A.S., Xi, Z., 2012. Wolbachia induces reactive oxygen species (ROS)-dependent activation of the Toll pathway to control dengue virus in the mosquito Aedes aegypti. Proceedings of the National Academy of Sciences of the United States of America 109, E23–31.

Panaram, K., Marshall, J.L., 2007. F supergroup Wolbachia in bush crickets: what do patterns of sequence variation reveal about this supergroup and horizontal transfer between nematodes and arthropods? Genetica 130, 53–60.

Pannebakker, B.A., Pijnacker, L.P., Zwaan, B.J., Beukeboom, L.W., 2004. Cytology of Wolbachia-induced parthenogenesis in Leptopilina clavipes (Hymenoptera : Figitidae). Genome 303, 299–303.

Park, J., Kim, K.J., Choi, K., Grab, D.J., Dumler, J.S., 2004. Anaplasma phagocytophilum AnkA binds to granulocyte DNA and nuclear proteins. Cellular Microbiology 6, 743–51.

Petrônio, M.S., Zeraik, M.L., Fonseca, L.M. Da, Ximenes, V.F., 2013. Apocynin: chemical and biophysical properties of a NADPH oxidase inhibitor. Molecules (Basel, Switzerland) 18, 2821–39.

Pichon, S., Bouchon, D., Cordaux, R., Chen, L., Garrett, R. a, Grève, P., 2009. Conservation of the Type IV secretion system throughout Wolbachia evolution. Biochemical and biophysical research communications 385, 557–62.

Pitzschke, A., Hirt, H., 2010. New insights into an old story: Agrobacterium-induced tumour formation in plants by plant transformation. The EMBO journal 29, 1021–32.

Popov, V.L., Han, V.C., Chen, S.M., Dumler, J.S., Feng, H.M., Andreadis, T.G., Tesh, R.B., Walker, D.H., 1998. Ultrastructural differentiation of the genogroups in the genus Ehrlichia. Journal of medical microbiology 47, 235–51.

Rabeling, C., Kronauer, D.J.C., 2013. Thelytokous parthenogenesis in eusocial hymenoptera. Annual review of entomology 58, 273–92.

Raja, S.J., Renkawitz-pohl, R., 2005. Replacement by Drosophila melanogaster Protamines and Mst77F of Histones during Chromatin Condensation in Late Spermatids and Role of Sesame in the Removal of These Proteins from the Male Pronucleus Replacement by Drosophila melanogaster Protamines and Ms.

Rasgon, J.L., Gamston, C.E., Ren, X., 2006. Survival of Wolbachia pipientis in cell-free medium. Applied and environmental microbiology 72, 6934–7.

Rathke, C., Baarends, W.M., Jayaramaiah-Raja, S., Bartkuhn, M., Renkawitz, R., Renkawitz-Pohl, R., 2007. Transition from a nucleosome-based to a protamine-based chromatin configuration during spermiogenesis in Drosophila. Journal of cell science 120, 1689–700.

Razzell, W., Evans, I.R., Martin, P., Wood, W., 2013. Calcium Flashes Orchestrate the Wound Inflammatory Response through DUOX Activation and Hydrogen Peroxide Release. Current biology : CB 23, 424–429.

Rikihisa, Y., 2010. Anaplasma phagocytophilum and Ehrlichia chaffeensis: subversive manipulators of host cells. Nature reviews. Microbiology 8, 328–39.

Riparbelli, M.G., Giordano, R., Ueyama, M., Callaini, G., 2012. Wolbachia-mediated male killing is associated with defective chromatin remodeling. PloS one 7, e30045.

Ritsick, D.R., Edens, W. a, Finnerty, V., Lambeth, J.D., 2007. Nox regulation of smooth muscle contraction. Free radical biology & medicine 43, 31–8.

Rogina, B., Reenan, R.A., Nilsen, S.P., Helfland, S.L., 2000. Extended Life-Span Conferred by Cotransporter Gene Mutations in Drosophila. Science 290, 2137–2140.

Rousset, F., Bouchon, D., Pintureau, B., Juchault, P., Solignac, M., 1992. Wolbachia endosymbionts responsible for various alterations of sexuality in arthropods. Proceedings. Biological sciences / The Royal Society 250, 91–8.

Ruang-areerate, T., Kittayapong, P., McGraw, E. a, Baimai, V., O'Neill, S.L., 2004. Wolbachia replication and host cell division in Aedes albopictus. Current microbiology 49, 10–2.

Ruangkiattikul, N., Bhubhanil, S., Chamsing, J., Niamyim, P., Sukchawalit, R., Mongkolsuk, S., 2012. Agrobacterium tumefaciens membrane-bound ferritin plays a role in protection against hydrogen peroxide toxicity and is negatively regulated by the iron response regulator. FEMS microbiology letters 329, 87–92.

Salzberg, S.L., Puiu, D., Sommer, D.D., Nene, V., Lee, N.H., 2009. Genome sequence of the Wolbachia endosymbiont of Culex quinquefasciatus JHB. Journal of bacteriology 191, 1725.

Saridaki, A., Sapountzis, P., Harris, H.L., Batista, P.D., Biliske, J. a, Pavlikaki, H., Oehler, S., Savakis, C., Braig, H.R., Bourtzis, K., 2011. Wolbachia prophage DNA adenine methyltransferase genes in different Drosophila-Wolbachia associations. PloS One 6, e19708.

Sasaki, T., Ishikawa, H., 1999. Wolbachia Infections and Cytoplasmic Incompatibility in the Almond Moth and the Mediterranean Flour Moth Wolbachia Infections and Cytoplasmic Incompatibility in the Almond Moth and the Mediterranean Flour Moth 16, 739–744.

Sem, X., Rhen, M., 2012. Pathogenicity of Salmonella enterica in Caenorhabditis elegans relies on disseminated oxidative stress in the infected host. PloS one 7, e45417.

Serbus, L.R., Ferreccio, A., Zhukova, M., McMorris, C.L., Kiseleva, E., Sullivan, W., 2011. A feedback loop between Wolbachia and the Drosophila gurken

mRNP complex influences Wolbachia titer. Journal of Cell Science 124, 4299–308.

Singh, S.R., Zheng, Z., Wang, H., Oh, S.-W., Chen, X., Hou, S.X., 2010. Competitiveness for the niche and mutual dependence of the germline and somatic stem cells in the Drosophila testis are regulated by the JAK/STAT signaling. Journal of Cellular Physiology 223, 500–510.

Stefanska, J., Pawliczak, R., 2008. Apocynin: molecular aptitudes. Mediators of inflammation 2008, 106507.

Stouthamer, R., Kazmert, D.J., 1994. Cytogenetics of microbe-associated parthenogenesis and its consequences for gene flow in Trichogramma wasps. Hereditas 73, 317–327.

Stouthamer, R., Luck, R.F., Hamilton, W.D., 1990. Antibiotics cause parthenogenetic Trichogramma (Hymenoptera / Trichogrammatidae) to revert to sex. Proceedings of the National Academy of Sciences of the United States of America 87, 2424–2427.

Stouthamer, R., Werren, J., 1993. Microbes associated with parthenogenesis in wasps of the genus Trichogramma. Journal of Invertebrate Pathology 61, 6–9.

Sturtevant AH, 1920. Genetic studies on Drosophila simulans. I. Introduction. Hybrids with Drosophila melanogaster. Genetics 5, 488–500.

Sugimoto, T.N., Ishikawa, Y., 2012. A male-killing Wolbachia carries a feminizing factor and is associated with degradation of the sex-determining system of its host. Biology Letters 8, 412–5.

Talà, A., Monaco, C., Nagorska, K., Exley, R.M., Corbett, A., Zychlinsky, A., Alifano, P., Tang, C.M., 2011. Glutamate utilization promotes meningococcal survival in vivo through avoidance of the neutrophil oxidative burst. Molecular microbiology 81, 1330–42.

Tanaka, K., Furukawa, S., Nikoh, N., Sasaki, T., Fukatsu, T., 2009. Complete WO phage sequences reveal their dynamic evolutionary trajectories and putative functional elements required for integration into the Wolbachia genome. Applied and environmental microbiology 75, 5676–86.

Tegtmeier F, Walter U, Schinzel R, Wingler K, Scheurer P, S.H., 2005. Compounds containing a N-heteroaryl moiety linked to fused ring moieties for the inhibition of NAD(P)H oxidases and platelet activation.

Tirone, F., Cox, J. a, 2007. NADPH oxidase 5 (NOX5) interacts with and is regulated by calmodulin. FEBS letters 581, 1202–8.

Tock, M.R., Dryden, D.T.F., 2005. The biology of restriction and anti-restriction. Current opinion in microbiology 8, 466–72.

Tokuyasu, K.T., Peacock, W.J., Hardy, R.W., 1972. Dynamics of spermiogenesis in Drosophila melanogaster. Zeitschrift für Zellforschung und Mikroskopische Anatomie 127, 492–525.

Tram, U., Sullivan, W., 2002. Role of delayed nuclear envelope breakdown and mitosis in Wolbachia-induced cytoplasmic incompatibility. Science (New York, N.Y.) 296, 1124–6.

Turelli, M., Hoffmann, A.A., 1991. Rapid spread of an inherited incompatibility factor in California Drosophila. Nature 353, 440–442.

Turelli, M., Hoffmann, A.A., 1995. Cytoplasmic Incompatibility in Drosophila simulans: Dynamics and Parameter Estimates from Natural Populations. Genetics 140, 1319–1338.

Vavre, F., Girin, C., Bouletreau, M., 1999. Phylogenetic status of a fecundity-enhancing Wolbachia that does not induce thelytoky in Trichogramma. Insect molecular biology 8, 67–72.

Veneti, Z., Clark, M.E., Karr, T.L., Savakis, C., Bourtzis, K., 2004. Heads or Tails : Host-Parasite Interactions in the Drosophila-Wolbachia System. Applied and environmental microbiology 70, 5366–5372.

Veneti, Z., Clark, M.E., Zabalou, S., Karr, T.L., Savakis, C., Bourtzis, K., 2003. Cytoplasmic incompatibility and sperm cyst infection in different Drosophila-Wolbachia associations. Genetics 164, 545–52.

Veneti, Z., Zabalou, S., Papafotiou, G., Paraskevopoulos, C., Pattas, S., Livadaras, I., Markakis, G., Herren, J.K., Jaenike, J., Bourtzis, K., 2012. Loss of reproductive parasitism following transfer of male-killing Wolbachia to Drosophila melanogaster and Drosophila simulans. Heredity 109, 306–12.

Vibranovski, M.D., Chalopin, D.S., Lopes, H.F., Long, M., Karr, T.L., 2010. Direct Evidence for Postmeiotic Transcription During Drosophila melanogaster Spermatogenesis. Genetics 186, 431–433.

Weeks, A.R., Stouthamer, R., 2004. Increased fecundity associated with infection by a cytophaga-like intracellular bacterium in the predatory mite,

Metaseiulus occidentalis. Proceedings of the Royal Society B: Biological Sciences 271 Suppl, S193–5.

Weldon, S.R., Strand, M.R., Oliver, K.M., 2013. Phage loss and the breakdown of a defensive symbiosis in aphids Phage loss and the breakdown of a defensive symbiosis in aphids. Proceedings of the Royal Society B 280.

Wernegreen, J.J., 2002. Genome evolution in bacterial endosymbionts of insects. Nature reviews. Genetics 3, 850–61.

Werren, J.H., Zhang, W., Guo, L.R., 1995. Evolution and phylogeny of Wolbachia: reproductive parasites of arthropods. Proceedings. Biological sciences / The Royal Society 261, 55–63.

Wieland, H., Ullrich, S., Lang, F., Neumeister, B., 2005. Intracellular multiplication of Legionella pneumophila depends on host cell amino acid transporter SLC1A5. Molecular microbiology 55, 1528–37.

Williams, B.C., Dernburg, A.F., Puro, J., Nokkala, S., Goldberg, M.L., 1997. The Drosophila kinesin-like protein KLP3A is required for proper behavior of male and female pronuclei at fertilization. Development 124, 2365–2376.

Wilson, K.L., Fitch, K.R., Bafus, B.T., Wakimoto, B.T., 2006. Sperm plasma membrane breakdown during Drosophila fertilization requires sneaky, an acrosomal membrane protein. Development (Cambridge, England) 133, 4871–9.

Wind, S., Beuerlein, K., Eucker, T., Müller, H., Scheurer, P., Armitage, M.E., Ho, H., Schmidt, H.H.H.W., Wingler, K., 2010. Comparative pharmacology of chemically distinct NADPH oxidase inhibitors. British Journal of Pharmacology 161, 885–98.

Wingler, K., Altenhoefer, S. a, Kleikers, P.W.M., Radermacher, K. a, Kleinschnitz, C., Schmidt, H.H.H.W., 2012. VAS2870 is a pan-NADPH oxidase inhibitor. Cellular and molecular life sciences : CMLS 69, 3159–60.

Wu, M., Sun, L. V, Vamathevan, J., Riegler, M., Deboy, R., Brownlie, J.C., McGraw, E. a, Martin, W., Esser, C., Ahmadinejad, N., Wiegand, C., Madupu, R., Beanan, M.J., Brinkac, L.M., Daugherty, S.C., Durkin, a S., Kolonay, J.F., Nelson, W.C., Mohamoud, Y., Lee, P., Berry, K., Young, M.B., Utterback, T., Weidman, J., Nierman, W.C., Paulsen, I.T., Nelson, K.E., Tettelin, H., O'Neill, S.L., Eisen, J. a, 2004. Phylogenomics of the reproductive parasite Wolbachia pipientis wMel: a streamlined genome overrun by mobile genetic elements. PLoS biology 2, E69.

Xi, Z., Gavotte, L., Xie, Y., Dobson, S.L., 2008. Genome-wide analysis of the interaction between the endosymbiotic bacterium Wolbachia and its Drosophila host. BMC genomics 9, 1.

Ximenes, V.F., Kanegae, M.P.P., Rissato, S.R., Galhiane, M.S., 2007. The oxidation of apocynin catalyzed by myeloperoxidase: proposal for NADPH oxidase inhibition. Archives of biochemistry and biophysics 457, 134–41.

Yamada, R., Iturbe-Ormaetxe, I., Brownlie, J.C., O'Neill, S.L., 2011. Functional test of the influence of Wolbachia genes on cytoplasmic incompatibility expression in Drosophila melanogaster. Insect Molecular Biology 20, 75–85.

Yen JH and Barr AR, 1973. The Etiological of Cytopiasmic Incompatibility Culex pipiens. Journal of Invertebrate Pathology 250, 242–250.

Zchori-Fein, E., Faktor, O., Zeidan, M., Gottlieb, Y., Czosnek, H., Rosen, D., 1994. Parthenogenesis-inducing microorganisms in Aphytis (Hymenoptera : Aphelinidae). Insect molecular biology 4, 173–178.

Zhao, D.-X., Zhang, X.-F., Chen, D.-S., Zhang, Y.-K., Hong, X.-Y., 2013. Wolbachia-Host Interactions: Host Mating Patterns Affect Wolbachia Density Dynamics. PLoS ONE 8, e66373.

Zheng, Y., Ren, P.-P., Wang, J.-L., Wang, Y.-F., 2011. Wolbachia-induced cytoplasmic incompatibility is associated with decreased Hira expression in male Drosophila. PloS One 6, e19512.

Zhou, W., Rousset, F., Neill, S.O., 1998. Phylogeny and PCR-based classification of Wolbachia strains using wsp gene sequences. Proceedings of the Royal Society B 265, 509–515.

Zug, R., Hammerstein, P., 2012. Still a host of hosts for Wolbachia: analysis of recent data suggests that 40% of terrestrial arthropod species are infected. PloS One 7, e38544.